Introduction

In this chapter, we are going to describe the main features as well as the basic steps of the Boundary Element Method (BEM) as applied to elastostatic problems and to compare them with other numerical procedures. As we shall show, it is easy to appreciate the advantages of the BEM, but it is also advisable to refrain from a possible unrestrained enthusiasm, as there are also limitations to its usefulness in certain types of problems. The number of these problems, nevertheless, is sufficient to justify the interest and activity that the new procedure has aroused among researchers all over the world.

Briefly speaking, the most frequently used version of the BEM as applied to elastostatics works with the fundamental solution, i.e. the singular solution of the governing equations, as an influence function and tries to satisfy the boundary conditions of the problem with the aid of a discretization scheme which consists exclusively of boundary elements. As in other numerical methods, the BEM was developed thanks to the computational possibilities offered by modern computers on a totally "classical" basis. That is, the theoretical grounds are based on linear elasticity theory, incorporated long ago into the curricula of most engineering schools. Its delay in gaining popularity is probably due to the enormous momentum with which Finite Element Methods (FEM) penetrated the professional and academic media. Nevertheless, the fact that these methods were developed before the BEM has been beneficial because the BEM successfully uses those results and techniques studied in past decades. Some authors even consider the BEM as a particular case of the FEM, while others view both methods as special cases of the general weighted residual technique [24].

The first paper usually cited in connection with the BEM as applied to elastostatics is that of Rizzo [95], even though the works of Jaswon et al. [65], Massonnet [79] and Oliveira [86] were published at about the same time, the reason probably being the attractiveness of the "direct" approach [95] over the "indirect" one [65, 79, 86]. The work of Rizzo [95] and the subsequent work of Cruse [45] initiated a fruitful period with applications of the direct BEM to problems of elastostatics, elastodynamics, fracture, etc. The next key contribution was that of Lachat and Watson [73] incorporating all the FEM discretization philosophy in what is sometimes called the "second BEM generation". This has, no doubt, led directly to the current developments.

Among the various researchers who worked on elastostatics by employing the

direct BEM, one can additionally mention Rizzo and Shippy [96–99], Cruse et al. [46–48], Lachat and Watson [74, 75], Alcarcón et al. [1–4], Brebbia et al. [26, 27], Brady et al. [22, 23], Wardle and Crotty [113], Dominguez et al. [53], Howell and Doyle [63, 64], Kuhn and Möhrmann [72] and Patterson and Sheikh [89–91], and among those who used the indirect BEM, one can additionally mention Benjumea and Sikarskie [20], Butterfield et al. [37–39], Tomlin and Butterfield [108], Banerjee et al. [13–15], Niwa et al. [85] and Altiero and Gavazza [10]. An interesting version of the indirect method, called the Displacement Discontinuity Method (DDM) has been developed by Crouch [42–44]. A comprehensive study on various special aspects of the elastostatic BEM has been done by Heisse [60–62], while review-type articles on the subject have been reported by Watson [114] and Hartmann [59].

At the present time, the method is well established and is being used for the solution of a variety of problems in engineering mechanics. Numerous introductory and advanced books have been published [66, 24, 28, 17, 44, 35] as well as research-oriented ones [16, 18, 31, 34]. In this sense, it is worth noting the series of conferences promoted by Brebbia since 1978 [25, 29, 30, 32, 33], which have provoked a continuous research effort all over the world in relation to the BEM.

In the following sections, we shall concentrate on developing the direct BEM as applied to elastostatics. Section 1 will present the fundamentals of the BEM, indicating its main features and fields of application as well as some general considerations on the different computational steps. The idea is to follow the well known path of the FEM and to comment on the major differences in a formal fashion. Section 2 contains more detailed material related to elastostatics problems, including such classical topics as the reciprocity theorem and Somigliana's identity, as well as the discretization procedure for both the direct and the indirect BEM. Special care has been taken to show the reduction to integrals on the boundary of several interesting body forces. Section 3 will present the development necessary for treating two-dimensional domains. The presentation will be done using linear elements and Kelvin-type fundamental solutions.

The method is particularly attractive in three-dimensional cases, and section 4 is dedicated to the corresponding implementation. It will be shown that owing to the properties of Kelvin's fundamental solution, the work is very simple and the treatment of conditions at infinity superior even to that of the plane case. Here the interpolation is presented with constant elements to prevent complications with corners, of the type treated in section 3, from shadowing the BEM properties. Section 5 discusses a special three-dimensional case, that of axisymmetric bodies. In this condition, the two-dimensional aspect is revised for the definition of elements although the fundamental solutions present typical features. Finally, section 6 briefly discusses the case of anisotropy, while section 7 is devoted to the special topics of bending of plates and shells, coupling of the BEM with the FEM and adaptive procedures in BEM analysis.

1. Fundamentals of the Boundary Element Method

1.1. Primary features of the method

The BEM proceeds by discretizing the boundary of the domain under study (Fig. 1) by subdivision into elements that support the zones where the data or the unknowns are supposed to vary according to a certain predefined fashion, e.g. linear, parabolic, cubic, etc. From that point of view, the BEM is similar to the FEM and the previous hypothesis would be identified with the usual "interpolation functions". A first and important difference is that of discretizing the boundary and not the domain with the logical advantages of simplification so conveyed.

Another important difference is with regard to the quantities used by the method. They correspond exactly to the field variables of the problem (stresses, displacements, temperatures, etc.) so that the concept of "equivalent nodal forces" disappears. That is essentially due to the fact that the above-mentioned interpolation is one simultaneously on the dual problem variables, i.e. stresses and displacements, temperature and fluxes, etc. It is worth noting that both interpolations can be independent because there is no relationship between their evolution along the boundary; nevertheless, it is common to apply the same degree of polynomial interpolation to both variables. In other cases, it could be advantageous to use a mixture of different degrees, generating the so-called "mixed elements" [78], or to incorporate in the polynomials the singular behavior of the solution near stress concentration or singular points [57]. In any case, it is logical to hope that the simultaneous interpolation of all field variables will produce more accurate results, as we shall see later.

It is important to point out from the beginning that the basis of the procedure hinges on the computation of the variables at the boundary. If it is desirable to compute values inside the domain, a relatively costly complementary algorithm must be established. It is well known that the FEM works precisely with values defined inside the domain and therefore, as a general conclusion, it can be said that the BEM is preferable in those cases where only the boundary values are

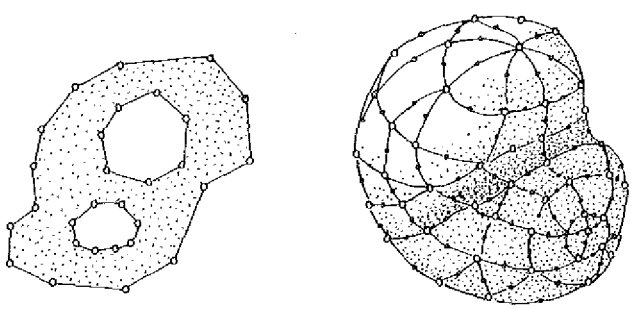

Fig. 1. Boundary element discretization of two- and three-dimensional domains.

needed, although it is important to remember the advantage of discretizing only the boundary.

Finally, a more technical peculiarity will be cited which is not obvious to the user but which hinges heavily on the programmer and on the effectiveness of the method. It is related to the "weighting functions" that, on the one hand form the core of the advantages of the method, while on the other hand burden it with their inconvenience. In short, the weighting functions are globally defined in opposition to the locally based FEM functions or to the interpolating functions. This implies two serious consequences: first, the resultant matrices are full and, second, they are not symmetric. Both conditions provoke the use of algorithms different from those of the FEM and which hinge on the storage and the methods used to solve the equations but do not substantially affect the user.

1.2. Fields of application

The areas to which the BEM can be applied are enormously varied, as can be seen by rereading the above-mentioned references. In principle, the ideal field of application includes linear problems defined over isotropic homogeneous domains, where a fundamental solution of the field problem is defined. In what follows, we shall restrict the appraisal to elastostatics.

The limitation on anisotropy is relatively easy to eliminate as is that of continuous heterogeneity, although, regarding the former, it is necessary to know the corresponding fundamental solution. The case of the piecewise heterogeneity is treated by a zoning technique (Fig. 2a), and the use for every subdomain of the

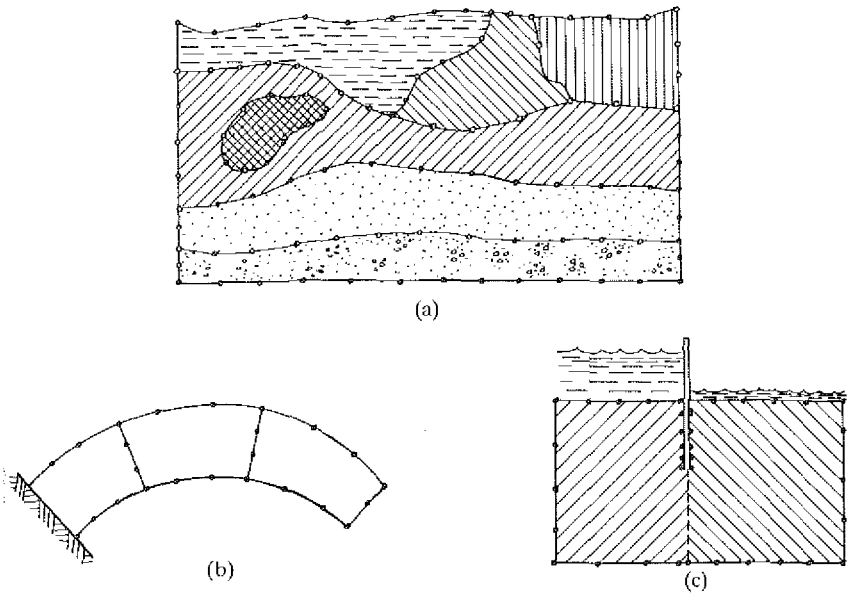

Fig. 2. Zoning technique in boundary element analysis.

corresponding fundamental solution. That is also interesting when treating aligned bodies, which would need a great number of boundary elements due to simple computational problems (Fig. 2b). A similar situation arises in cases with small or null distances (Fig. 2c), where it would be complicated to establish different conditions at the same node. Occasionally, this type of zoning is even included artificially to produce block matrices which can be favorably treated by the computer [74].

In problems with nonzero body forces or those in which an approximate fundamental solution is used, volume integrals on quantities varying in an arbitrary manner over the domain appear in the formulation. The usual technique is the definition of integration "cells" with a predefined evolution as a function of the nodal values (Fig. 3). They are not finite "elements" because they do not contribute unknowns to the equations. It is fair to recognize, nevertheless, that an important part of the spectacularity and advantages of the method are lost in those cases, because a domain mesh must be defined and values have to be computed at the mesh nodes. This is costly, although several attempts have been made to alleviate this disadvantage.

Another specific area of applicability is the treatment of areas with boundaries at infinity, as usually assumed in soil–structure interaction (Fig. 4). In those cases, the variables of interest are related to a small part of the domain (the structure) where a detailed knowledge of the field variables is important, while the other is a contact or interface boundary. A recommended procedure is then to

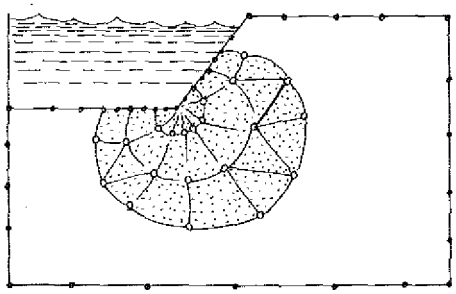

Fig. 3. Use of internal cells in the BEM.

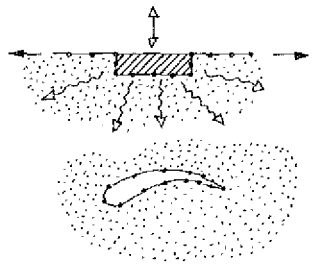

Fig. 4. Automatic treatment of domains with infinite boundaries by the BEM

apply the FEM to the structure and to model the rest of the media by the BEM in a "marriage à la mode", as it was called by Zienckiewicz, where "the best of both worlds" is used [117].

1.3. Basic steps of the method

As in every engineering situation, the initial step is the selection of the mathematical model best suited to the properties of the problem at hand and consideration of this model from the point of view of the BEM possibilities. If the answer is affirmative, the steps are similar to those used in the FEM, i.e.:

(a) The domain is subdivided into the number of subregions necessary to reflect its peculiarities, either of heterogeneity or of a geometrical nature.

(b) The boundaries of each subregion are subdivided, using the concept of "element", i.e. the degree of interpolation on that part of the boundary is chosen. Usually, the boundary is discretized by the same shape functions (isoparametric elements), although that is not strictly necessary.

(c) In order to build the pre-established degree of interpolation, a number of nodes is defined. It is important to note that these nodes can be anywhere that they are needed (Fig. 5a). In general, it is common to work with compatible elements, in the sense that neighboring elements share nodes at their sides or vertex. This has the advantage of reducing the number of equations to be solved

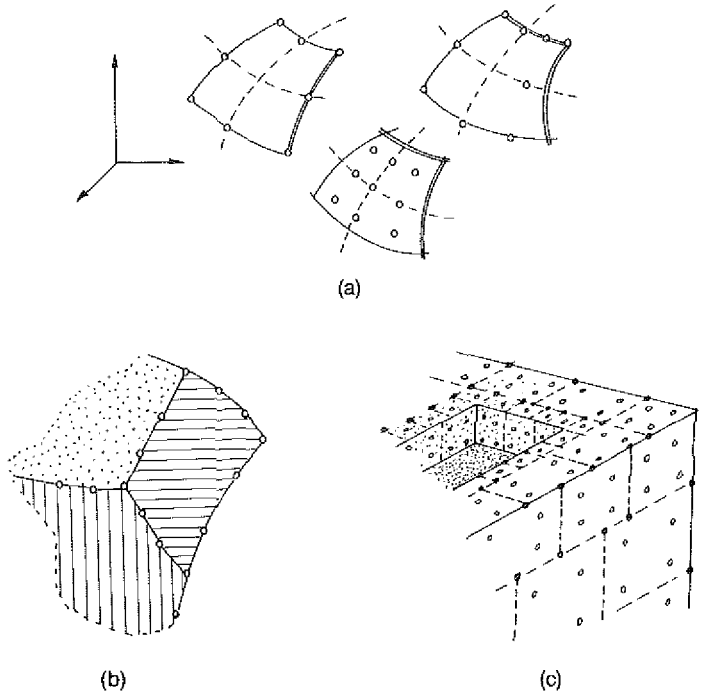

Fig. 5. Various types of higher-order boundary elements.

but may present complications with discontinuities, interfaces or singularities where it is most convenient to give the model more adaptiveness (Fig. 5b). Some authors prefer the first working possibility, especially in three-dimensional problems, where an extraordinary capacity for adaptation to the peculiarities of the problem can be achieved (Fig. 5c).

(d) For every degree of freedom (d.o.f.) at each node, an equation is built through an integral representation formula, using as weighting functions the fields of displacements and stresses generated by unit loads along the d.o.f. acting (in general) on an infinite space with the same material properties of the body under study. At this point, important computational problems appear, due to the necessity of computing singular integrals with accuracy and effectiveness. Usually, those unit loads are placed at the previously defined nodes. It is possible, nevertheless, that in some problems it might be interesting to define new nodes to which those loads would be applied. This is precisely what is done in the so-called "indirect methods" where, on occasion, the nodes are situated outside the domain, or in the "hierarchical elements" where collocation points are completely independent of the geometry.

(e) The natural and essential variables in the boundary are contained in two vectors that will be called, respectively, $\boldsymbol{t}$ and $\boldsymbol{u}$ and the previously computed factors are stored in matrices $\boldsymbol{A}$ and $\boldsymbol{B}$, forming a system

$$\boldsymbol{A}\boldsymbol{u} = \boldsymbol{B}\boldsymbol{t}\,, \tag{1.1}$$

where $\boldsymbol{u}$ and $\boldsymbol{t}$ contain data as well as unknowns.

(f) Once $\boldsymbol{A}$ and $\boldsymbol{B}$ have been built (or simultaneously, to gain time), the boundary conditions are established, imposing the known values of the variables on the different pieces. The problem is then reduced to the classical form

$$\boldsymbol{K}\boldsymbol{x} = \boldsymbol{F}\,, \tag{1.2}$$

that is, to a system of equations where $\boldsymbol{x}$ contains all the boundary unknowns and $\boldsymbol{F}$, the product of the $\boldsymbol{A}$ and $\boldsymbol{B}$ coefficients by the corresponding data.

(g) Solution of the system (1.2) allows the determination of all the boundary information. If results at internal points are sought, an additional step is required. New $\boldsymbol{A}$ and $\boldsymbol{B}$ matrices have to be computed (one set for each internal point) and multiplied by the boundary values, as will be shown later. In this process of computing new $\boldsymbol{A}$ and $\boldsymbol{B}$ matrices, a significant amount of time is used, so that, if the number of internal points is large, the advantages of using the BEM may disappear.

1.4. The fundamental solution

As we mentioned in point (d) above, the construction of every equation follows the general pattern of the FEM, i.e. an integral formula relates internal and

external energy of loads and stresses. There are two main differences between the method under study and the Displacements Finite Element Method. First, the basic integral formula is a reciprocity relationship among the actual problem and a series of virtual problems. That means that there are energies due to virtual stresses as well as those related to virtual displacements, so that it will be necessary to discretize both the actual stresses and the displacements. Second, the virtual state is chosen so that the field equations can be satisfied. There are several ways of doing that, but the classical BEM technique uses the so-called fundamental solution, that is, the fields generated by point loads acting on an infinite space. Thus, if $\mathscr{A}$ represents the operator of the problem, the weighting functions are the fields related to the solution of

$$\mathscr{A}\boldsymbol{u}^*(\boldsymbol{x}) = \delta(\boldsymbol{x} - \boldsymbol{x}_\mathrm{p})\boldsymbol{e} \tag{1.3}$$

where δ is the Dirac (delta) function, $\boldsymbol{x}$ represents an arbitrary point inside an infinite space, $\boldsymbol{x}_\mathrm{p}$ are the coordinates of point P (where the unit load is applied) and $\boldsymbol{e}$ is a unit vector pointing in the d.o.f. direction.

By varying the point P, it is possible to generate as many weighting functions as necessary, the simplest way being the use of the same points defined to interpolate the actual variables. The above-mentioned fundamental solution for linear elasticity is well known. It is the solution to the so-called Kelvin problem [76] and is the most appropriate for general purposes. Other fundamental solutions are related to special conditions. For instance, the Mindlin problem [35] can be used to model half-spaces, the Boussinesq problem [112] can be applied to certain soil-fundation situations, etc. Two features related to the special choice of weighting functions are worth noting. First, the reduction to only one term of the energy related to virtual loads, i.e. the work of the applied Dirac delta on the actual $u(\boldsymbol{x}_\mathrm{p})$ of point P. This implies elimination of the trouble related to computations of domain integrals. Then the "globally based" property of the weighting functions will produce interactions with all the interpolating ones, independently of their global or local definition. In other words, as we said in section 1.1, the matrices to be obtained are full, as opposed to the FEM matrices. Finally, the special character of the delta function will cause trouble in the computation, especially when trying to compute integrals relating the same collocation and interpolation points. This problem will be dealt with in subsequent sections.

2. Classical relationships in linear elasticity

In this section, the formulas controlling the response of linear elastic bodies to static loads will be established and some classical relationships directly related to boundary methods will be presented.

2.1. Elasticity problems

In what follows, the discussion will be organized around problems controlled by the Navier equation for linear isotropic and homogeneous elastostatics [76]

$$(\lambda + G)\ \text{grad div}\ \boldsymbol{u} + G\nabla^2\boldsymbol{u} + \boldsymbol{X} = \boldsymbol{0}\,, \tag{2.1}$$

where u is the displacement vector

$$\boldsymbol{u}^{\mathrm{T}} = \{u_1, u_2, u_3\}\,, \tag{2.2}$$

$\boldsymbol{X}$ is the body force vector

$$\boldsymbol{X}^{\mathrm{T}} = \{X_1, X_2, X_3\}\,, \tag{2.3}$$

while λ and G are the classical Lame constants related to the Young modulus E and Poisson ratio ν by

$$\lambda = \frac{\nu E}{(1+\nu)(1-2\nu)}\,, \qquad G = \frac{E}{2(1+\nu)}\,. \tag{2.4}$$

The solution of Eqs. (2.1) has been treated largely from a mathematical point of view and several well known closed-form solutions constitute the experience of the academic community. Nevertheless, the solution of situations with arbitrary geometry and general conditions on the boundary can still be considered to offer computational and practical interest.

It is well known that, for the problem to be "well posed", the field equations must be completed with the specification of suitable boundary conditions. Those conditions for a body Ω with boundary $\partial\Omega$ can be of the following types:

1. Essential conditions:

The displacements are prescribed on the boundary, i.e.

$$\boldsymbol{u}(\boldsymbol{x}) = \boldsymbol{u}_0(\boldsymbol{x})\,, \qquad \boldsymbol{x} \in \partial\Omega\,. \tag{2.5}$$

This is similar to the Dirichlet-type conditions in potential problems.

2. Natural conditions:

The stresses are prescribed on the boundary, i.e.

$$\overset{n}{\boldsymbol{T}}(\boldsymbol{x}) = \overset{n}{\boldsymbol{T}}_0(\boldsymbol{x}) \qquad \boldsymbol{x} \in \partial\Omega \tag{2.6}$$

where $\overset{n}{\boldsymbol{T}}$ is the traction vector at a point $\boldsymbol{x}$ where the normal to the boundary is $\boldsymbol{n}$.

It is well known that

$$\overset{n}{T} = \boldsymbol{\sigma} \cdot \boldsymbol{n} \tag{2.7}$$

where $\boldsymbol{\sigma}$ is the stress tensor, and the material law is the Hooke's relationship

$$\sigma_{ij} = \lambda \varepsilon_{mm} \delta_{ij} + 2G\varepsilon_{ij} \tag{2.8}$$

with

$$\begin{aligned} \varepsilon_{ij} &= \tfrac{1}{2}(u_{i,j} + u_{j,i}) \\ \delta_{ij} &= \begin{cases} 0 & \text{if} \quad i \neq j \\ 1 & \text{if} \quad i = j \end{cases} \end{aligned} \tag{2.9}$$

a comma denoting derivative and a repeated index summation.

Using (2.7), (2.8), (2.9) and (2.6), it is possible to write the natural conditions in terms of the displacement vector as

$$\lambda \boldsymbol{n} \operatorname{div} \boldsymbol{u} + 2G \frac{\partial \boldsymbol{u}}{\partial \boldsymbol{n}} + G(\boldsymbol{n} \times \operatorname{rot} \boldsymbol{u}) = \overset{n}{\boldsymbol{T}}_0(\boldsymbol{x}) \,. \tag{2.10}$$

It is possible to see that this condition is similar to the Neumann-type conditions in potential problems, only with respect to the second term on the left-hand side of (2.10).

3. Mixed conditions:

They are a combination of the previous conditions, either on different parts of the boundary or on a fixed one, where several stresses (normal, for example) and several displacements (tangential, for example) are given.

As examples, Figs. 6 and 7 offer several familiar cases of what has been said. Thus the problem depicted by Fig. 6(a) corresponds to simple traction of a strip. Obviously, the basic variables here are the displacement vector $\boldsymbol{u}$ and its dual, the traction $\boldsymbol{T}$. Apparently the displacement is constant along BC while the tractions

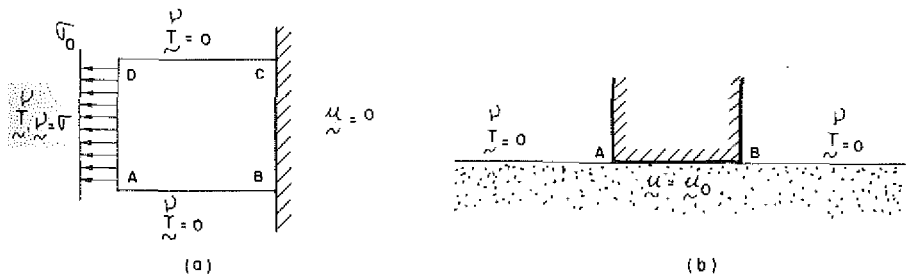

Fig. 6. Typical boundary-value problems in elastostatics with mixed boundary conditions.

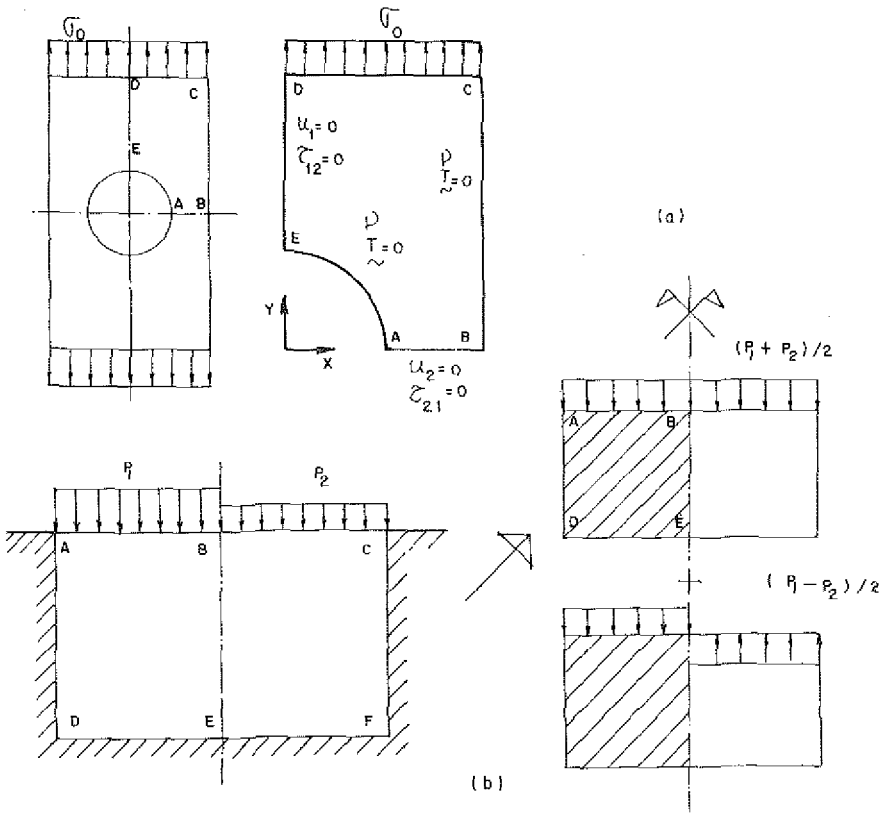

Fig. 7. Use of symmetry and antisymmetry in elastostatic boundary-value problems.

are null along AB and DC and $\boldsymbol{\sigma}_0 \cdot \boldsymbol{n}$ along DA. The problem shown in Fig. 6(b), where a rigid punch is applied to an elastic half-space, is also familiar. Along AB, the displacement is constant, while the free boundary offers no traction. Conditions at infinity are more complicated to establish. In general, it is assumed that stresses become bounded and displacements tend to zero. It is interesting to note that points A and B are singular points due to the sudden change in conditions from pure natural to pure essential. This implies the presence of infinite stresses and the need to solve an interesting numerical problem.

Occasionally, the conditions of symmetry or antisymmetry will allow a mixed problem, which is interesting for the good conditioning of matrices. In Fig. 7(a), we can see how a problem with natural boundary conditions can be transformed into a mixed one, taking advantage of the symmetry of the perforated strip and of the load. The first problem is undetermined, in the sense that a rigid-body displacement can be superimposed without affecting the state of stresses. On the other hand, after applying the conditions of symmetry, as indicated in Fig. 7(a), the displacements are relative to those specified. Problem 7(a) is also interesting because, along DE or AB, conditions are mixed in displacements and stresses.

Similarly, Fig. 7(b) presents the way to treat symmetrical geometry with antisymmetrical loads. The problem is decomposed into another two. In the first one, the interface BE cannot move horizontally, while in the second the vertical displacement is nil. The symmetry in the first case impedes the development of tangential vertical stresses, while, in the second, the antisymmetry along BE precludes the development of normal horizontal stresses. If, in addition, walls AD and CF are smooth, the first problem is a trivial one and is solved immediately. Once again a singular situation will develop at B, where the stress tensor has to produce two different traction values p_1 and p_2 at a point B with only one normal.

In the previous examples, it has been implicitly assumed that the medium was isotropic and homogeneous. For piecewise heterogeneities, as in Fig. 8(a), it is possible to establish a zoning scheme and, for each zone, apply the previous equations along with the specific material properties. In addition to the conditions at the exterior boundary, it is necessary now to introduce the compatibility of displacements and equilibrium of tractions along the interfaces. The zoning is also an artifice allowing the solution of asymmetric situations such as that of Fig. 8(b), by the introduction of an artificial interface.

In addition to the three classical boundary conditions, there are occasions in which the natural values are combined with the esential ones, either in a Robin–Newton mode of the form

$$a\boldsymbol{u} + b\overset{n}{\boldsymbol{T}} = \boldsymbol{c}\,, \tag{2.11}$$

or in a generalized oblicuum derivative, relating different components of $\overset{n}{\boldsymbol{T}}$, according to

$$a(\overset{n}{\boldsymbol{T}} \cdot \boldsymbol{n}) + b(\overset{n}{\boldsymbol{T}} \cdot \boldsymbol{s}) = c\,, \tag{2.12}$$

where $\boldsymbol{s}$ indicates the tangent unit vector.

An example of the first situation is a beam resting on springs (Fig. 9a), while the second one can be represented by Coulomb-like interfaces, as in Fig. 9(b).

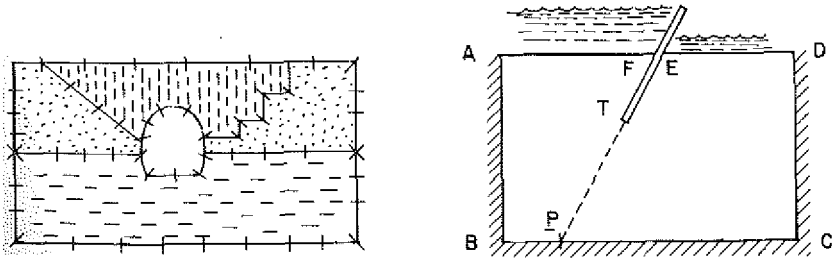

(a) (b)

Fig. 8. Use of the zoning technique for heterogeneous or asymmetric domains.

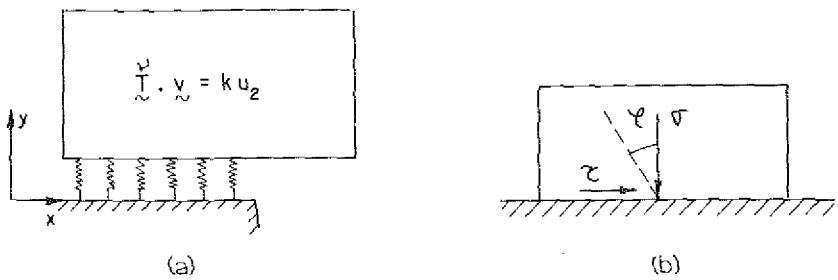

Fig. 9. Boundary-value problems with non-classical boundary conditions.

2.2. *Virtual work and reciprocity theorem*

It is known that the equilibrium equations inside the domain can be written as

$$\sigma_{ij,j} + X_i = 0 .$$

If a displacement field u_i^* is imagined, then it is possible to write

$$\int_{\mathcal{N}} \sigma_{ij,j} u_i^* + \int_{\Omega} X_i u_i^* = 0 , \tag{2.13}$$

where Ω represents the body, and where here and throughout, the differentials of volume are omitted for the sake of convenience. On account of

$$(\sigma_{ij} u_i^*)_{,j} = \sigma_{ij,j} u_i^* + \sigma_{ij} u_{i,j}^* \tag{2.14}$$

and due to the symmetry of σ_{ij}

$$(\sigma_{ij} u_i^*)_{,j} = \sigma_{ij,j} u_i^* + \sigma_{ij} \varepsilon_{ij}^*$$

so that, application of the divergence theorem yields

$$\int_{\Omega} \sigma_{ij,j} u_i^* = \int_{\Omega} (\sigma_{ij} u_i^*)_{,j} - \int_{\Omega} \sigma_{ij} \varepsilon_{ij}^* = \int_{\partial\Omega} \sigma_{ij} n_j u_i^* - \int_{\Omega} \sigma_{ij} \varepsilon_{ij}^* . \tag{2.15}$$

Thus, introduction of (2.15) in (2.13) results in

$$\int_{\partial\Omega} \overset{n}{T}_i u_i^* + \int_{\Omega} X_i u_i^* = \int_{\Omega} \sigma_{ij} \varepsilon_{ij}^* . \tag{2.16}$$

This is the principle of virtual work, relating an equilibrium set $(\overset{n}{T}_i, X_i, \varepsilon_{ij})$ to a completely independent, compatible one $(u_i^*, \varepsilon_{ij}^*)$.

The right-hand side of Eq. (2.16) can be rewritten by using Hooke's law as

follows:

$$\int_{\Omega} \sigma_{ij}\varepsilon^*_{ij} = \lambda \int_{\Omega} \varepsilon_{mm}\delta_{ij}\varepsilon^*_{ij} + 2G \int_{\Omega} \varepsilon_{ij}\varepsilon^*_{ij}$$
$$= \lambda \int_{\Omega} \varepsilon_{mm}\varepsilon^*_{mm} + 2G \int_{\Omega} \varepsilon_{ij}\varepsilon^*_{ij} . \tag{2.17}$$

Due to the symmetry of the right-hand side, it is clear that

$$\int_{\Omega} \sigma_{ij}\varepsilon^*_{ij} = \int_{\Omega} \varepsilon_{ij}\sigma^*_{ij} \tag{2.18}$$

and thus, introducing (2.18) in (2.16), we obtain

$$\int_{\partial\Omega} \overset{n}{T}_i u^*_i + \int_{\Omega} X_i u^*_i = \int_{\partial\Omega} \overset{n}{T}^*_i u_i + \int_{\Omega} X^*_i u_i , \tag{2.19}$$

expressing the Maxwell–Betti reciprocity relationship between two different elastic problems established on the same domain.

2.4. *Somigliana's identity*

An interesting application of Eq. (2.19) is obtained when

$$X^*_i = e\delta(x - \mathrm{P}) ,$$

where e denotes a direction and $\delta(x - \mathrm{P})$ represents a unit value concentrated force applied at point $x = \mathrm{P}$.

Due to the properties of the Dirac δ-function, the last term of the right-hand of Eq. (2.19) reduces to u_i and thus a representation formula can be obtained of the form

$$u_i(\mathrm{P}) = \int_{\partial\Omega} \overset{n}{T}_i(\mathrm{Q})u^*_i(\mathrm{P},\mathrm{Q}) - \int_{\partial\Omega} \overset{n}{T}^*_i(\mathrm{P},\mathrm{Q})u_i(\mathrm{Q}) + \int_{\Omega} X_i(\mathrm{Q})u^*_i(\mathrm{Q}) ; \qquad \mathrm{P} \in \Omega . \tag{2.20}$$

This formula, along with other interesting contributions, was developed by the Italian mathematician Somigliana [101–103]. It is important to note that, on the right-hand side of (2.20), only the first two terms include unknowns. The third is completely known. Let us forget it, however, for a moment and imagine that there are no body forces.

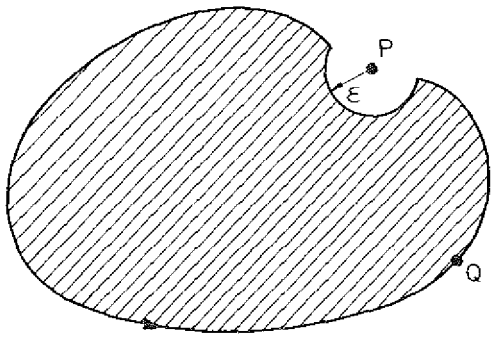

Fig. 10. Illustration of the limiting procedure as an interior point P approaches the boundary.

If P is located at the boundary, a limiting procedure (Fig. 10) allows (2.20) to be written as

$$u_i(\mathrm{P}) = \lim_{\varepsilon \to 0} \Bigg[\int_{\partial(\Omega - \mathscr{E})} \overset{n}{T}_i(\mathrm{Q}) u_i^*(\mathrm{P}, \mathrm{Q}) + \int_{\partial \mathscr{E}} \overset{n}{\mathrm{T}}_i(\mathrm{Q}) \mathrm{u}_i^*(\mathrm{P}, \mathrm{Q}) - \int_{\partial(\Omega - \mathscr{E})} \overset{n}{T}_i^*(\mathrm{P}, \mathrm{Q}) u_i(Q) - \int_{\partial \mathscr{E}} \overset{n}{T}_i^*(\mathrm{P}, Q) u_i(\mathrm{Q}) \Bigg] . \tag{2.21}$$

The second integral on the right-hand side of (2.21) represents the work done by the resultant real force on $\partial\mathscr{E}$ on the virtual displacement $\boldsymbol{u}^*$ and tends to zero with ε. On the other hand, the last integral represents the resultant of the virtual stresses around $\partial\mathscr{E}$ on the real displacement of the point Q. When the boundary at P is smooth and based on the symmetry and antisymmetry conditions with respect to the normal and with respect to the tangent, it is clear that

$$\lim_{\varepsilon \to 0} \int_{\partial \mathscr{E}} \overset{n}{T}_i^*(\mathrm{P}, \mathrm{Q}) u_i(\mathrm{Q}) = -\tfrac{1}{2} u_i(\mathrm{P}) , \tag{2.22}$$

i.e. each half of the load is supported by a half-space. The minus sign is due to the change in positive directions on normals to the surface and $\partial\mathscr{E}$. This condition is proved rigorously by Rizzo [95], using the expression for the fundamental solution.

When the boundary is not smooth, the resultant of the stresses along the surface $\partial\mathscr{E}$ will have to be computed explicity by means of

$$\lim_{\varepsilon \to 0} \int_{\partial \mathscr{E}} T_{ij}^*(\mathrm{P}, \mathrm{Q}) , \tag{2.23}$$

where T_{ij}^* are the stresses $\overset{n}{T}_i^*$ at point Q in direction j, provoked by a unit load acting at P and directed along i.

In general, it would be possible then to write (2.20) as

$$c_{ji}(\mathrm{P})u_i(\mathrm{P}) = \int_{\partial\Omega} T_i(\mathrm{Q})U^*_{ij}(\mathrm{P},\mathrm{Q}) - \int_{\partial\Omega} T^*_{ji}(\mathrm{P},\mathrm{Q})u_i(\mathrm{Q}) + \int_{\Omega} U^*_{ji}(\mathrm{P},\mathrm{Q})X_i(\mathrm{R}), \qquad \mathrm{P},\mathrm{Q}\in\partial\Omega; \qquad \mathrm{R}\in\Omega, \tag{2.24}$$

where points P and Q are on the boundary, point R is inside the domain,

$$C_{ji}(\mathrm{P}) = \delta_{ji} - \lim_{\varepsilon\to 0}\int_{\partial\mathscr{E}} T^*_{ji}(\mathrm{P},\mathrm{Q}) \tag{2.25}$$

and U^*_{ji} is the displacement at point Q in direction i when a unit load of direction j has been applied at point P. The pair of tensors U^*_{ji} and T^*_{ji} constitutes the fundamental solution of the problem.

2.4. *Boundary integral equation*

Equations (2.24) and (2.25) are ideally suited to solve the case when $X = 0$, i.e. when there are no body forces. In this case

$$c_{ji}u_i(\mathrm{P}) = \int_{\partial\Omega} U^*_{ji}(\mathrm{P},\mathrm{Q}) - \int_{\partial\Omega} T^*_{ji}(\mathrm{P},\mathrm{Q}), \qquad \mathrm{P},\mathrm{Q}\in\partial\Omega, \tag{2.26}$$

and both P and Q are along the boundary. The representation formula (2.26) is similar to the classical one in potential theory, offering the solution at a boundary point as a contribution from single and double layer potentials.

Explicit expressions for the Kelvin's fundamental solution of elastostatics are given in three dimensions by [76, 35]

$$U^*_{ij} = \frac{1}{16\pi G(1-\nu)}\frac{1}{r}\left[(3-4\nu)\delta_{ij} + r_{,i}r_{,j}\right]$$
$$T^*_{ij} = \frac{-1}{8\pi(1-\nu)}\frac{1}{r^2}\left\{\frac{\partial r}{\partial n}\left[(1-2\nu)\delta_{ij} + 3r_{,i}r_{,j}\right] - (1-2\nu)(r_{,i}n_j - r_{,j}n_i)\right\} \tag{2.27}$$

and in two dimensions (plane strain) by

$$U^*_{ij} = \frac{1}{8\pi G(1-\nu)}\left[(3-4\nu)\ln\frac{1}{r}\,\delta_{ij} + r_{,i}r_{,j}\right],$$
$$T^*_{ij} = -\frac{1}{4\pi(1-\nu)}\frac{1}{r}\left\{\frac{\partial r}{\partial n}\left[(1-2\nu)\delta_{ij} + 2r_{,i}r_{,j}\right] - (1-2\nu)\,(r_{,i}n_j - r_{,j}n_i)\right\}, \tag{2.28}$$

where $r = r(\mathrm{P},\mathrm{Q})$ is the distance between the points P and Q. The singular

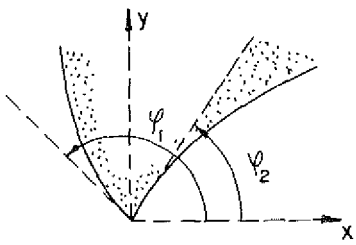

Fig. 11. Geometry of a non-smooth boundary point.

character of the above fundamental solutions is apparent. Indeed, as $r \to 0$, we have from (2.27) and (2.28) that $U^*_{ij} = O(1/r)$ and $T^*_{ij} = O(1/r^2)$ for three dimensions and $V^*_{ij} = O(\ln r)$ and $T^*_{ij} = O(1/r)$ for two dimensions.

On the other hand, for non-smooth boundary points, the tensor c_{ij} is given explicitly in two dimensions by

$$c_{ij} = \frac{1}{4\pi(1-\nu)} \times \begin{bmatrix} 2(1-\nu)(\varphi_1 - \varphi_2) + \frac{1}{2}(\sin 2\varphi_1 - \sin 2\varphi_2) & \sin^2 \varphi_1 - \sin^2 \varphi_2 \\ \sin^2 \varphi_1 - \sin^2 \varphi_2 & 2(1-\nu)(\varphi_1 - \varphi_2) - \frac{1}{2}(\sin^2 \varphi_1 - \sin^2 \varphi_2) \end{bmatrix}, \tag{2.29}$$

where the angles φ_1 and φ_2 are shown in Fig. 11, while for three dimensions, Hartmann [59] has presented expressions for c_{ij} for the following cases:

Quarter of a sphere:

$$c_{ij} = \frac{1}{8\pi} \begin{bmatrix} 2\pi & 0 & 0 \\ 0 & 2\pi & 2/(1-\nu) \\ 0 & 2/(1-\nu) & 2\pi \end{bmatrix}. \tag{2.30}$$

Eighth of a sphere:

$$c_{ij} = \frac{1}{8\pi} \begin{bmatrix} \pi & 1/(1-\nu) & 1/(1-\nu) \\ 1/(1-\nu) & \pi & 1(1-\nu) \\ 1/(1-\nu) & 1/(1-\nu) & \pi \end{bmatrix}.$$

It will be shown in the following sections that the exact computation of c_{ij} is, in general, not necessary, because if the boundary is not smooth c_{ij} can be obtained through the imposition of rigid-body displacements. However, for smooth boundary points the tensor $c_{ij} = \frac{1}{2}I$, where I is the identity matrix.

2.5. *The direct method*

Equation (2.26) is the basis for the BEM. The idea is to interpolate the unknowns by means of predefined shape functions in the same fashion as with the FEM, but

simultaneously. That is, it is assumed that

$$\begin{aligned} \boldsymbol{u} &= \boldsymbol{N}\boldsymbol{a}\,, \\ \boldsymbol{T} &= \boldsymbol{M}\cdot\boldsymbol{b}\,, \end{aligned} \tag{2.31}$$

where $\boldsymbol{u}$ and $\boldsymbol{T}$ are the displacement and traction vectors along some piece of boundary, $\boldsymbol{N}$ and $\boldsymbol{M}$ are matrices containing the interpolating functions and $\boldsymbol{a}$ and $\boldsymbol{b}$ are vectors with the unknowns. The support of $\boldsymbol{N}$ and $\boldsymbol{M}$ define the "elements" on the boundary over which the integrals appearing in (2.26) will be calculated. $\boldsymbol{N}$ and $\boldsymbol{M}$ can be locally or globally based, they can be different and, finally, they are completely independent of the approximation used to represent the geometry.

The first idea by Rizzo [95] and Cruse [45] was the simplest one, i.e. to divide the boundary into pieces, where both $\boldsymbol{u}$ and $\boldsymbol{T}$ were assumed to remain constant. In this case, Eq. (2.26) simplifies to

$$c_{ji}u_i(\mathrm{P}) = \sum_k T_i(\mathrm{Q}) \int_{\partial\Omega_k} U^*_{ji}(\mathrm{P},\mathrm{Q}_k) - \sum_k u_i(\mathrm{Q}) \int_{\partial\Omega_k} T^*_{ji}(\mathrm{P},\mathrm{Q}_k)\,. \tag{2.32}$$

The pieces $\partial\Omega_k$ must still be selected, that is the boundary must be discretized and the k points P where Eq. (2.32) will be applied must be chosen. In this way, a system $(k \times k)$ given by

$$\boldsymbol{A}\boldsymbol{u} = \boldsymbol{B}\boldsymbol{t} \tag{2.33}$$

will be formed, where $\boldsymbol{A}$ contains the coefficients c_{ij} plus the last integrals of the right-hand side of Eq. (2.32) and $\boldsymbol{B}$ contains the first integrals of the right-hand side of Eq. (2.32). Several examples of this procedure will be shown in the following sections. In general, the actual geometry is substituted by plane triangular facets as in Fig. 21(a), and the collocation points are taken at the centroids of the facets. The representative values for $\boldsymbol{u}$ and $\boldsymbol{t}$ are assumed to be those occurring at the centroids.

Equation (2.33) can be transformed in a classical system of linear equations by imposing the boundary conditions at the element centroids, thereby reducing the number of unknowns. If all the displacements are known, for instance

$$\boldsymbol{t} = \boldsymbol{B}^{-1}\boldsymbol{A}\boldsymbol{u}\,, \tag{2.34}$$

while if the stresses are known (except rigid-body displacements)

$$\boldsymbol{u} = \boldsymbol{A}^{-1}\boldsymbol{B}\boldsymbol{t}\,. \tag{2.35}$$

In general, in a mixed problem, (2.33) yields

$$\begin{aligned} \boldsymbol{F} &= \boldsymbol{K}\boldsymbol{X} \\ \boldsymbol{X} &= \boldsymbol{K}^{-1}\boldsymbol{F} \end{aligned} \tag{2.36}$$

where X contains all the boundary unknowns and F all the boundary data. The problem is then formally solved.

Lachat and Watson [73] proposed to use the finite element isoparametric idea to improve the acuracy of the previous method, that is to use

$$\begin{aligned} u &= Nu^e , \\ T &= NT^e , \\ x &= Nx^e , \end{aligned} \tag{2.37}$$

where N is the common set of interpolatory serendipity polynomial functions and u^e, T^e, x^e are, respectively, the displacements, tractions and coordinates of the points chosen to discretize the boundary. In addition, the same set of points is used to locate the fundamental solution. In this way, the rigidity of the method is balanced by the simplicity of the procedure. As soon as the user selects a degree for the interpolatory polynomial, and the collocation points have been selected, everything is fixed, and the method can be completely computerized.

It is important to notice that the fundamental solution is defined everywhere so that, although functions N are locally based, the matrices A and B will be full. Nevertheless, u^e, T^e and x^e retain a physical significance. On the other hand, a close look at A or B will show that these matrices need not be square.

Also worth noting is the fact that, when the body force $X \neq 0$, the last integral of Eq. (2.24) must be computed. In general, X will not follow any analytical law, so that the integral will have to be computed numerically along cells, as suggested by Fig. 3. However, there are important cases where, for the sake of elegance, this volume integral can be reduced to a boundary one. Imagine, for instance, that

$$X = \nabla \Phi , \tag{2.38}$$

i.e. the body forces are derived from a potential Φ. In this case

$$I = \int_\Omega X u^* = \int_\Omega u^* \nabla \phi . \tag{2.39}$$

Use of the identity

$$\nabla(\phi u^*) = u^* \nabla \phi + \phi \nabla u^* ,$$

or

$$u^* \nabla \phi = \operatorname{div}(\phi u^*) - \phi \operatorname{div} u^* , \tag{2.40}$$

in conjunction with the divergence theorem, transforms I of (2.39) into

$$I = \int_\Omega \operatorname{div}(\phi u^*) - \int_\Omega \phi \operatorname{div} u^* = \int_{\partial\Omega} \phi u^* \cdot n - \int_\Omega \phi \operatorname{div} u^* . \tag{2.41}$$

On the other hand, use of the Galerkin vector G for the representation of the fundamental solution by

$$u^* = \frac{1-2\nu}{2(1-\nu)} \operatorname{grad} \operatorname{div} \boldsymbol{G} - \operatorname{rot} \operatorname{rot} \boldsymbol{G} ,$$

or, because of

$$\nabla^2 \boldsymbol{G} = \operatorname{grad} \operatorname{div} \boldsymbol{G} + \operatorname{rot} \operatorname{rot} \boldsymbol{G}$$

by

$$\boldsymbol{u}^* = \nabla^2 \boldsymbol{G} - \frac{1}{2(1-\nu)} \operatorname{grad} \operatorname{div} \boldsymbol{G} , \tag{2.42}$$

in conjunction with the fact that $\operatorname{div}(\operatorname{rot}) = 0$, leads to

$$\operatorname{div} \boldsymbol{u}^* = \frac{1-2\nu}{2(1-\nu)} \nabla^2 (\operatorname{div} \boldsymbol{G}) . \tag{2.43}$$

If we take into account that (e.g. for three-dimensions)

$$\boldsymbol{G} = \frac{1+\nu}{4\pi E} \boldsymbol{re} , \tag{2.44}$$

and call

$$\boldsymbol{W} = \frac{(1-2\nu)(1+\nu)}{8\pi E(1-\nu)} \boldsymbol{re} , \tag{2.45}$$

then (2.43) becomes

$$\operatorname{div} \boldsymbol{u}^* = \nabla^2 (\operatorname{div} \boldsymbol{W}) = \nabla^2 H , \tag{2.46}$$

where

$$H = \operatorname{div} \boldsymbol{W} = \frac{(1-2\nu)(1+\nu)}{8\pi E(1-\nu)} (r_{,x} + r_{,y} + r_{,z}) . \tag{2.47}$$

Thus, the volume integral on the right-hand side of (2.41) takes the form

$$-\int_{\Omega} \phi \operatorname{div} \boldsymbol{u}^* = -\int_{\Omega} \phi \nabla^2 H , \tag{2.48}$$

or, upon using Green's theorem, the form

$$-\int_{\Omega} \phi \operatorname{div} \boldsymbol{u}^* = \int_{\partial\Omega} H \cdot \operatorname{grad} \phi \cdot \boldsymbol{n} - \int_{\partial\Omega} \phi \operatorname{grad} H \cdot \boldsymbol{n} - \int_{\Omega} H \nabla^2 \phi . \tag{2.49}$$

If the function ϕ satisfies the equation

$$\nabla^2\phi = k_0 , \tag{2.50}$$

where k_0 is a constant, then

$$\int_\Omega H\nabla^2\phi = k_0 \int_\Omega \operatorname{div} \boldsymbol{W} = k_0 \int_{\partial\Omega} \frac{\partial \boldsymbol{W}}{\partial \boldsymbol{n}} \tag{2.51}$$

and in view of (2.49) and (2.51), Eq. (2.41) yields

$$I = \int_{\partial\Omega} \phi \boldsymbol{u}^* \cdot \boldsymbol{n} - \int_{\partial\Omega} \phi \operatorname{grad} H \cdot \boldsymbol{n} - k_0 \int_{\partial\Omega} \frac{\partial \boldsymbol{W}}{\partial \boldsymbol{n}} \tag{2.52}$$

as presented by Rizzo and Shippy [97]. For the case of the self-weight, for instance $k_0 = 0$, while for the case of the centrifugal force, $k_0 = \rho\omega^2$, where ρ is the material density and ω is the angular velocity of the rotating body. A review type of article on the treatment of body forces in elasticity has been written by Danson [50].

2.6. *The indirect method*

The indirect boundary element method proceeds directly from the physical meaning of the fundamental solution on a heuristic basis. Only a brief description is given here. A full treatment of the indirect method can be found in Banerjee and Butterfield [17].

A unit load applied to the boundary at point Q produces displacements $\boldsymbol{u}$ and tractions $\boldsymbol{T}$ defined by

$$\begin{aligned} u_i(\mathrm{P}) &= U^*_{ij}(\mathrm{P}, \mathrm{Q}) e_j(\mathrm{Q}) , \\ T_i(\mathrm{P}) &= T^*_{ij}(\mathrm{P}, \mathrm{Q}) e_j(\mathrm{Q}) , \end{aligned} \tag{2.53}$$

and, thus, a fictitious load $\boldsymbol{t}(\mathrm{Q})$ continuously distributed along the boundary will produce

$$u_i(\mathrm{P}) = \int_{\partial\Omega} U^*_{ij}(\mathrm{P}, \mathrm{Q}) t_j(\mathrm{Q}) , \tag{2.54a}$$

$$T_i(\mathrm{P}) = \int_{\partial\Omega} T^*_{ij}(\mathrm{P}, \mathrm{Q}) t_j(\mathrm{Q}) , \tag{2.54b}$$

$$\mathrm{P} \in \Omega ; \mathrm{Q} \in \partial\Omega ,$$

When P is moved to the boundary, Eq. (2.54b) is transformed into

$$T_i(\mathrm{P}) = \tfrac{1}{2} t_i(\mathrm{P}) + \int_{\partial\Omega} T^*_{ij}(\mathrm{P}, \mathrm{Q}) t_j(\mathrm{Q}) \,, \tag{2.55}$$

while Eq. (2.54a) remains of the same form.

Provided that P is not a corner point, the two Eqs. (2.54a) and (2.55) can be used to repeat the discretization process described above for the direct BEM. In this way, the system:

$$\begin{aligned} \boldsymbol{u} &= \boldsymbol{A}\boldsymbol{t} \\ \boldsymbol{T} &= \boldsymbol{B}\boldsymbol{t} \end{aligned} \tag{2.56}$$

is applied to every collocation point around the boundary, where either $\boldsymbol{u}$ or $\boldsymbol{T}$ is known. After all conditions on $\boldsymbol{u}$ or $\boldsymbol{T}$ have been imposed, there results the system

$$\boldsymbol{F} = \boldsymbol{K}\boldsymbol{t} \tag{2.57}$$

from which the unknown fictitious distribution $\boldsymbol{t}$ can be evaluated. As soon as $\boldsymbol{t}$ is known around the boundary, Eq. (2.56) can be applied to those points where either $\boldsymbol{u}$ or $\boldsymbol{T}$ is needed.

It is possible to see that recovery of the main unknowns is done after an intermediate quantity $\boldsymbol{t}$ has been evaluated, and this is why the method is called "*indirect*" *in opposition to the* "*direct*" *one, where the basic unknowns are* directly incorporated into the system to be solved.

Of course, it is possible to use a distribution of $\boldsymbol{t}$ along a fictitious boundary, as several authors have proposed. In addition to complicating the data input, these methods seem to present several mathematical objections, the nature of which is out of context here.

It is also important to note the sensitivity of the results to sharp corners. This sensitivity has caused the trend to move towards the direct method.

2.7. *The displacement discontinuity method*

This interesting method is a special case of the indirect method, where the fundamental solution is substituted by an ingenious artifice, the opening or closure of fictitious cracks. The method is fully described in the works of Crouch [42–44], which the interested reader can consult for more details. Extension of the DDM to three dimensions has been reported by Dunbar and Anderson [54].

In summary, equations are established for the displacements and tractions along the given plane boundary of the form

$$\begin{aligned} u_i(\mathrm{P}) &= \sum B_{ij} D_j \,, \\ T_i(\mathrm{P}) &= \sum A_{ij} D_j \,, \end{aligned} \qquad i, j = 1, 2, \ldots, N \tag{2.58}$$

provoked by arbitrary displacements D_j given along N cracks distributed either on the boundary or outside it.

Equations (2.58) are applied at a series of N points where $\boldsymbol{u}$ or $\boldsymbol{T}$ is known, and from them, an equation of the form

$$\boldsymbol{F} = \boldsymbol{K}\boldsymbol{D} \tag{2.59}$$

can be established which, when solved, gives the values $\boldsymbol{D}$ inducing $\boldsymbol{u}$ and $\boldsymbol{T}$ along the boundary. Equation (2.58) can be applied now to the points where $\boldsymbol{u}$ and $\boldsymbol{T}$ are unknowns in order to obtain the final results.

2.8. Computational aspects

The most important computational aspects of the direct BEM are discussed in some detail in the next two sections dealing with two- and three-dimensional elastostatics. Thus, the use of linear elements and the treatment of corners are discussed in connection with two-dimensional problems, while the use of constant and higher-order elements as well as the computation of the influence matrices $\boldsymbol{A}$ and $\boldsymbol{B}$ are presented in connection with three-dimensional problems.

3. Plane problems

In this section, we shall present, from an elementary point of view, the steps needed to develop the BEM in plane-stress or plane-strain elastostatic problems. The essential boundary conditions will be on the displacements $\boldsymbol{u}$ and the natural ones on the tractions $\boldsymbol{T}$ of the two-dimensional body. After establishing the usual notions, we shall offer the computation of the influence matrices and present some simple examples.

3.1. Definitions and notations

As we indicated above, the main objective of the method is the computation of values taken by the basic variables at the boundary. The first noteworthy idea is that it is necessary to interpolate those variables both when they are data and when they are unknowns, in order to approximate their behavior by a finite number of "ad-hoc" functions.

In order to stabilize these ideas, consider the problem shown in Fig. 12 which deals with the stress analysis of the square disk ABCD. Along AB and CD, the displacements are known to be zero and the tractions are unknown, while along BC and DA, the situation is reciprocal.

In order to reduce the unknowns to a finite number, the quest for unknown values has been limited to a finite number $1, 2, \ldots, n$ of points. In addition, it is assumed that both displacements and tractions will be interpolated by "shape"

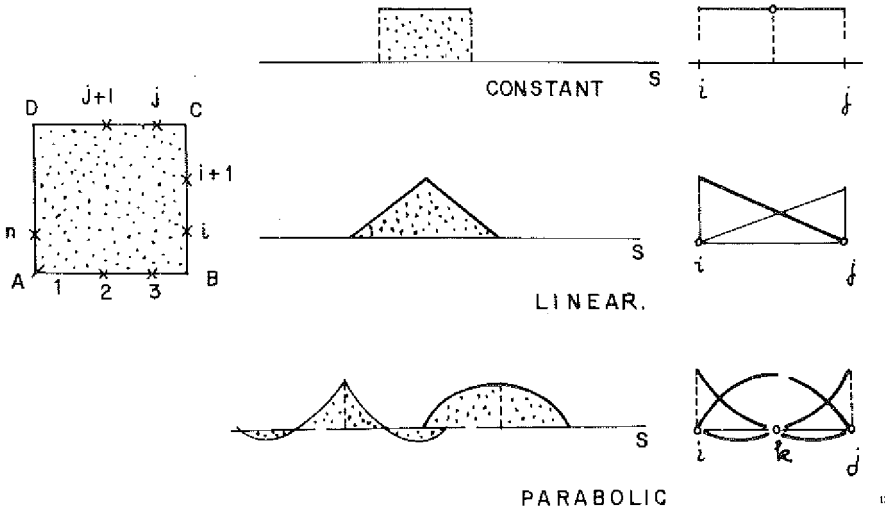

Fig. 12. Constant, linear and parabolic interpolation functions for boundary elements.

functions $N(i)$, $M(i)$, taking unit values in turn at each of the chosen points (nodes) and zero at the others, so that in an interpolation of the type

$$\begin{aligned} u &= a(i)\ N(i) \\ v &= b(i)\ N(i) \\ \bar{X} &= c(i)\ M(i) \\ \bar{Y} &= d(i)\ M(i) \qquad i = 1, 2, \ldots, n \end{aligned} \tag{3.1}$$

the $a(i)$, $b(i)$, $c(i)$, $d(i)$ will be the values taken by the components u, v, of $\boldsymbol{u}$ and the components $\bar{X}$ and $\bar{Y}$ of $\boldsymbol{T}$, respectively, at point i.

Figure 12 shows the constant, linear and parabolic interpolations with polynomials that are zero along important parts of the boundary, simplifying the above-mentioned idea of giving physical meaning to the coefficients.

As with the FEM, it can be seen that this type of interpolation generates the concept of "element" naturally, i.e. that zone of the boundary where the approximating shape is repeated. This allows the computations (basically integrations) to be done in a local sense and in a repetitive manner, which is ideal for a treatment by the computer.

The idea of geometrical approximation of the boundary also appears by interpolating among the points chosen to define the variables. That is

$$\begin{aligned} x &= x(i) \cdot R(i) \\ y &= y(i) \cdot R(i) \end{aligned} \qquad i = 1, 2, \ldots, n \tag{3.2}$$

where $R(i)$ are again locally based functions.

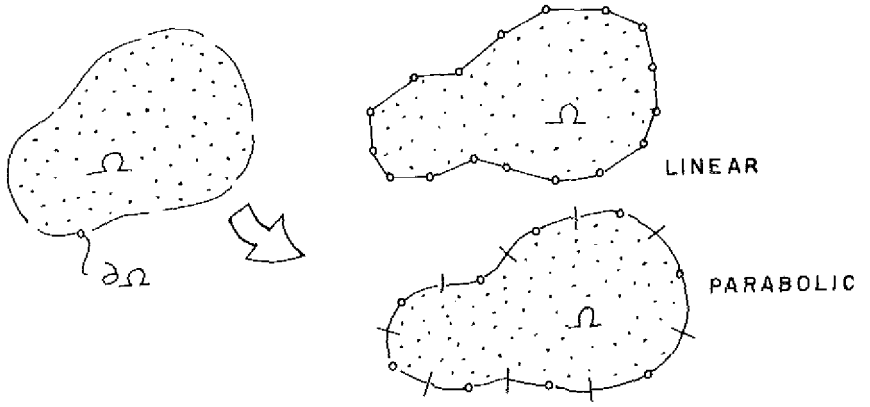

Fig. 13. Linear and parabolic isoparametric boundary element discretization of a plane domain.

In principle N, M and R are independent, but traditionally they are taken as equal, thus introducing the idea of isoparametric elements. So the analyst's first task is to discretize, that is to choose those boundary points which are going to guide the interpolation of variables and geometry (Fig. 13). After that, the method is limited to the procedure for determining the parameters $a(i)$, $b(i)$, $c(i)$, $d(i)$, which are unknown at the boundary. In general, there will be N unknowns so that N independent equations are needed. In the BEM they are obtained through the representation formula (2.26) of section 2, which must be applied as many times as necessary, as we shall see below.

3.2. Linear elements

The general analysis can be subdivided into the following steps:

(a) Selection of boundary elements (Fig. 14).

As usual, the mesh is refined in the areas with larger curvature where the variables could have higher gradients as shown in Fig. 14(a).

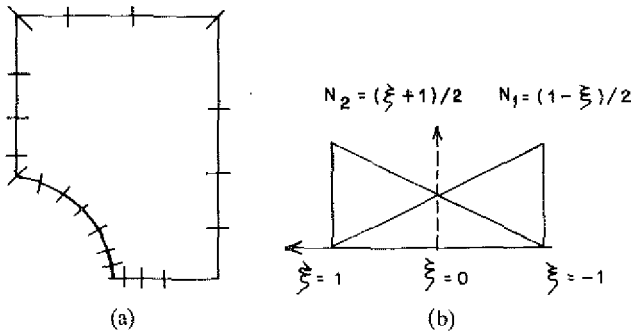

Fig. 14. Selection of size of boundary elements based on linear interpolation functions.

(b) Linear interpolation (Fig. 14).

Inside each element, both displacements and stresses are approximated by linear shape functions of the form

$$N_1(\xi) = -\tfrac{1}{2}(\xi - 1); \qquad N_2(\xi) = \tfrac{1}{2}(\xi + 1); \qquad \xi = s/L, \tag{3.3}$$

as shown in Fig. 14(b).

In general, it is assumed that the displacements are continuous along the boundary while it is necessary to allow discontinuous tractions around each sharp corner. The following analysis is based on the work of Alarcón et al. [2].

Using the notation of Fig. 15(c) and assuming that a subscript indicates "node" and a superscript "element", it is possible to write for element j

$$\boldsymbol{u} = \begin{Bmatrix} u \\ v \end{Bmatrix} = \begin{bmatrix} N_1 & N_2 & 0 & 0 \\ 0 & 0 & N_1 & N_2 \end{bmatrix} \begin{Bmatrix} u_j^j \\ u_{j+1}^j \\ v_j^j \\ v_{j+1}^j \end{Bmatrix} \tag{3.4a}$$

and

$$\boldsymbol{T} = \begin{Bmatrix} \boldsymbol{X} \\ \boldsymbol{Y} \end{Bmatrix} = \begin{bmatrix} N_1 & N_2 & 0 & 0 \\ 0 & 0 & N_1 & N_2 \end{bmatrix} \begin{Bmatrix} \boldsymbol{X}_j^j \\ \boldsymbol{X}_{j+1}^j \\ \boldsymbol{Y}_j^j \\ \boldsymbol{Y}_{j+1}^j \end{Bmatrix}. \tag{3.4b}$$

The general boundary integral equation (2.26) can be written now for every collocation point i as follows:

$$2c(i)\begin{Bmatrix} u_i \\ v_i \end{Bmatrix} + \sum_{j=1}^{N} L_j \begin{bmatrix} \int_{\partial\Omega_j} N_1 T_{11}^* & \int_{\partial\Omega_j} N_2 T_{11}^* & \int_{\partial\Omega_j} N_1 T_{12}^* & \int_{\partial\Omega_j} N_2 T_{12}^* \\ \int_{\partial\Omega_j} N_1 T_{21}^* & \int_{\partial\Omega_j} N_2 T_{21}^* & \int_{\partial\Omega_j} N_1 T_{22}^* & \int_{\partial\Omega_j} N_2 T_{22}^* \end{bmatrix} \begin{Bmatrix} u_j^j \\ u_{j+1}^j \\ v_j^j \\ v_{j+1}^j \end{Bmatrix}$$

$$= \sum_{j=1}^{N} L_j \begin{bmatrix} \int_{\partial\Omega_j} N_1 U_{11}^* & \int_{\partial\Omega_j} N_2 U_{11}^* & \int_{\partial\Omega_j} N_1 U_{12}^* & \int_{\partial\Omega_j} N_2 U_{12}^* \\ \int_{\partial\Omega_j} N_1 U_{21}^* & \int_{\partial\Omega_j} N_2 U_{21}^* & \int_{\partial\Omega_j} N_1 U_{22}^* & \int_{\partial\Omega_j} N_2 U_{22}^* \end{bmatrix} \begin{Bmatrix} \bar{X}_j^j \\ \bar{X}_{j+1}^j \\ \bar{Y}_j^j \\ \bar{Y}_{j+1}^j \end{Bmatrix} \tag{3.5}$$

where (u, v) and $(\bar{X}, \bar{Y})$ are the components of boundary displacements and

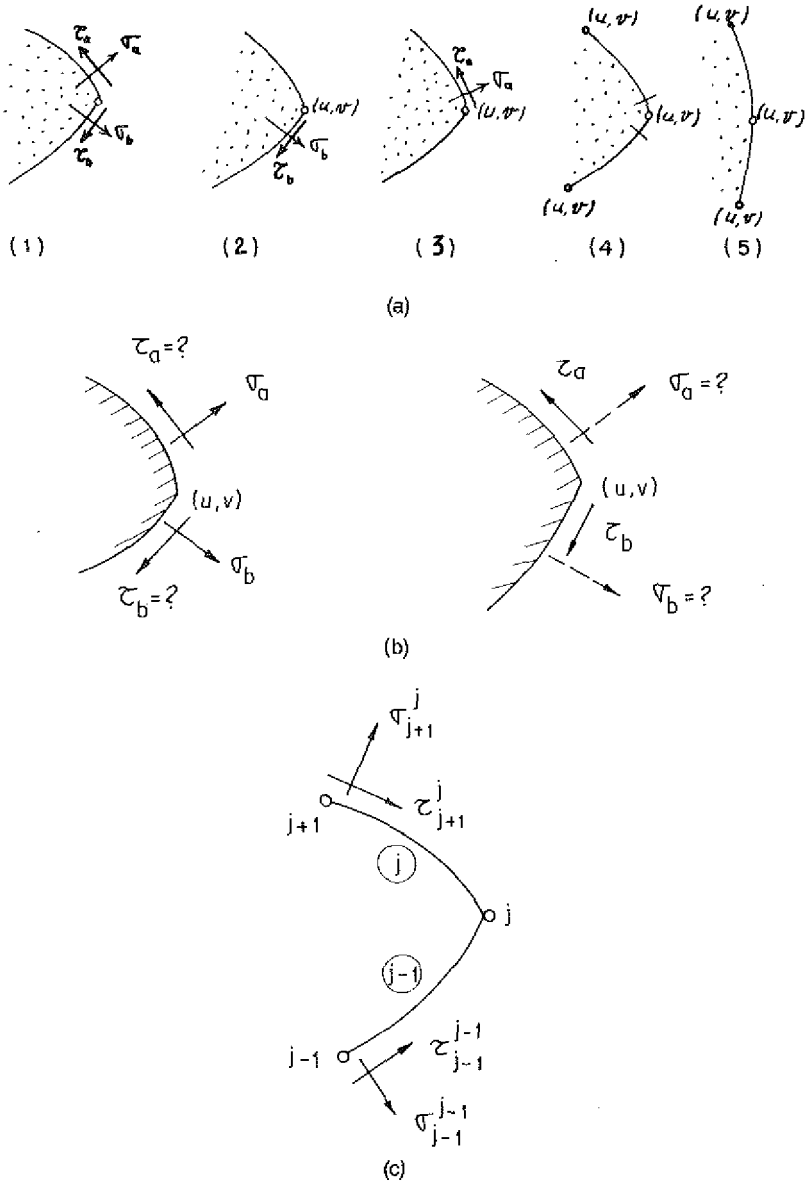

Fig. 15. Boundary condition cases at a corner.

tractions, respectively, in global coordinates and T^*_{ij}, U^*_{ij} are the components of the fundamental solution for stresses and displacements, respectively.

In general, it is more useful to express tractions as normal σ and tangential τ components. This can be done simply by using the transformation

$$\begin{Bmatrix} \sigma \\ \tau \end{Bmatrix}^e = \begin{bmatrix} \cos\alpha_e & \sin\alpha_e \\ -\sin\alpha_e & \cos\alpha_e \end{bmatrix} \begin{Bmatrix} \bar{X} \\ \bar{Y} \end{Bmatrix}, \tag{3.6}$$

where α_e is the angle between the x-axis and the unit normal vector to the element e.

Equation (3.5) can now be written in terms of σ and τ as

$$c(i)\begin{Bmatrix} u_i \\ v_i \end{Bmatrix} + \sum_{j=1}^{N} \begin{bmatrix} A_{11}^j & A_{12}^j & A_{13}^j & A_{14}^j \\ A_{21}^j & A_{22}^j & A_{23}^j & A_{24}^j \end{bmatrix} \begin{Bmatrix} u_j^j \\ u_{j+1}^j \\ v_j^j \\ v_{j+1}^j \end{Bmatrix}$$

$$= \sum_{j=1}^{N} \begin{bmatrix} B_{11}^j & B_{12}^j & B_{13}^j & B_{14}^j \\ B_{21}^j & B_{22}^j & B_{23}^j & B_{24}^j \end{bmatrix} \begin{Bmatrix} \sigma_j^j \\ \sigma_{j+1}^j \\ \tau_j^j \\ \tau_{j+1}^j \end{Bmatrix} \tag{3.7}$$

Varying i, one obtains from (3.7) a system of $2N$ equations of the form

$$\boldsymbol{Au} = \boldsymbol{B\sigma} \tag{3.8}$$

The scheme of contribution of each element is as follows:

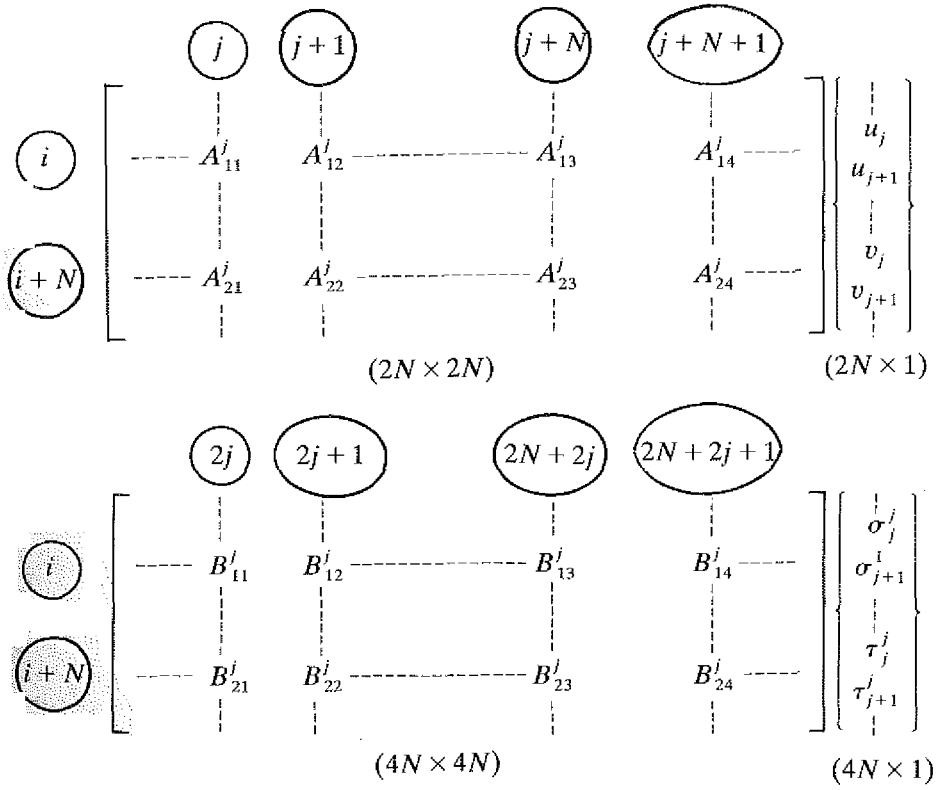

The double size of the stress vector $\boldsymbol{\sigma}$ is due to the double normal around each node. To proceed with the method, it is necessary now to establish conditions related to the continuity of the functions. This is done by identifying the different cases that can occur around a corner. The basic possibilities are those five included in Fig. 15(a) and having as follows:

(1) presents tractions which are specified at both sides of the corner with (u, v) remaining as local unknowns.

(2) presents a case where the data are the tractions before the node (σ_b, τ_b) and the node displacements (u, v). Two unknowns, the tractions after the node (σ_a, τ_a), remain.

(3) is the reciprocal of (2) with (σ_b, τ_b) as unknowns.

(4) deals with a sharp corner where there are four unknowns (σ_b, τ_b) and (σ_a, τ_a).

(5) is like (4) except that the boundary is smooth, with only one normal so that

$$\sigma_a = \sigma_b \,, \qquad \tau_a = \tau_b \tag{3.9}$$

reducing the unknowns to two.

It is also possible to imagine mixed combinations like those of Fig. 15(b) but there are always only two unknowns per node, except for case (4) above.

If there is no singularity at the sharp corner, this situation is easily solvable because knowing the derivatives of u and v along the boundary (computable since one knows the evolution of the data) allows the computation of their gradients at the corner and then the strains ε_{ij}. Using Hooke's material law, the stresses are obtained immediately so that the corner is completely solved. We are, in fact, facing a corner element in Fig. 15(c), where there are two nodes to collocate, namely $(j-1)$ and $(j+1)$ and four unknowns, namely the tractions "after" node $j-1$ and the tractions "before" node $j+1$. Another alternative can be seen in [2].

In that way, matrix $\boldsymbol{B}$ is reduced to size $2N \times 2N$ and after imposing boundary conditions, it is possible to reduce (3.8) to the system

$$\boldsymbol{KX} = \boldsymbol{F} \,. \tag{3.10}$$

For the sake of computing efficiency, the theoretical scheme described above has been slightly modified. Instead of forming $\boldsymbol{A}$ and $\boldsymbol{B}$ by rows, they are formed by columns; that is, in place of computing the integrals, viewing the elements from each node (implying the computation of normals, lengths, etc.), it is better to fix an element and to compute the contributions affecting each node. Another important aspect is the computation of the constants $c(i)$ by using a fictitious problem, i.e. by imagining rigid-body displacements which implies $\boldsymbol{\sigma} = 0$ and then imposing the condition of nullity for the sum of the row coefficients in $\boldsymbol{A}$. A more detailed description of a computer program called SERBA incorporating this approach can be seen in [2].

Figure 16 presents results obtained by Domínguez [52], using constant elements, while studying the distribution of stresses produced around rigid anchors modelled by a semirigid crack, when the anchor is near a free boundary.

An example with linear elements taken from [57] is plotted in Fig. 17, where a rectangular plate, fissured by a crack, is analyzed in order to determine the stress intensity factor. As it is shown, in spite of the fine mesh used near the singularity,

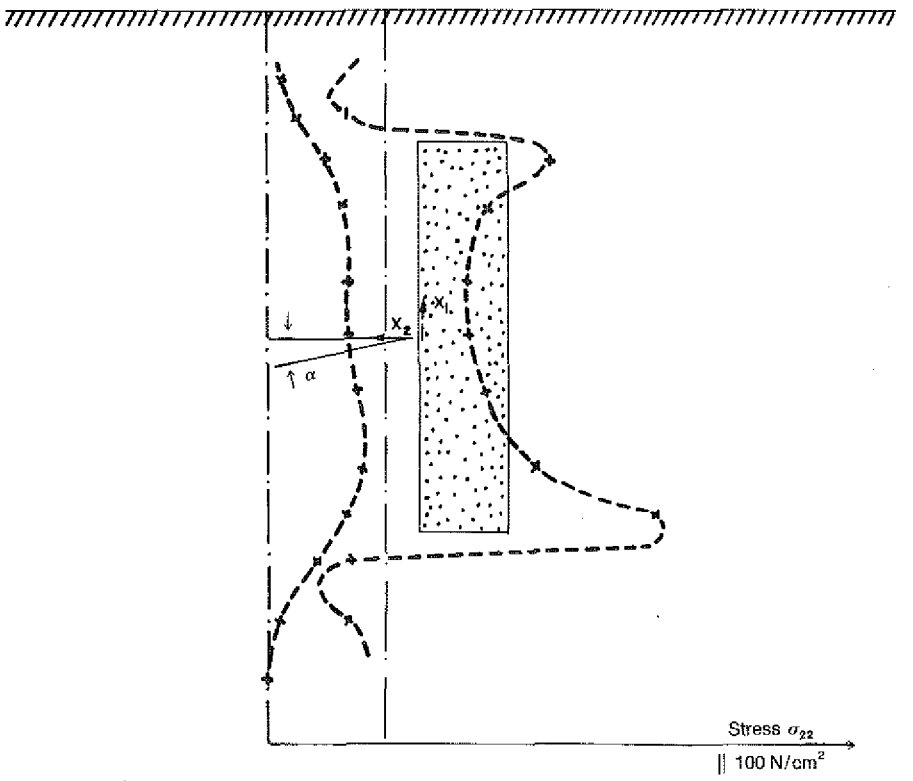

Fig. 16. Stress distribution around a rigid anchor near a free boundary.

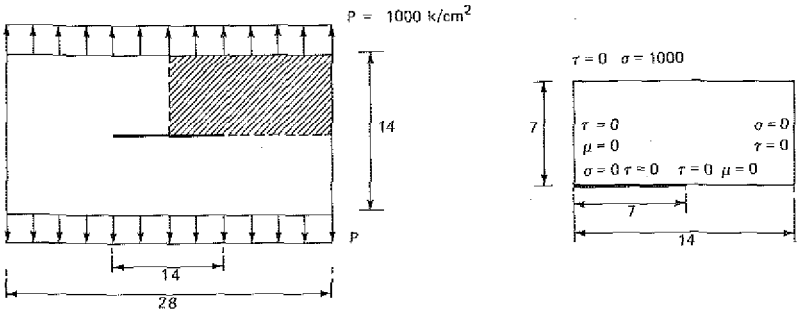

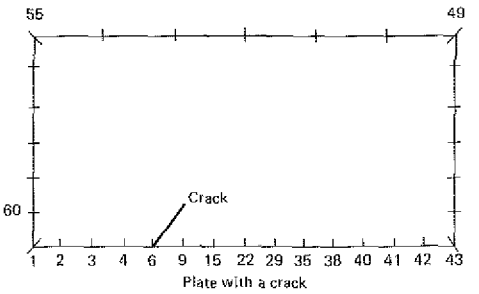

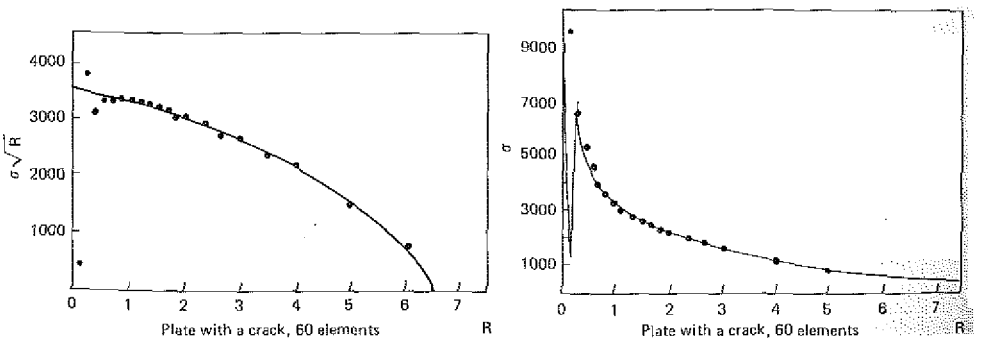

Fig. 17. Stress intensity factor for cracked rectangular plate.

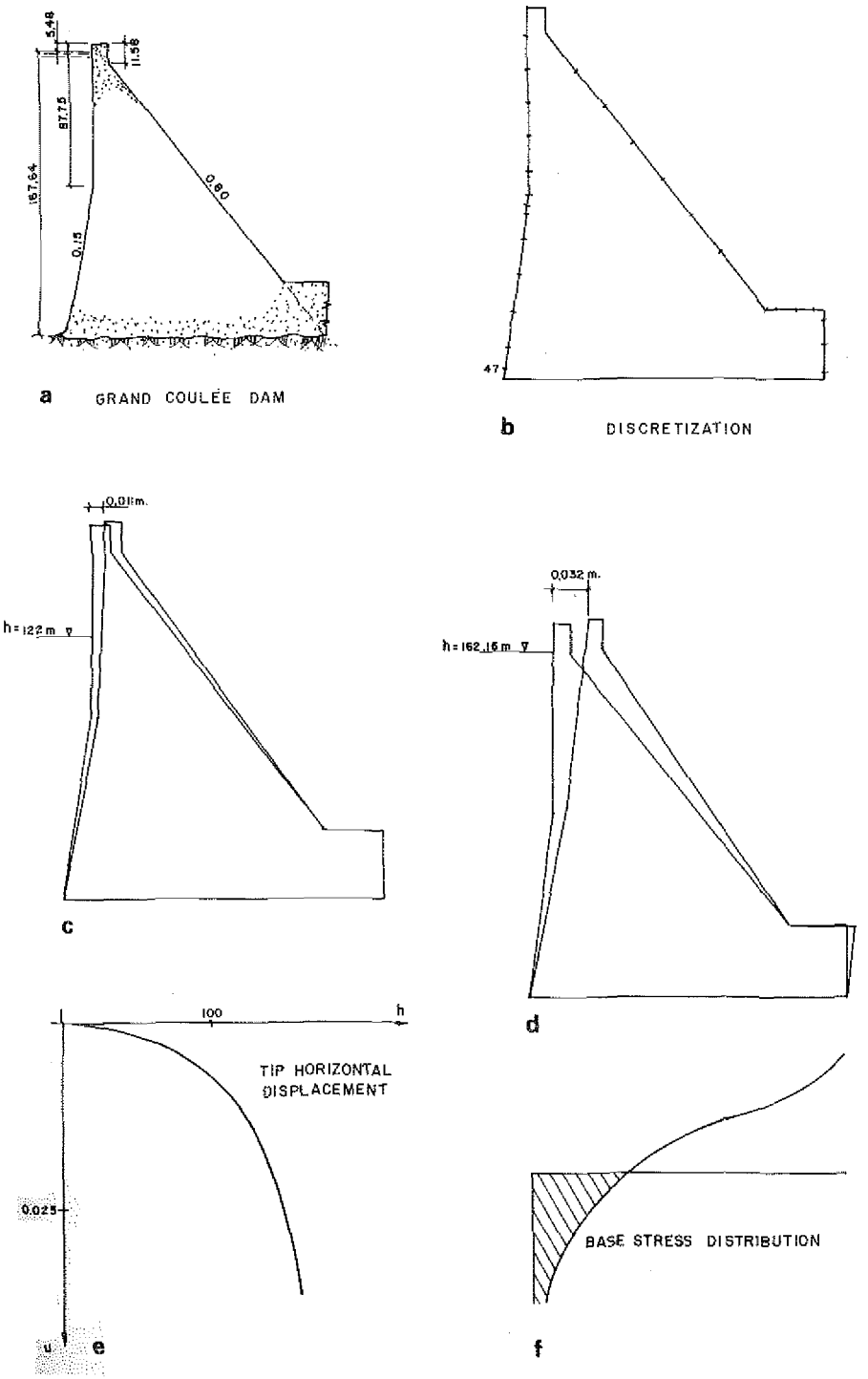

Fig. 18. Stress analysis of the Grand Coulee gravity dam.

there is contamination of results which can only be eliminated through interpolation of the results or by using singular elements.

Figure 18 is a classical example borrowed from civil engineering. It represents a simplified section of a famous gravity dam, the Grand Coulee dam. The general geometry is given in Fig. 18(a), while 18(b) presents the boundary element discretization. It is possible to observe that the mesh is finer near the sharp corner in order to take into account the higher gradients nearby. The base is assumed to be completely fixed against displacements so that, as Fig. 18(f) shows, there are singular points near the corners. Except for those points, the stresses follow the general pattern of the well known Levy's solution. The dashed zone represents tension areas. Figures 18(c) and (d) show the dam deformations for two different water levels, and Fig. 18(e) presents the evolution of the tip horizontal displacement as a function of the dam's degree of filling.

In Fig. 19(a) we have plotted the cross section of a reinforced concrete syphon

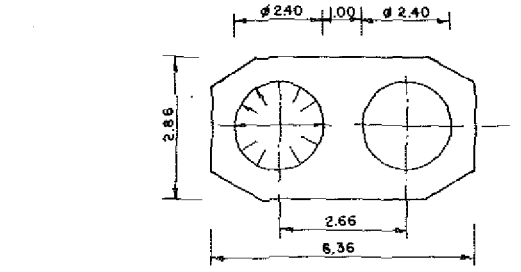

(a) SYPHON GEOMETRY AND DIMENSIONS

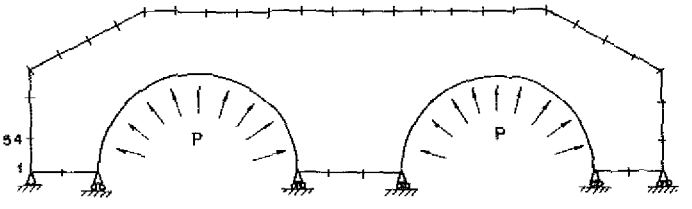

P=60T/m²

(b) DISCRETIZATION FOR INTERNAL PRESSURE

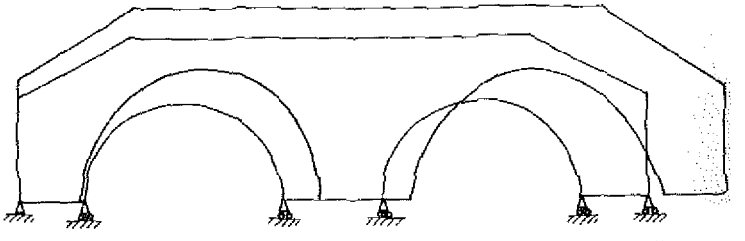

(c) DISPLACEMENTS FOR INTERNAL PRESSURE

Fig. 19. Deformation analysis of a reinforced concrete syphon under external and internal loads.

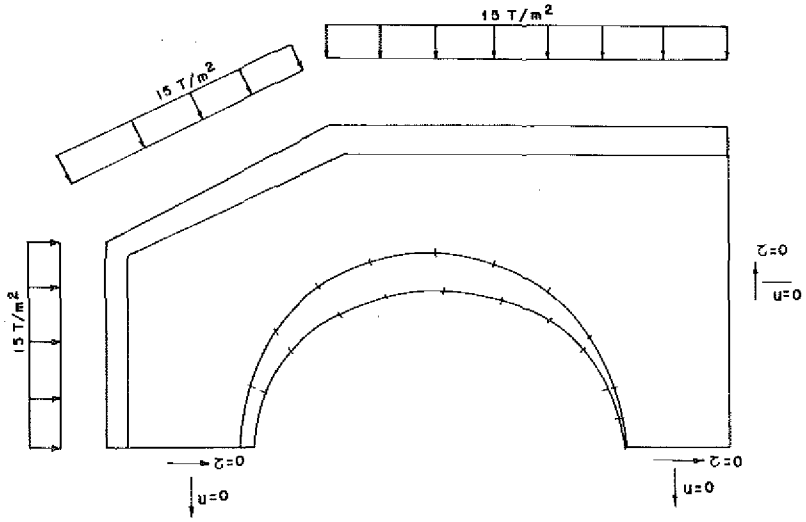

DISPLACEMENTS FOR EXTERNAL LOADS

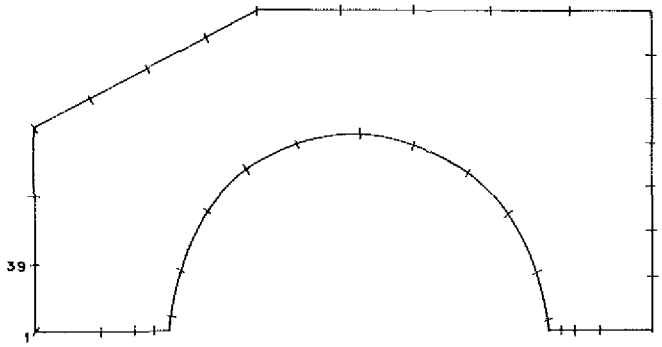

(d) DISCRETIZATION FOR EXTERNAL LOAD

Fig. 19. (continued).

designed to sustain an interior pressure equivalent to 6 m of water and working under an exterior pressure on the order of 15 m of water. In Fig. 19(b), we show the discretization used to analyze the boundary displacements under internal pressure. Due to the symmetry with respect to the horizontal axis, it is possible to analyze only half of the section. Of course, it would also be possible to establish a vertical axis of symmetry where both cavities are equally pressurized, but it has been decided to maintain only one axis in order to study the asymmetric situation. It is worth noting, then, that the model can suffer rigid-body horizontal displacements. In order to avoid this situation, node 1 has been completely fixed and so the displacements shown in Fig. 19(c) are relative to that point. It is possible to establish that condition in several ways. What we did here was to delete the first

row and column of the final matrix, substitute the diagonal elements by a 1 and changing the first element of the "force" vector to a zero [3]. As we can see, this is the classical solution used in similar situations with the FEM or the matrix analysis of beam structures. Figure 19(d) shows the discretization used for a totally symmetrical external load. In this case, there is no room for rigid-body displacements and the computation follows the usual patterns of the method.

4. Three-dimensional problems

In this section, we are going to develop some ideas related to three-dimensional geometry. If the domain presents a large ratio volume/surface, the economies that can be obtained, compared with other methods, are important.

After describing some typical problems, the simplest approach utilizing constant elements as well as some of the integration problems that arise, will be developed. We shall also indicate the treatment of higher-order elements and, finally, we shall show some examples, including the application of volume integrals to the thermoelastic case.

4.1. Typical problems

Typical problems are governed by Eq. (2.1) along with boundary conditions (2.5), (2.6), etc. In the majority of the cases, however, the situation is not strictly pure and even. Mixed conditions, can be artifically generated. In Fig. 20, for enstance, several different cases are presented for fan annular cylinder. Thus, in Fig. 20(b), the displacements are imposed along the internal and external boundaries, while in Fig. 20(c), the same happens with tractions, and Fig. 20(d) represents a mixed problem. Finally, in Figs. 20(e) and (f) we suggest the

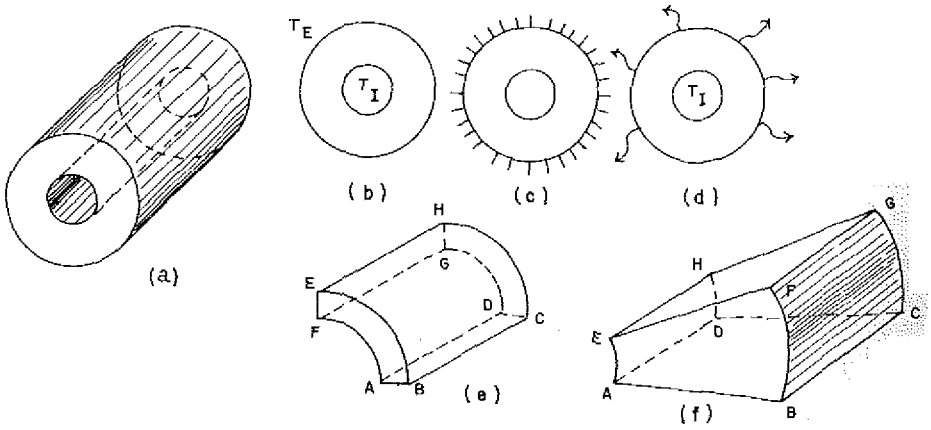

Fig. 20. Mixed boundary conditions for an annular cylinder.

possibility of using symmetry for the walls ABCD and EFGH to model mixed conditions of the type zero normal displacements plus zero tangential stresses thereby producing artificial mixed problems from the initial pure ones of Figs. 20(b, c). We shall show below that this situation can be managed in an automatic fashion while forming the matrix $\boldsymbol{K}$ of (2.36)

4.2. Boundary elements

Imagine for a moment that body forces are zero. The representation formula will then include variables defined only at the boundary where the discretization process has to be carried out. The "elements" are generated while interpolating with locally based functions. The simplest examples is obtained with "constant elements", i.e. plane facets where both displacements and stresses are assumed constant. In addition, the facets are taken to have triangular shapes and the representative points for displacements and stresses are taken at the centroid of every triangle as shown in Fig. 21(a).

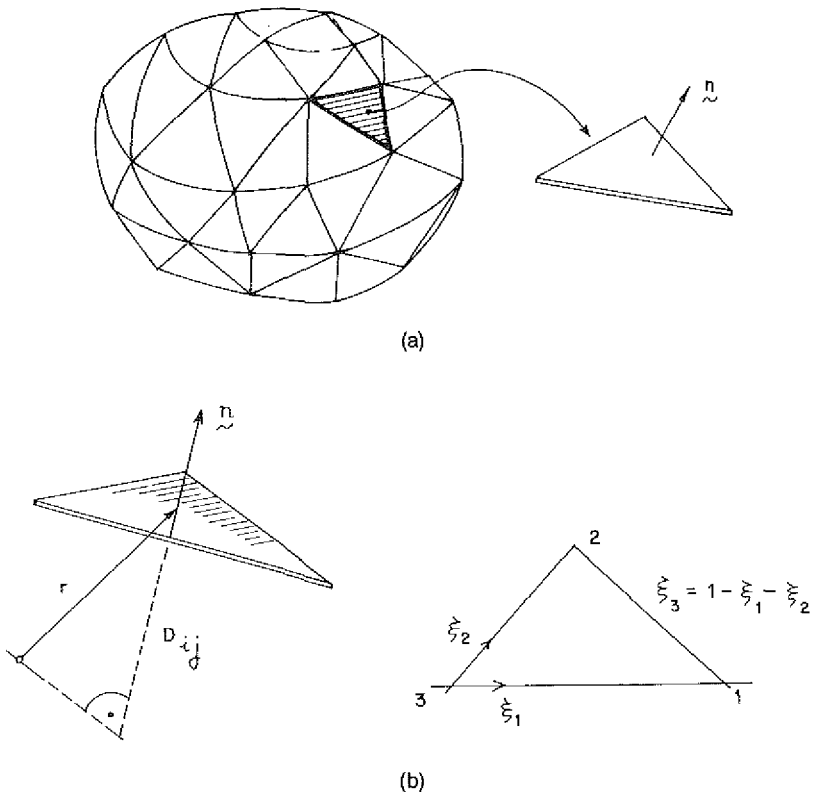

Fig. 21. Constant triangle boundary element discretization of a three-dimensional body.

The general boundary equation (2.26) then takes the form

$$\tfrac{1}{2}u_j(\boldsymbol{x}_L) + \sum_{K=1}^{N} \int_{\partial\Omega_K} T_{ji}(\boldsymbol{x}_L, \boldsymbol{x}_K) u_i(\boldsymbol{x}_K) = \sum_{K=1}^{N} \int_{\partial\Omega_K} U_{ji}(\boldsymbol{x}_L, \boldsymbol{x}_K) t_i(\boldsymbol{x}_K) , \qquad (4.1)$$

where $i, j = 1, 2, 3$; $K, L = 1, 2, \ldots, N$ and where $\boldsymbol{x}_L$ represents the collocation point and $\boldsymbol{x}_K$, the running point inside the element K.

If $u_i(\boldsymbol{x}_K)$ and $t_i(\boldsymbol{x}_K)$ are constant inside the element K

$$\begin{aligned} u_i(\boldsymbol{x}_K) &= u_i(K) , \\ t_i(\boldsymbol{x}_K) &= t_i(K) , \end{aligned} \qquad (4.2)$$

and the system of $3N$ equations

$$\tfrac{1}{2}u_j(\boldsymbol{x}_L) + \sum_{K=1}^{N} A_{ji}^{LK} u_i(K) = \sum_{K=1}^{N} B_{ji}^{LK} t_i(K) , \qquad (4.3)$$

is obtained from (4.1) where

$$\begin{aligned} A_{ji}^{LK} &= \int_{\partial\Omega_K} T_{ji}(\boldsymbol{x}_L, \boldsymbol{x}_K) , \\ B_{ji}^{LK} &= \int_{\partial\Omega_K} U_{ji}(\boldsymbol{x}_L, \boldsymbol{x}_K) , \end{aligned} \qquad (4.4)$$

and T_{ji}, U_{ji} are defined in Eq. (2.27). Equation (4.3) can be written in matrix form as

$$\boldsymbol{A}\boldsymbol{u} = \boldsymbol{B}\boldsymbol{t} . \qquad (4.5)$$

The integrals in (4.4) can be computed either numerically or analytically. The first procedure is implemented when the collocation point is outside the element (Fig. 21b). Change of coordinates from the global Cartesian (x_1, x_2, x_3) to the local triangular (ξ_1, ξ_2, ξ_3) ones according to the relation $\mathrm{d}x_1\,\mathrm{d}x_2\,\mathrm{d}x_3 = |J|\,\mathrm{d}\xi_1\,\mathrm{d}\xi_2\,\mathrm{d}\xi_3$ where $|J|$ is the Jacobian of the transformation, reduces the problem to the computation of the typical integral

$$I = \int_0^1 \int_0^{1-\xi_2} f(\xi_1\xi_2\xi_3)\,\mathrm{d}\xi_1\,\mathrm{d}\xi_2 = \sum_{i=1}^{n} w_i f(\xi_1^i \xi_2^i \xi_3^i), \qquad (4.6)$$

through a quadrature scheme involving a certain number of integration points $(\xi_1^i, \xi_2^i, \xi_3^i)$ and corresponding weights w_i [106]. A typical quadrature scheme is shown in Table 1 taken from refs. [118, 17].

Table 1
Integration points and weights for a typical quadrature scheme.

n	i	ξ_1^i	ξ_2^i	ξ_3^i	$2w_i$
1	1	1/3	1/3	1/3	1
2	1	1/2	1/2	0	1/3
	2	0	1/2	1/2	1/3
	3	1/2	0	1/2	1/3
4	1	1/3	1/3	1/3	−9/16
	2	3/5	1/5	1/5	25/48
	3	1/5	3/5	1/5	25/48
	4	1/5	1/5	3/5	25/48
7	1	0.33333333	0.33333333	0.33333333	0.22500000
	2	0.79742699	0.10128651	0.10128651	0.12593918
	3	0.10128651	0.79742699	0.10128651	0.12593918
	4	0.10128651	0.10128651	0.79742699	0.12593918
	5	0.05971587	0.47014206	0.47014206	0.13239416
	6	0.47014206	0.05971587	0.47014206	0.13239416
	7	0.47014206	0.47014206	0.05971587	0.13239416

When the point is inside the element, singularities appear in the fundamental solution. Then the integration is usually done analytically by subdividing the triangle into three parts as shown in Fig. 22 and taking the (ξ_1, ξ_2, ξ_3) to be the local coordinate system such that ξ_1 is parallel to the side 2–1 and with the same orientation, ξ_3 is normal to the element and $\xi_2 = \xi_3 \times \xi_1$. If

$$\xi_i = e_{ij} X_j \tag{4.7}$$

it is possible to show that

$$\begin{aligned} A_{ij}^{LK} &= A_{ij}|_1^2 + A_{ij}|_2^3 + A_{ij}|_3^1 , \\ B_{ij}^{LK} &= B_{ij}|_1^2 + B_{ij}|_2^3 + B_{ij}|_3^1 , \end{aligned} \tag{4.8}$$

and, for instance

$$\begin{aligned} A_{ij}|_1^2 &= \frac{1-2\nu}{8\pi(1-\nu)}\, \xi_{ijk} e_{1k} L(r+\xi_1)|_1^2 , \\ B_{ij}|_1^2 &= \frac{D}{16\pi G(1-\nu)} \left\{ (3-4\nu)\delta_{ij} L \left(\tan\phi + \frac{1}{\cos\phi} \right) + e_{1i} e_{1j} \right. \\ &\quad \times \left[-\sin\phi + L\left(\tan\phi + \frac{1}{\cos\phi} \right) \right] \\ &\quad \left. + e_{2i} e_{2j} \sin\phi - (e_{1i} e_{2j} + e_{2i} e_{1j}) \cos\phi \right\} \Big|_{\phi_1}^{\phi_2} , \end{aligned} \tag{4.9}$$

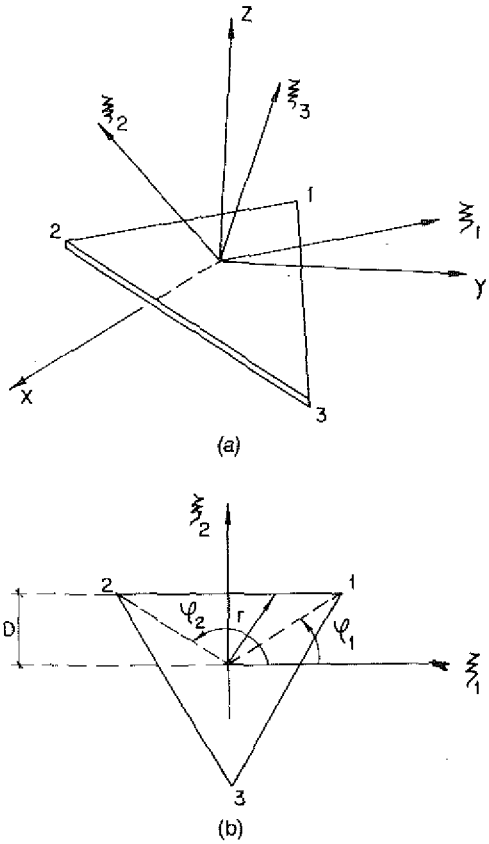

Fig. 22. Constant triangular boundary element with the collocation point inside the element.

where ξ_{ijk} is the permutation symbol.

Numerical integration in the presence of singularities is also possible [41].

4.3. *Volume integrals. Thermoelasticity*

As we stated in Eq. (2.38) and the following ones, in special cases it is possible to reduce volume integrals to boundary ones. An important case is thermoelasticity, where the body forces are proportional to the temperature Θ, which satisfies the steady-state heat conduction equation

$$\nabla^2\Theta = 0\,. \tag{4.10}$$

The volume integral due to these body forces becomes

$$-\gamma \int_{\partial\Omega} \Omega_j(x_L, x_K)\, \frac{\partial\Theta}{\partial n}\,(x_K) + \gamma \int_{\partial\Omega} \Theta(x_K)\, \frac{\partial\Omega_j}{\partial n}\,(x_L, x_K)\,, \tag{4.11}$$

where $\Omega_j = W_{,j}$ and $\gamma = \alpha G(1+\nu)/(1-\nu)$ with α being the coefficient of thermal expansion.

If the same constant elements are defined for the temperature, as for the displacements and stresses, (4.11) takes the form

$$\sum_{1}^{N}\left[-\gamma\frac{\partial\Theta(K)}{\partial n}\int_{\partial\Omega_K} W_{,j}(x_L, x_K) + \gamma\Theta(K)n_i^K\int_{\partial\Omega_K} W_{,ji}(x_L, x_K)\right], \tag{4.12}$$

or

$$-\gamma\sum_{K=1}^{N} C_j^{LK}\frac{\partial\Theta}{\partial n}(K) + \gamma\sum_{K=1}^{N} D_{ji}^{LK}n_i^K\Theta(K)\,, \tag{4.13}$$

with

$$\begin{aligned} C_j^{LK} &= \int_{\partial\Omega_K} W_{,j}(x_L, x_K)\,,\\ D_{ji}^{LK} &= \int_{\partial\Omega_K} W_{,ji}(x_L, x_K)\,. \end{aligned} \tag{4.14}$$

The computation of the C_j and D_{ji} elements is done analogously to that for the A and B matrices of (4.4), i.e.

$$\begin{aligned} C_j^{KK} &= C(1-2\nu)(I_{21} + I_{32} + I_{31})\,,\\ K_{ji}^{KK} &= C(1-2\nu)(I'_{21} + I'_{32} + I'_{31})\,, \end{aligned} \tag{4.15}$$

where, for instance

$$\begin{aligned} I_{12} &= D[\delta_{ij}L\tan(\phi/2) - e_{1i}e_{1j}(L\tan(\phi/2) + \cos\phi)\\ &\quad - (e_{1i}e_{2j} + e_{2i}e_{1j})\sin\phi + e_{2i}e_{2j}\cos\phi]\Big|_{\phi_1}^{\phi_2}\,,\\ I'_{12} &= \frac{D^3}{3}\left(-\frac{\cos\phi}{2\sin^2\phi} + \tfrac{1}{2}L\tan(\phi/2)\right)\Big|_{\phi_1}^{\phi_2}. \end{aligned} \tag{4.16}$$

The following example was developed by Anza [11] and deals with the thermoelastic analysis of cylinders and spheres subjected to different exterior and interior temperatures, as shown in Fig. 23. Using symmetry, discretization of the sphere can be simulated, for instance, by the mesh shown in Fig. 24(b). For the evolution of temperature, elements 1 to 48 have the zero flux condition while elements 49 to 56 are supposed to be maintained at fixed temperatures. In this example, the temperature data are

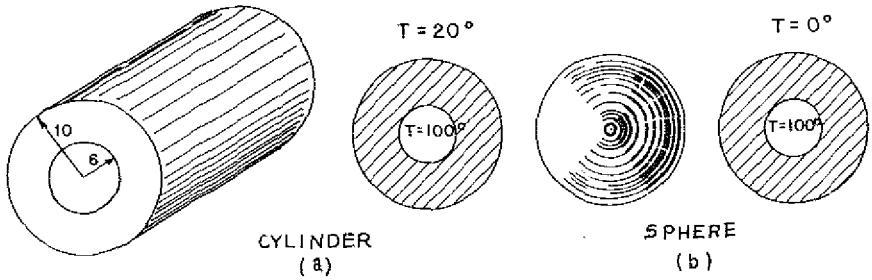

Fig. 23. Cylinder and sphere under different exterior and interior temperatures.

$$\Theta_{\text{int}} = 100^\circ, \qquad \Theta_{\text{ext}} = 0^\circ. \tag{4.17}$$

The elastic conditions are also imposed by the symmetry. Elements 1 to 48 present zero normal displacements and zero tangential stress, while elements 49 to 56 present known tractions (zero in this case). In addition, $\nu = 0.25$, $G = 1$, $\alpha = 1$. The closed-form solution of this problem in terms of the temperature Θ, the radial displacement u and the radial and hoop stresses σ_r and σ_θ, respectively, is given by

$$\begin{aligned}
&\Theta = 1800(1/r) - 100, \\
&u = -42.86r - 1500 - 69428.5(1/r^2), \\
&\sigma_r = 285.72 - 600(1/r) + 277713.9(1/r^3), \\
&\sigma_\theta = 285.71 - 3000(1/r^2) - 138857(1/r^3),
\end{aligned} \tag{4.18}$$

and it is plotted in Figs. 25(a, b and c) against the results obtained by the BEM. As we can see, the results are very good in a qualitative sense and the maximum error in displacements is of 4.7%. In general, the errors can be attributed to poor representation of the geometry. It is also important to point out that the example was chosen only to show the possibilities of the method. The symmetry conditions can be managed without elements 1 to 48 by a careful assembling of the A_{ij} and B_{ij} elements due to each element and all their symmetric ones. In this way, the number of equations could have been reduced and precision increased.

4.4. *Higher-order elements*

The method can easily be generalized to higher-order elements, for instance, to parabolic interpolation type of elements by shape functions which allow the adjustment by triangular or quadrilateral shells approaching complex geometry as shown in Fig. 26(a).

There are, nevertheless, problems with corner nodes that are similar to those

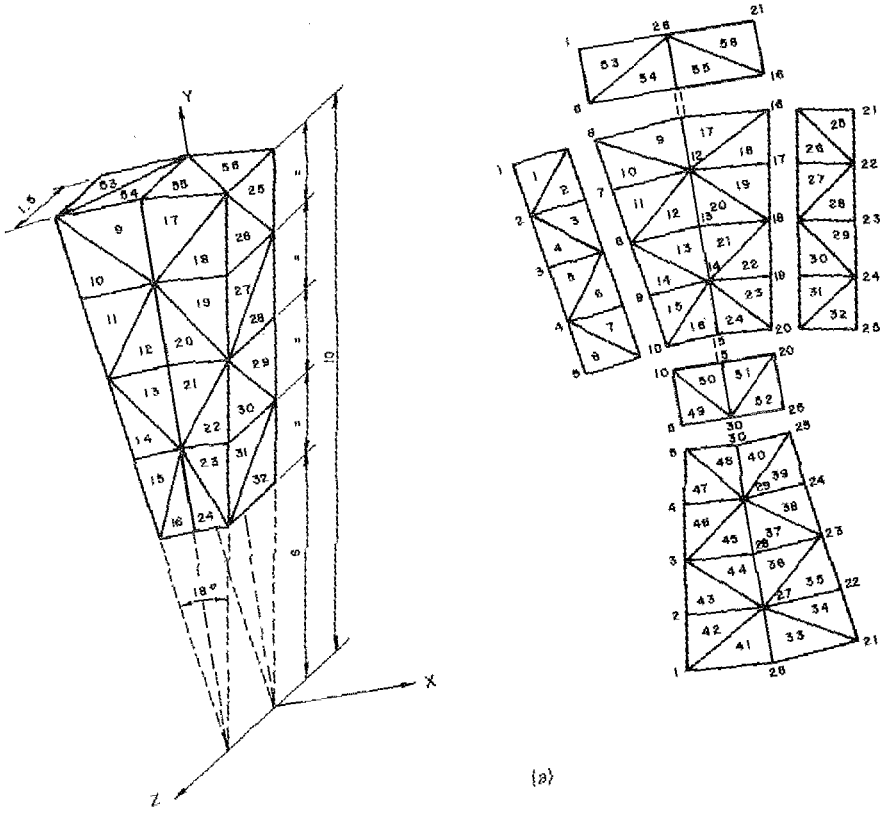

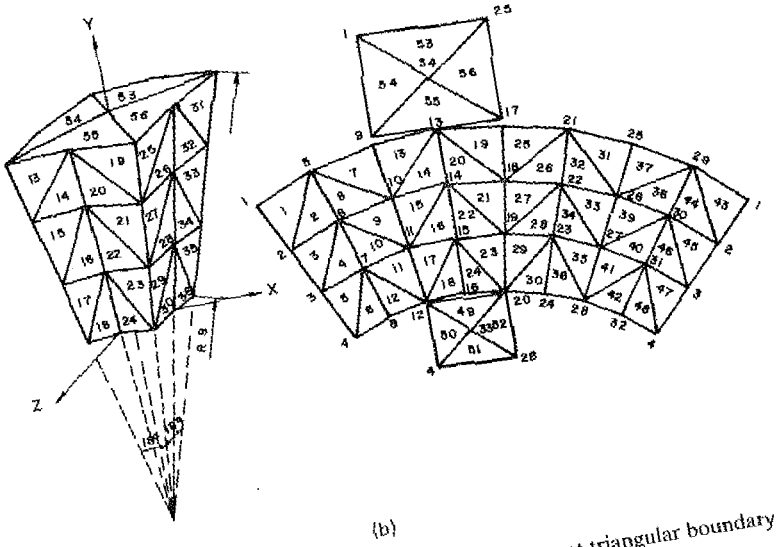

Fig. 24. Discretization of the cylinder and sphere of Fig. 23 by constant triangular boundary elements.

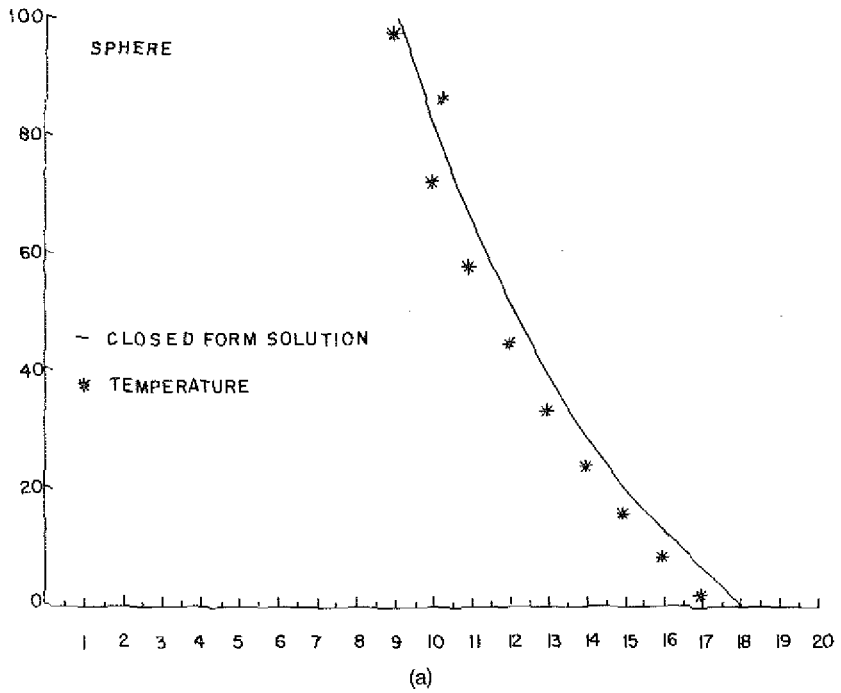

(a)

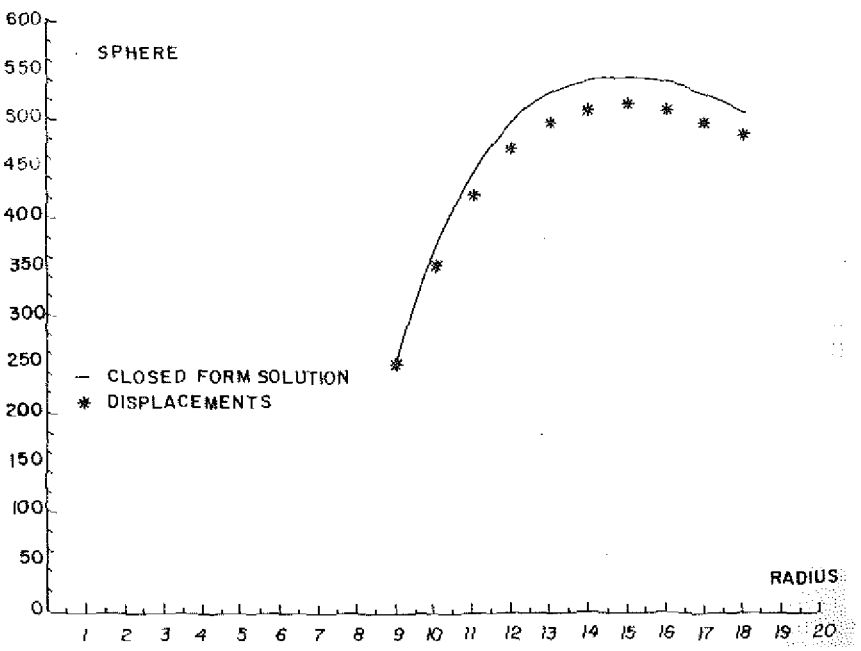

(b)

Fig. 25. Thermoelastic analysis results for the sphere of Fig. 23(b)

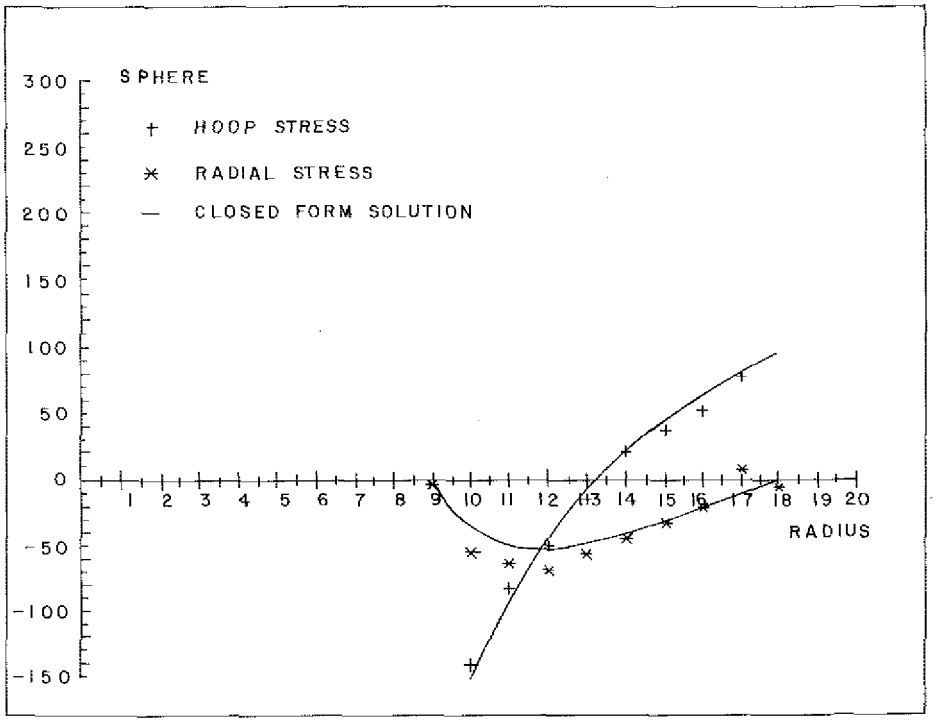

(c)

Fig. 25. (continued).

presented in plane problems. That is, for sharp corner nodes shared by different elements, there are different normals and hence different tractions which, in the assembling process, produce a rectangular $\boldsymbol{B}$ matrix. It is necessary, then, to supplement either a code or some artifice such as corner elements, master and slave degrees of freedom, etc., to eliminate the difficulty. That is why some authors prefer to define the elements by internal nodes (Fig. 4c) that eliminate the problem at the price of the size of the system of equations. The problem is really serious in piecewise heterogeneous media where it is usual to find singular behavior of fluxes or tractions.

The computation of the elements of each of the matrices $\boldsymbol{A}$, $\boldsymbol{B}$, cannot easily be done analytically because of the complexity of the Jacobian of the parabolic elements. For this reason, a numerical approach is usually followed. However, the singularity of kernels U_{ik} and T_{ik}, which tend to ∞ when r tends to zero, implies that the integration scheme needs to be done carefully while integrating over the elements near the collocation point in order to reduce the integration error. An adaptive process has been proposed by Lachat and Watson [74] which uses the standard Gaussian process, but divides each of the elements into a certain number of sub-elements and chooses the number of integration points for each of these sub-elements according to an error bound previously defined as a

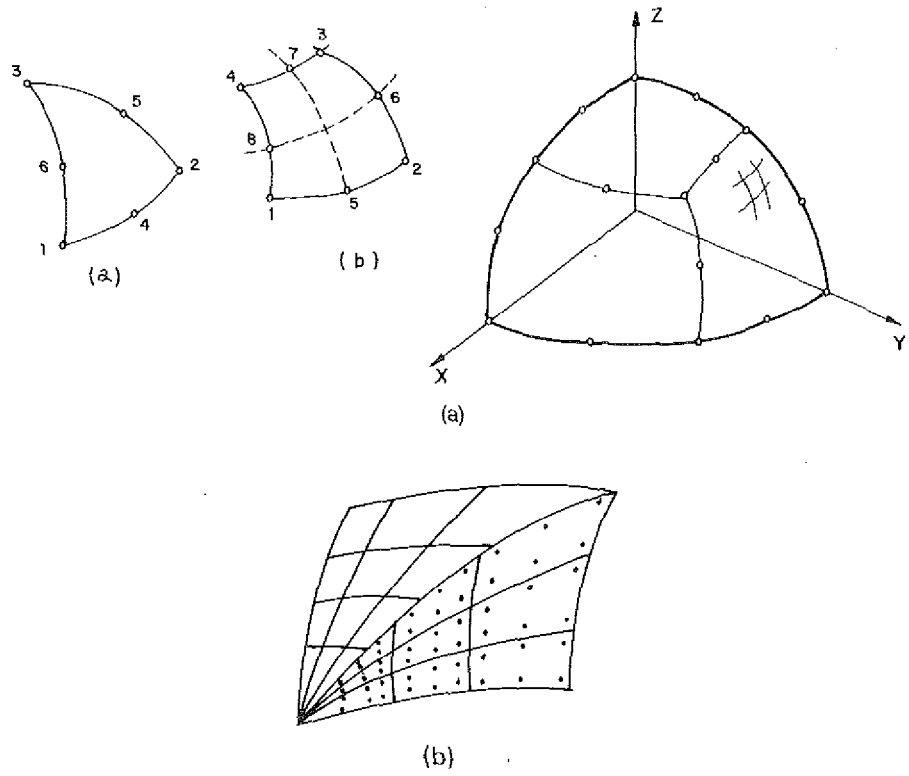

Fig. 26. Higher-order triangular and quadrilateral boundary elements.

function of some variables, as for example, the distance between the element and the singular point, the size, and the geometry of the element, etc. When the nodal point belongs to the integration element, a different approach is used in order to place a great number of integration points near the singular one. The element is divided into two or three triangles and each of them is considered as a degenerated quadrilateral sub-element. The disposition of integration points is shown in Fig. 26(b). More details can be seen in Doblaré and Alarcón [51]. Other alternatives are discussed by Watson [114] and by Rizzo and Shippy [98].

Once the equilibrium and compatibility equations have been introduced for the interface nodes, the complete linear system is reduced to a problem with $\sum_{r=1}^{R} p(r) \times 3$ equations where r is the total number of equations. However, the number of unknowns can be greater than the number of equations. This number of unknowns is $\sum_{i=1}^{I} 6p(i) + \sum_{c=1}^{R} 3p(c)$ where I is the number of interfaces and $p(i)$ and $p(c)$ are the number of nodes of each interface or subregion external boundary of the problem.

Two different problems arise during the formation of the linear system:

(a) To reduce the number of unknowns at interface nodes.

(b) To obtain a matrix structure adapted to the subsequent solving process, it is

possible to choose a structure which, by a systematic process of storage, allows an appropriate situation of the zeros in order to eliminate them during the storing process and, finally, an adequate disposition for the solving process.

The first point is treated by using a new interpolation function for the stress vector in the element to which the node with more unknowns than equations belongs. Each of these functions, with a lower order than the usual ones, takes the value 1 at each node and 0 at the rest, except for the special node. After this, it is possible to extrapolate the stress vector, as Fig. 27 shows, and obtain the expressions

$$t_i = a_{1i} + a_{2i}\xi + a_{3i}\eta + a_{4i}\xi^2 + a_{5i}\eta^2 + a_{6i}\eta^2\xi + a_{7i}\xi^2\eta$$
$$t_1 = t_4 + t_2 - t_3 . \tag{4.19}$$

The second point is resolved by following Lachat and Watson [74, 75] and ordering the subregions as in Fig. 28, thereby obtaining a great number of grouped zeros, which are not stored, and thus saving a lot of memory.

The following three illustrative examples of three-dimensional elastic analysis by parabolic isoprametric boundary elements have been taken from [51]. The first example deals with the analysis of a sphere subject to internal pressure. This has been solved and compared with the theoretical solution given in [112]. The sphere has an internal radius of 30 and an external radius of 110, consists of a material with a Young's modulus of 2.5 and Poisson's ratio of 0.25 and is subjected to an internal pressure of 1000. The discretization of 18 elements and 36 nodes is shown in Fig. 29 and a computer memory of only 6K was used in the program for the given data. The results in terms of the radial displacement u_r and the tangential stress σ_t are shown in Table 2. The total computer time needed was 24'50", which is very high. However, this is logical because the amount of time of input–output is very important in this case and the access time of the computer used was also very high.

Another typical test is that of a cube subjected to internal point loads. The problem consists of a simple cube supported at three different faces and subjected to two point loads of 1000 acting in the interior of the body as shown in Fig. 30(a).

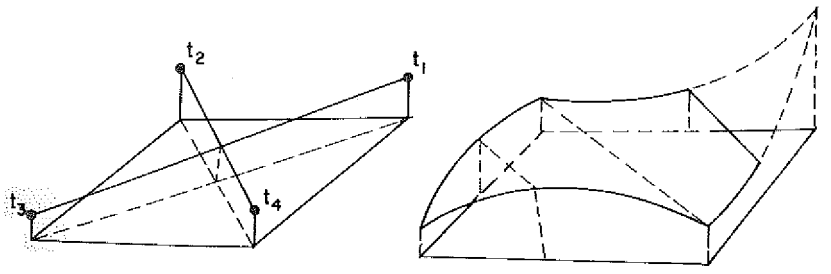

Fig. 27. Schematic illustration of a special stress vector interpolation.

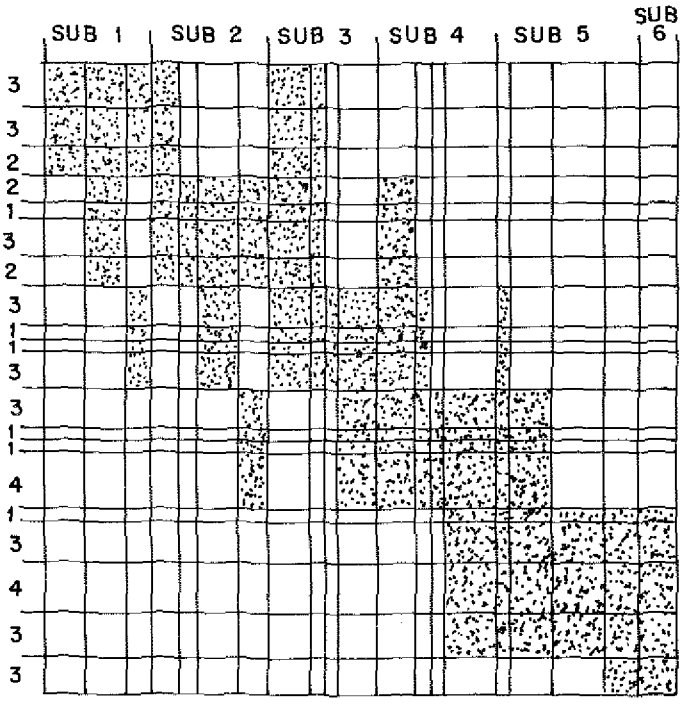

Fig. 28. Efficient ordering of subregions in the BEM.

The deformation of the cube can be seen in Fig. 30(b). Finally, as an example of the treatment of boundary conditions, the analysis of the dolos of Fig. 31(a) was also performed. The discretization of a quarter of the dolos is shown in Fig. 31(b) while the boundary conditions are such that the normal displacement restricted at the planes of symmetry, the tangential stresses are zero on them, and all the displacements for elements of the base are zero. The discretization presented was obtained using a preprocessor described in [36].

Table 2
Numerical results for the sphere of Fig. 29.

Node	Variable	Theory	BEM	Error %
1	u_r	6428.57	6401.0	−0.43
17	u_r	7164.72	7109.0	−0.78
23	u_r	8492.06	8406.0	−1.01
35	u_r	10928.57	10800.0	−1.17
41	u_r	15714.29	15590.0	−0.79
1	σ_t	214.29	207.5	−3.17
17	σ_t	249.48	250.9	0.57
23	σ_t	312.17	303.9	−2.65
35	σ_t	435.43	433.5	−0.44
41	σ_t	714.29	757.0	5.98

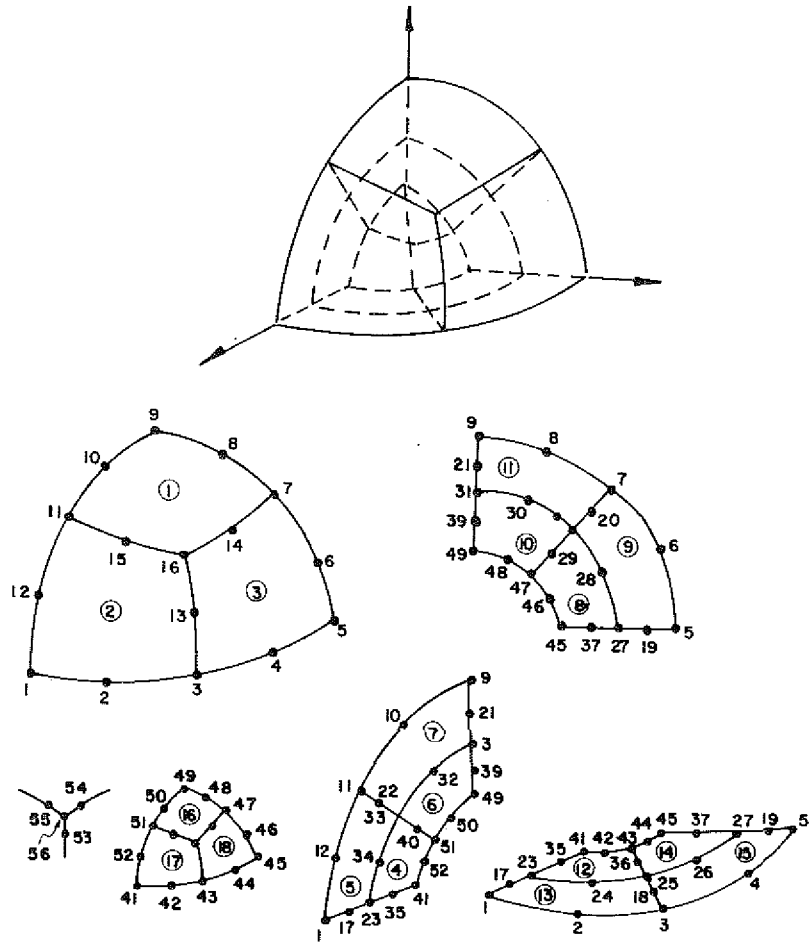

Fig. 29. Discretization of a sphere by parabolic isoparametric quadrilateral boundary elements.

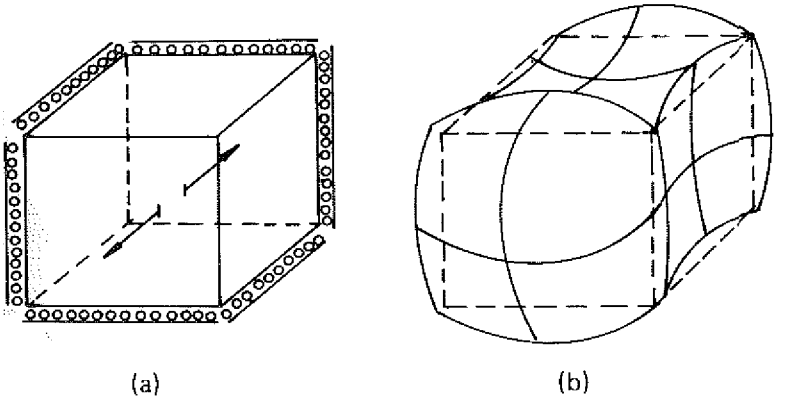

Fig. 30. Deformational configuration of a cube subjected to internal point loads.

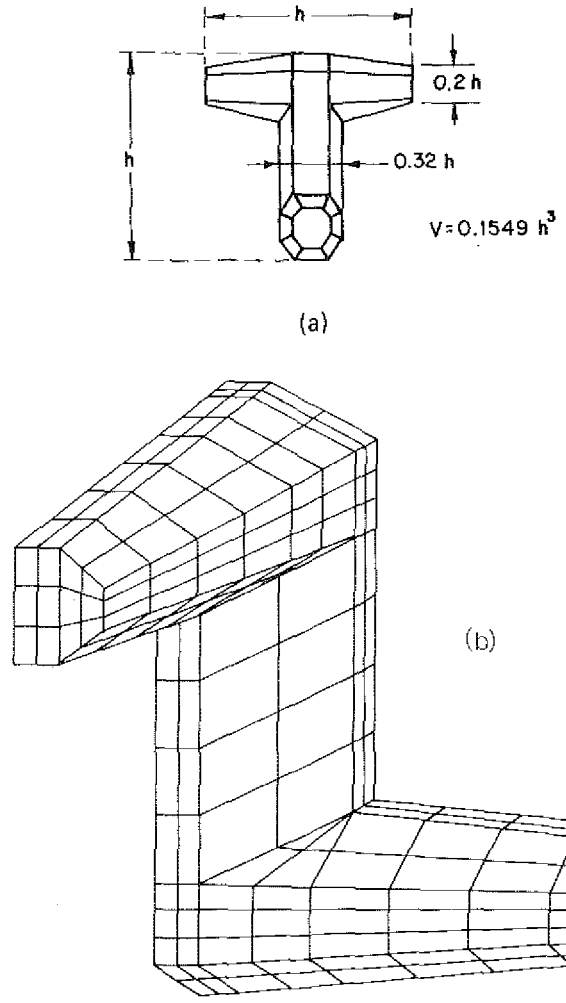

Fig. 31. Boundary element discretization of a dolos.

5. Axisymmetric problems

In this section, we shall consider those bodies whose geometry and load state have have axial symmetry (Fig. 32). The engineering applications are numerous, including, for example, rotating disks, bins, silos, reservoirs, etc.

5.1. The fundamental solution

The starting equation is Somigliana's integral equation 2.20, but now the matrices U^*_{ik}, T^*_{ik}, can be specialized by using a ring load like that in Fig. 33. A

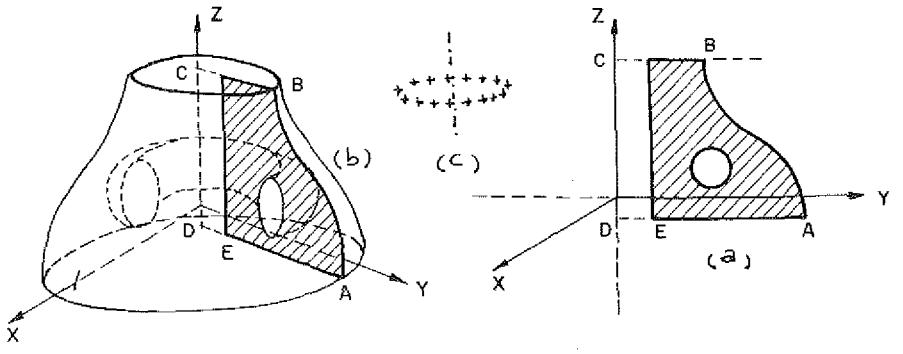

Fig. 32. Geometry of a general axisymmetric body.

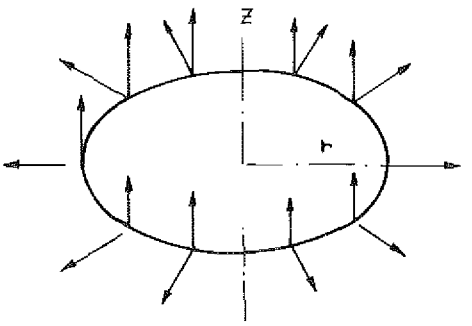

Fig. 33. Radial and axial unit concentrated loads.

current procedure for computing the fundamental solution is through the displacement function introduced by Galerkin [48, 70]. The subsequent analysis is based on the work of Cruse et al. [48]. In cylindrical coordinates, the components X_r and X_z of the Galerkin vector for a ring radial load F_r and an axial one F_z of the form

$$\begin{Bmatrix} F_r \\ F_z \end{Bmatrix} = \begin{Bmatrix} 1 \\ 1 \end{Bmatrix} \delta(R-r, Z-z)/2\pi r \tag{5.1}$$

satisfy the equations

$$\begin{aligned} &\left(\nabla^2 - \frac{1}{r^2}\right)\left(\nabla^2 - \frac{1}{r^2}\right) X_r = -\frac{F_r}{G}, \\ &\nabla^2\nabla^2 X_z = -\frac{F_z}{G}; \qquad \nabla^2 = \frac{\partial^2}{\partial r^2} + \frac{1}{r}\frac{\partial}{\partial r} + \frac{\partial^2}{\partial z^2}, \end{aligned} \tag{5.2}$$

The solution of (5.2) written in terms of the Legendre functions of zero order

$Q_{\pm 1/2}(\gamma)$ is

$$X_r = \frac{1}{12\pi^2 G}\sqrt{Rr}(\gamma Q_{1/2} - Q_{-1/2}),$$
$$X_z = \frac{-1}{4\pi^2 G}\sqrt{Rr}(Q_{1/2} - \gamma Q_{-1/2}), \tag{5.3}$$

where

$$\gamma = 1 + \frac{(R-r)^2 + (Z-z)^2}{2Rr}, \tag{5.4}$$

and where R, Z are the coordinates of the point of application of the load and r, z those of the running point.

The expressions for U^*_{ij} are as follows [48]:

$$2(1-\nu)U^*_{rr} = (1-2\nu)\left(\nabla^2 - \frac{1}{r^2}\right)X_r + \frac{\partial^2 X_r}{\partial z^2},$$
$$2(1-\nu)U^*_{zr} = -\frac{\partial^2 X_z}{\partial r \partial z} - \frac{1}{r}\frac{\partial X_r}{\partial z},$$
$$2(1-\nu)U^*_{rz} = -\frac{\partial^2 X_z}{\partial r \partial z}, \tag{5.5}$$
$$2(1-\nu)U^*_{zz} = (1-2\nu)\nabla^2 X_z + \frac{\partial^2 X_z}{\partial r^2} + \frac{1}{r}\frac{\partial X_z}{\partial r},$$

or in view of (5.3)

$$U^*_{rr} = \frac{1}{16\pi^2 G(1-\nu)\sqrt{Rr}}\left((3-4\nu)Q_{1/2} + \frac{(Z-z)^2}{Rr}\frac{\mathrm{d}Q_{1/2}}{\mathrm{d}\gamma}\right),$$
$$U^*_{zr} = \frac{1}{16\pi^2 G(1-\nu)}\frac{Z-z}{r\sqrt{Rr}}\left[\frac{Q_{1/2}}{2} - \left(\gamma - \frac{r}{R}\right)\frac{\mathrm{d}Q_{+1/2}}{\mathrm{d}\gamma}\right],$$
$$U^*_{rz} = \frac{-1}{16\pi^2 G(1-\nu)}\frac{Z-z}{r\sqrt{Rr}}\left[\frac{Q_{-1/2}}{2} + \left(\gamma - \frac{r}{R}\right)\frac{\mathrm{d}Q_{-1/2}}{\mathrm{d}\gamma}\right], \tag{5.6}$$
$$U^*_{zz} = \frac{1}{16\pi^2 G(1-\nu)\sqrt{Rr}}\left((3-4\nu)Q_{-1/2} - \frac{(Z-z)^2}{Rr}\frac{\mathrm{d}Q_{-1/2}}{\mathrm{d}\gamma}\right)$$

The computation of T^*_{ik} is obtained using the equilibrium equations

$$T^*_{rr} = \sigma^*_{rrr}n_r + \sigma^*_{rzr}n_z,$$
$$T^*_{zr} = \sigma^*_{rzr}n_r + \sigma^*_{zzr}n_z,$$
$$T^*_{rz} = \sigma^*_{rrz}n_r + \sigma^*_{rzz}n_z, \tag{5.7}$$
$$T^*_{zz} = \sigma^*_{rzz}n_r + \sigma^*_{zzz}n_z,$$
$$T^*_{\theta r} = 0; \qquad T^*_{\theta z} = 0,$$

where

$$\sigma^*_{rrr} = 2G\left[\frac{1-\nu}{1-2\nu}\frac{\partial U^*_{rr}}{\partial r} + \frac{\nu}{1-2\nu}\left(\frac{1}{r}U^*_{rr} + \frac{\partial U^*_{zr}}{\partial z}\right)\right],$$

$$\sigma^*_{rzr} = G\left[\frac{\partial U^*_{rr}}{\partial z} + \frac{\partial U^*_{zr}}{\partial r}\right],$$

$$\sigma^*_{zzr} = 2G\left[\frac{1-\nu}{1-2\nu}\frac{\partial U^*_{zr}}{\partial r} + \frac{\nu}{1-2\nu}\left(\frac{1}{r}U^*_{rr} + \frac{\partial U^*_{rr}}{\partial r}\right)\right],$$

$$\sigma^*_{rrz} = 2G\left[\frac{1-\nu}{1-2\nu}\frac{\partial U^*_{rz}}{\partial r} + \frac{\nu}{1-2\nu}\left(\frac{1}{r}U^*_{rz} + \frac{\partial U^*_{zz}}{\partial z}\right)\right], \tag{5.8}$$

$$\sigma^*_{rzz} = G\left(\frac{\partial U^*_{rz}}{\partial z} + \frac{\partial U^*_{zz}}{\partial r}\right),$$

$$\sigma^*_{zzz} = 2G\left[\frac{1-\nu}{1-2\nu}\frac{\partial U^*_{zz}}{\partial z} + \frac{\nu}{1-2\nu}\left(\frac{1}{r}U^*_{rz} + \frac{\partial U^*_{zz}}{\partial z}\right)\right].$$

5.2. Displacements and stresses on the boundary

The reduction to the boundary is done by transporting $x(R, Z)$ to the boundary by a standard limiting process. When $x(R, Z) \to x(r, z)$, we have that $\gamma \to 1$ and the Legendre functions can be approximated by logarithmic functions of the type

$$Q_{-1/2}(\gamma) \simeq -\tfrac{1}{2}\ln\left(\frac{\gamma-1}{32}\right), \qquad Q_{1/2}(\gamma) \simeq -\tfrac{1}{2}\ln\left(\frac{\gamma-1}{32}\right) - 2, \tag{5.9}$$

with derivatives

$$\frac{\mathrm{d}Q_{1/2}}{\mathrm{d}\gamma} = \frac{\mathrm{d}Q_{-1/2}}{\mathrm{d}\gamma} = \frac{-1}{2(\gamma-1)}, \tag{5.10}$$

and then the integrals must be computed in the sense of their Cauchy principal value. The final boundary integral equation is then

$$(\delta_{ik} - C_{ik})u_i(x) = \int_{\partial\Omega} U^*_{ik}(x, y)t_i(y) - \int_{\partial\Omega} T^*_{ik}(x, y)u_i(y) + \int_{\Omega} U^*_{ik}(x, z)X_i(z),$$

$$x, y \in \partial\Omega; z \in \Omega, \tag{5.11}$$

and the stress components can be obtained from

$$\sigma_{ij}(x) = \int_{\partial\Omega} D^*_{ijk}t_k - \int_{\partial\Omega} S^*_{ijk}u_k + \int_{\Omega} S^*_{ijl}X_l, \tag{5.12}$$

where

$$D^*_{ijk} = \lambda U^*_{lk,l}\delta_{ij} + G(U^*_{lj,i} + U^*_{jk,i}),$$
$$S^*_{ijk} = \lambda T^*_{lk,l}\delta_{ij} + G(T^*_{ik,j} + T^*_{jk,i}). \tag{5.13}$$

5.3. Discretization and treatment of the integral equation

As the discretization is limited to the meridian curve, it is possible to use constant, linear, parabolic, etc., elements as shown in Fig. 34.

If the constant element approach is used and the procedure developed in section 2.5 is applied, it is possible to write (5.11) in the form

$$\tfrac{1}{2}\delta_{ik}u_i = \sum_{i=1}^{N}\left[\int_{\partial\Omega} U_{ik}^{*}t_i\,\mathrm{d}s - \int_{\partial\Omega} T_{ij}^{*}u_i\,\mathrm{d}s + \int_{\partial\Omega} E_{ik}^{*}X_i\,\mathrm{d}s + \int_{\partial\Omega} F_k\,\mathrm{d}s\right], \quad (5.14)$$

where the E_{ik}^{*}, F_k represent the contribution of volumetric forces reducible to the boundary, or

$$\begin{aligned}\tfrac{1}{2}\begin{Bmatrix} u_r \\ u_z \end{Bmatrix} = \sum_{n=1}^{N}\Bigg[&\int_{\partial\Omega_n}\begin{bmatrix} U_{rr}^{*} & U_{zr}^{*} \\ U_{rz}^{*} & U_{zz}^{*}\end{bmatrix}\begin{Bmatrix} t_r \\ t_z\end{Bmatrix}_{(\text{centroid})_n} \\ &- \int_{\partial\Omega_n}\begin{bmatrix} T_{rr}^{*} & T_{zr}^{*} \\ T_{rz}^{*} & T_{zz}^{*}\end{bmatrix}\begin{Bmatrix} u_r \\ u_z\end{Bmatrix}_{(\text{centroid})_n} \\ &+ \int_{\partial\Omega_n}\begin{bmatrix} E_{rr}^{*} & E_{zr}^{*} \\ E_{rz}^{*} & E_{zz}^{*}\end{bmatrix}\begin{Bmatrix} X_r \\ X_z\end{Bmatrix}_{(\text{centroid})_n} + \int_{\partial\Omega_n}\begin{Bmatrix} F_r \\ F_z\end{Bmatrix}\mathrm{d}s_n\Bigg], \end{aligned} \quad (5.15)$$

which will produce a $2N \times 2N$ system, once $2N$ boundary conditions have been fixed.

Following Eq. (5.12), the stresses are then

$$\begin{aligned}\sigma_{ij} = \sum_{n=1}^{N}\Bigg[&\int_{\partial\Omega_n} D_{ijk}t_k\,\mathrm{d}s_n - \int_{\partial\Omega_n} S_{ijk}u_k\,\mathrm{d}s_n \\ &+ \frac{1-2\nu}{2(1-\nu)}\int_{\partial\Omega_n}[X_kH_{ij} - H_{ijk}X_{k,k}]n_k - \int_{\partial\Omega_n} X_kI_{ijk}\,\mathrm{d}s_n\Bigg], \end{aligned} \quad (5.16)$$

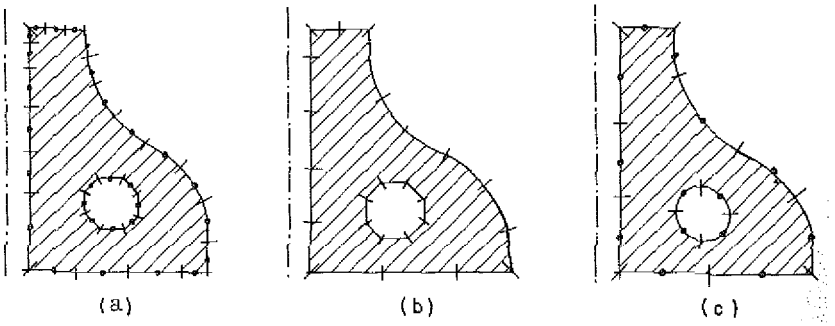

Fig. 34. Constant, linear and parabolic boundary element discretization of an axisymmetric body

where the new tensors appear after substituting the expressions of the previously mentioned volumetric forces reducible to the boundary.

Thus, finally, Eqs. (5.15) and (5.16) can be written symbolically as

$$\begin{aligned} \boldsymbol{Bu} &= \boldsymbol{At} + \boldsymbol{P} , \\ \boldsymbol{\sigma} &= \boldsymbol{Dt} - \boldsymbol{Su} + \boldsymbol{P}' . \end{aligned} \tag{5.17}$$

For the computation of the coefficients in the influence matrices, two cases are usually distinguished:

(a) If the running point does not coincide with the collocation point, computation of the coefficients is carried out by a Gauss quadrature as

$$\int_{\partial\Omega_m} f \, \mathrm{d}S_m = \int_{-L/2}^{L/2} 2rf \, \mathrm{d}l = \int_{-1}^{1} 2\pi rfL/2 \, \mathrm{d}\xi = L \sum_{k=1}^{N} w_k r(\xi_k) f(\xi_k) . \tag{5.18}$$

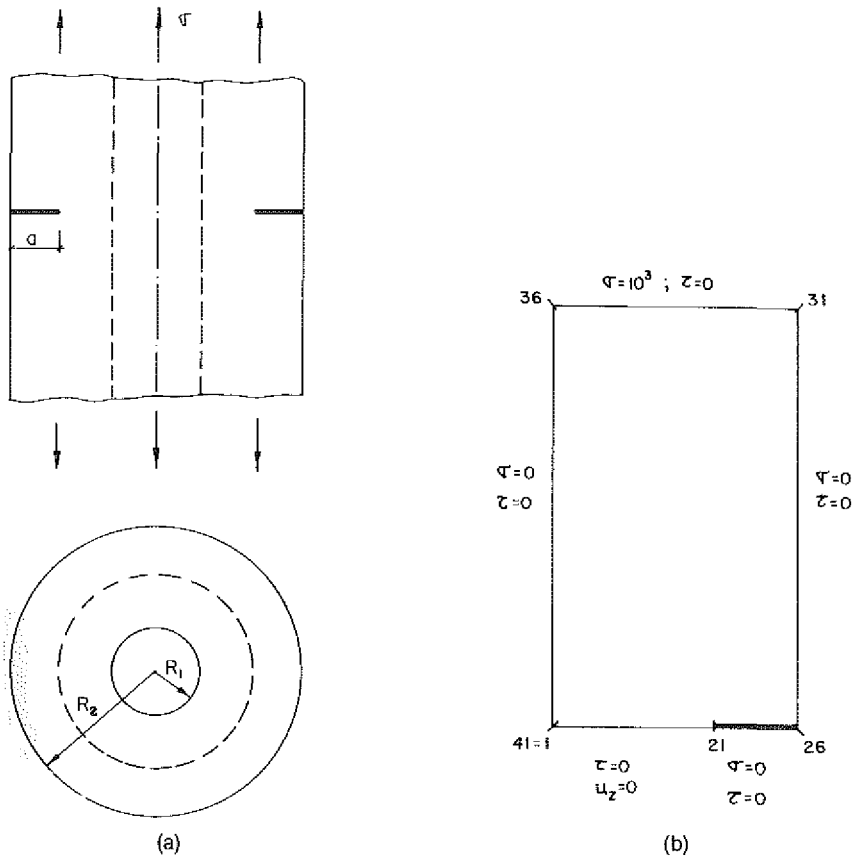

Fig. 35. Axially loaded thick walled cracked tube.

(b) If both points coincide, we use a semianalytic approach producing a closed-form solution around the singularity where the Legendre functions can be expressed by a relatively simple formula and a numerical integration of the remaining parts of the element.

5.4. *Numerical examples*

The first example is shown in Fig. 35(a). A thick walled tube is loaded axially and presents a crack along its exterior boundary. It is well known that the stress distribution follows the law

$$\sigma_{ij}(r,\theta) = \frac{K}{\sqrt{2\pi r}} f_{ij}(\theta) ,$$

where K is the stress intensity factor. Fig. 35(b) shows the discretization that produces the results shown in Table 3. The computed stress intensity factor is $K = 2908.372$ (Fig. 36) with an error of 4.05% against the closed-form solution in spite of the poor discretization that has been used.

Another example is presented in Fig. 37(a), where the same cylinder is

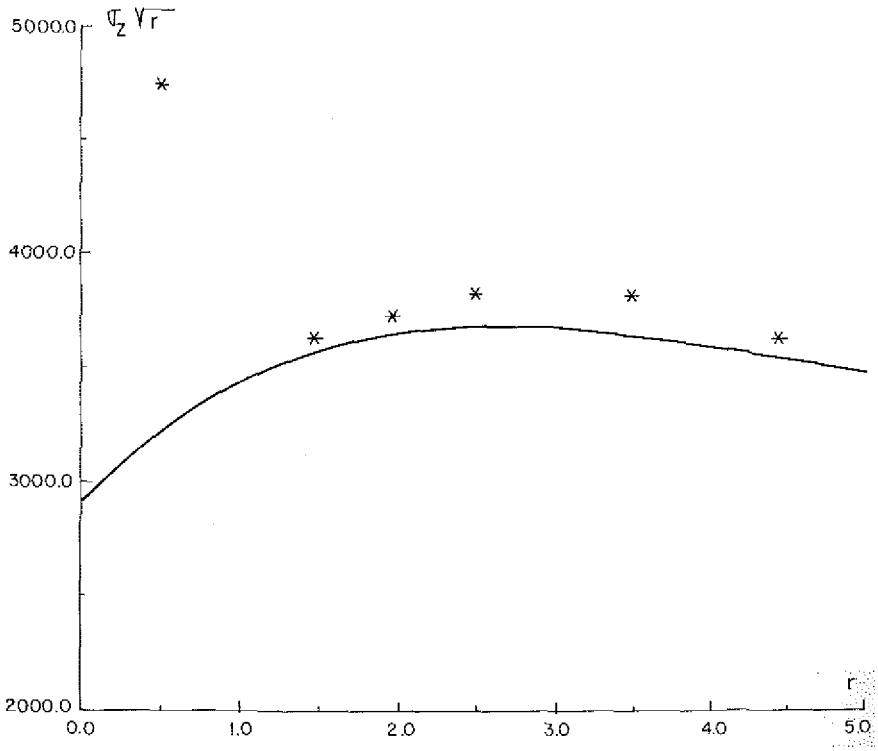

Fig. 36. Stress intensity factor for the structure of Fig. 35(a).

Table 3
Numerical results from the analysis of the thick walled tube of Fig. 35.

Node	Distance to the crack tip r (cm)	σ_z (kg/cm^2)	$\sigma_z\sqrt{r}$ (kg · cm$^{-5/2}$)
20	0.5	6856.35	4848.17
19	1.5	2899	3550.54
18	2.5	2336.135	3693.75
17	3.5	2001.184	3743.87
16	4.5	1557.939	3304.89
15	5.5	1562.348	3664.03
14	6.5	1307.604	3494.37
13	7.5	1273.738	3488.28
12	8.5	1166.764	3401.67
11	9.5	1136.31	3502.67
10	10.5	908.003	3147.98

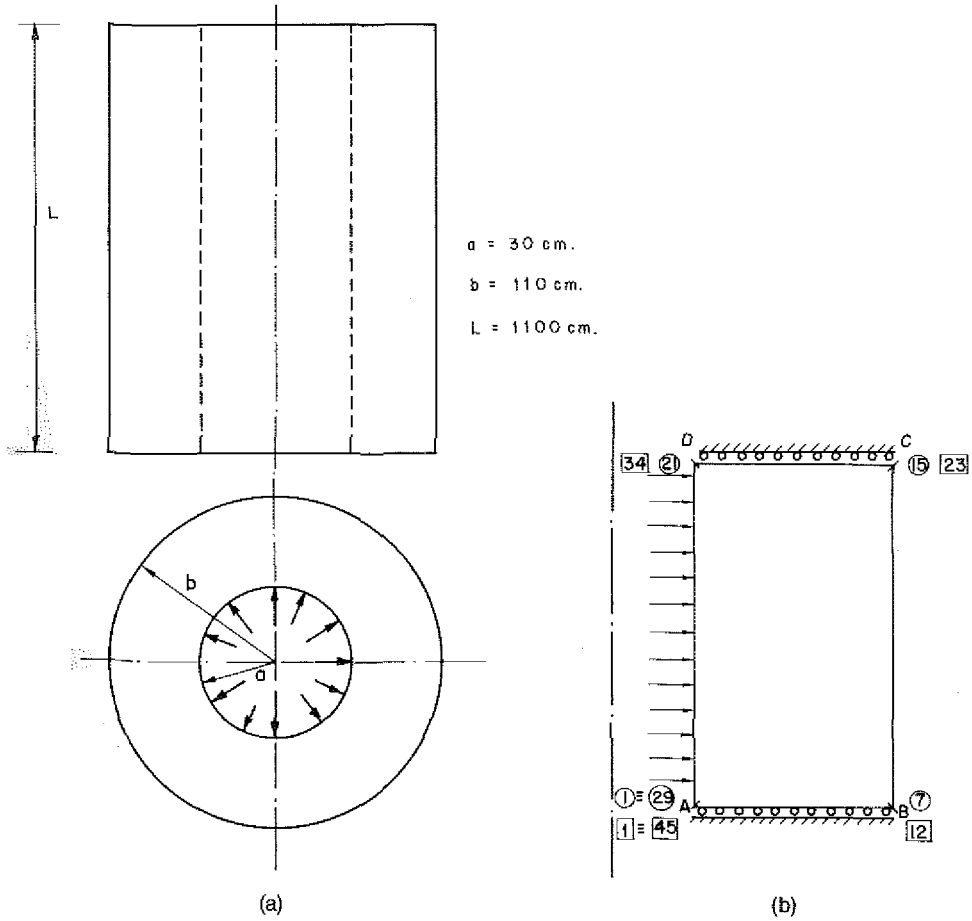

Fig. 37. Thick walled tube under internal pressure.

Table 4
Numerical results from the analysis of the cylinder of Fig. 37.

Face	Discretization	Variable	Results	Error %
AB,CD	28 elements	$\sigma_z(\mathrm{kg/cm^2})$	37.55	6.55
	44 elements		40.27	0.22
BC	28 elements	$u_r(\mathrm{cm})$	6680.75×10^{-5}	7.97
	44 elements		6627.18×10^{-5}	7.11
DA	28 elements	$u_r(\mathrm{cm})$	17362.5×10^{-5}	4.04
	44 elements		17200.91×10^{-5}	3.08

submitted to internal pressure. Nodes with the symbol ○ correspond to a 28-element discretization, while those with the □ represent a discretization with 44 elements (Fig. 37b). The results are as shown in Table 4.

5.5. *Use of the Cartesian fundamental solution*

As an alternative to the use of the axisymmetric fundamental solution, it is possible to treat the Cartesian equation with two changes to polar coordinates. If the field point has coordinates (ρ, θ, z) and the collocation point (ρ', θ', z'), it can be seen immediately that the boundary integral equation can be written for a smooth boundary such as

$$\tfrac{1}{2}\boldsymbol{u}^{\mathrm{p}}(\mathrm{P}) + \int_{\partial\Omega} (\boldsymbol{\Omega}'\boldsymbol{T}^{\mathrm{c}}\boldsymbol{\Omega})\boldsymbol{u}^{\mathrm{p}} = \int_{\partial\Omega} (\boldsymbol{\Omega}'\boldsymbol{U}^{\mathrm{c}}\boldsymbol{\Omega})\boldsymbol{t}^{\mathrm{p}}\,, \tag{5.19}$$

where superscripts c and p mean Cartesian and polar, respectively, and Ω and Ω' are defined by

$$\boldsymbol{\Omega} = \begin{pmatrix} \cos\theta & -\sin\theta & 0 \\ \sin\theta & \cos\theta & 0 \\ 0 & 0 & 1 \end{pmatrix}, \qquad \boldsymbol{\Omega}' = \begin{pmatrix} \cos\theta' & \sin\theta' & 0 \\ -\sin\theta' & \cos\theta' & 0 \\ 0 & 0 & 1 \end{pmatrix}. \tag{5.20}$$

If the collocation point P has $\theta' = 0$, then, for instance

$$\boldsymbol{T}^{\mathrm{p}} = \boldsymbol{\Omega}'\boldsymbol{T}^{\mathrm{c}}\boldsymbol{\Omega} = \begin{bmatrix} T_{11}\cos\theta + T_{12}\sin\theta & -T_{11}\sin\theta + T_{12}\cos\theta & T_{13} \\ T_{21}\cos\theta + T_{22}\sin\theta & -T_{21}\sin\theta + T_{22}\cos\theta & T_{23} \\ T_{31}\cos\theta + T_{32}\sin\theta & -T_{31}\sin\theta + T_{32}\cos\theta & T_{33} \end{bmatrix}. \tag{5.21}$$

In general, point P has to be chosen judiciously, depending on problem conditions.

A very interesting situation arises, for instance, when trying to compute the impedance of rigid circular foundations. In general, one is interested in obtaining

the stresses developed under the footing when subjected to torsional, vertical, horizontal or rocking unit displacements. The distribution of displacements and stresses is given in Table 5.

Assuming constant values of u' and τ' inside concentric rings and that the collocation points P are situated at $\theta = 0$, it is easy to see that cases (a) and (b) can be solved simultaneously through the system

$$\frac{1}{2}\begin{Bmatrix} u'_\rho \\ u'_\theta \\ u'_z \end{Bmatrix} + 2\int \left[\begin{array}{c|c|c} T_{11}\cos\theta + T_{12}\sin\theta & 0 & T_{13} \\ \hline 0 & -T_{21}\sin\theta + T_{22}\cos\theta & 0 \\ \hline T_{31}\cos\theta + T_{32}\sin\theta & 0 & T_{33} \end{array}\right] \begin{Bmatrix} u'_\rho(\mathrm{Q}) \\ u'_\theta(\mathrm{Q}) \\ u'_z(\mathrm{Q}) \end{Bmatrix}$$

$$= 2\int \left[\begin{array}{c|c|c} U_{11}\cos\theta + U_{12}\sin\theta & 0 & U_{13} \\ \hline 0 & -U_{21}\sin\theta_{22} + U_{22}\cos\theta & 0 \\ \hline U_{31}\cos\theta + U_{32}\sin\theta & 0 & U_{23} \end{array}\right] \begin{Bmatrix} \tau'_\rho(\mathrm{Q}) \\ \tau'_\theta(\mathrm{Q}) \\ \sigma'_z(\mathrm{Q}) \end{Bmatrix} \tag{5.22}$$

where the integration is done only along the half ring, such that $0 \leqslant \theta \leqslant \pi$. For cases (c) and (d), the situation is similar although the second equation has to be computed by locating P somewhere with $\theta \neq 0$. Choosing, for instance, $\theta = -\pi/2$, the final system for every ring is

$$\frac{1}{2}\begin{Bmatrix} u'_\rho \\ u'_\theta \\ u'_z \end{Bmatrix} + 2\int \left[\begin{array}{c|c|c} T_{11}C^2 + T_{12}SC & T_{11}S^2 - T_{12}SC & T_{13}C \\ \hline T^*_{11}C^2 + T^*_{12}SC & T^*_{11}S^2 - T^*_{12}SC & T^*_{13}C \\ \hline T_{31}C^2 + T_{32}SC & T_{31}S^2 - T_{32}SC & T_{33}C \end{array}\right] \begin{Bmatrix} u'_\rho \\ u'_\theta \\ u'_z \end{Bmatrix}$$

$$= 2\int \left[\begin{array}{c|c|c} U_{11}C^2 + U_{12}SC & U_{11}S^2 - U_{12}SC & U_{13}C \\ \hline U^*_{11}C^2 + U^*_{12}SC & U^*_{11}S^2 - U_{12}SC & U^*_{13}C \\ \hline U_{31}C^2 + U_{32}SC & U_{31}S^2 - U_{32}SC & U_{33}C \end{array}\right] \begin{Bmatrix} \tau'_\rho \\ \tau'_\theta \\ \sigma'_z \end{Bmatrix} \tag{5.23}$$

where

$$C = \cos\theta,\ S = \sin\theta,\ SC = \cos\theta \cdot \sin\theta,\ C^2 = \cos^2\theta,\ S^2 = \sin^2\theta\ ,$$

and the integration for the first and third equation is carried out inside the half ring $0 \leqslant \theta \leqslant \pi$, while the second one is extended over $-\pi \leqslant \theta \leqslant \pi$.

This procedure is also useful for treating embedded foundations or piles with

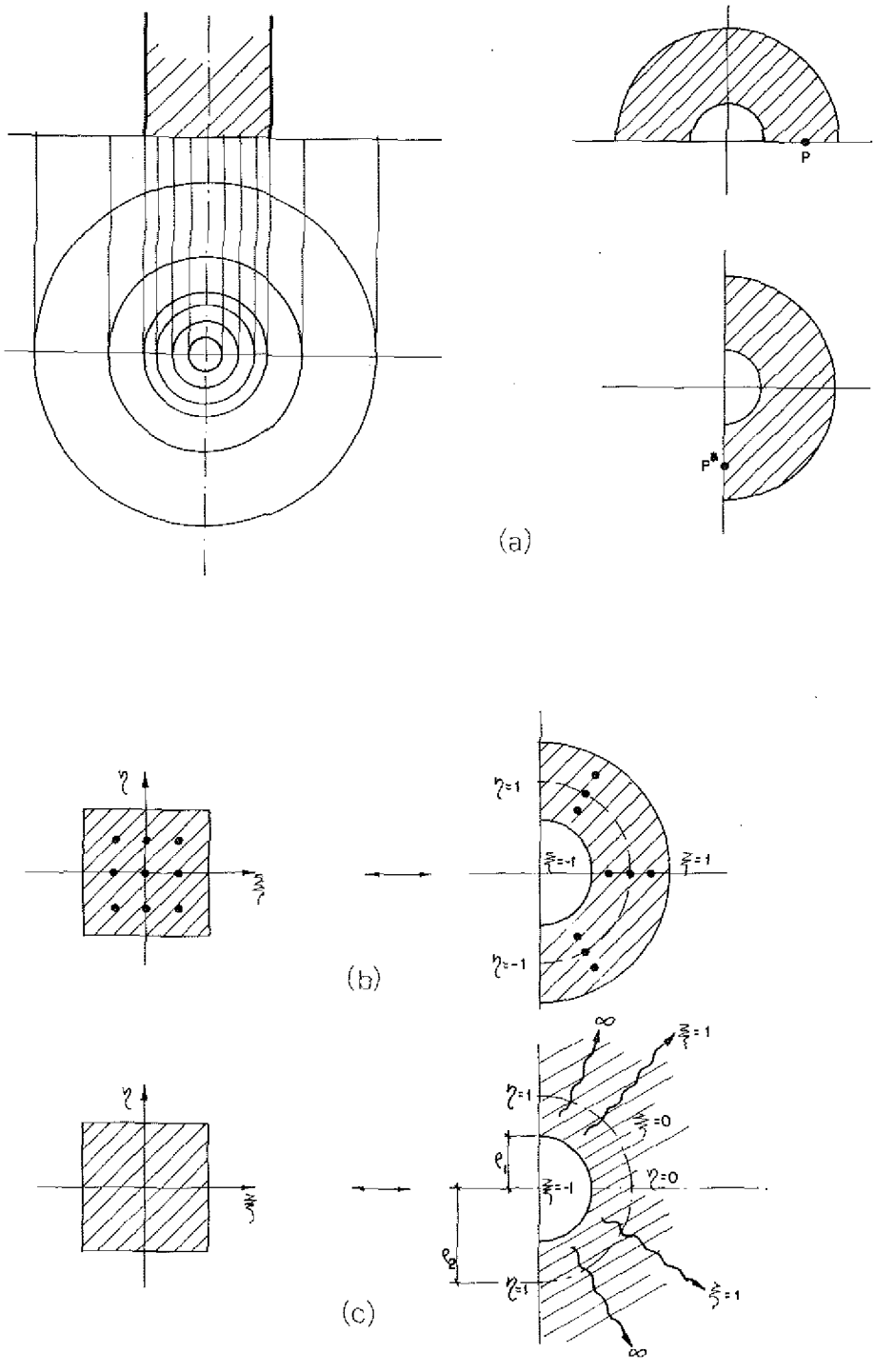

Fig. 38. Coordinate transformations for the treatment of axisymmetric structures.

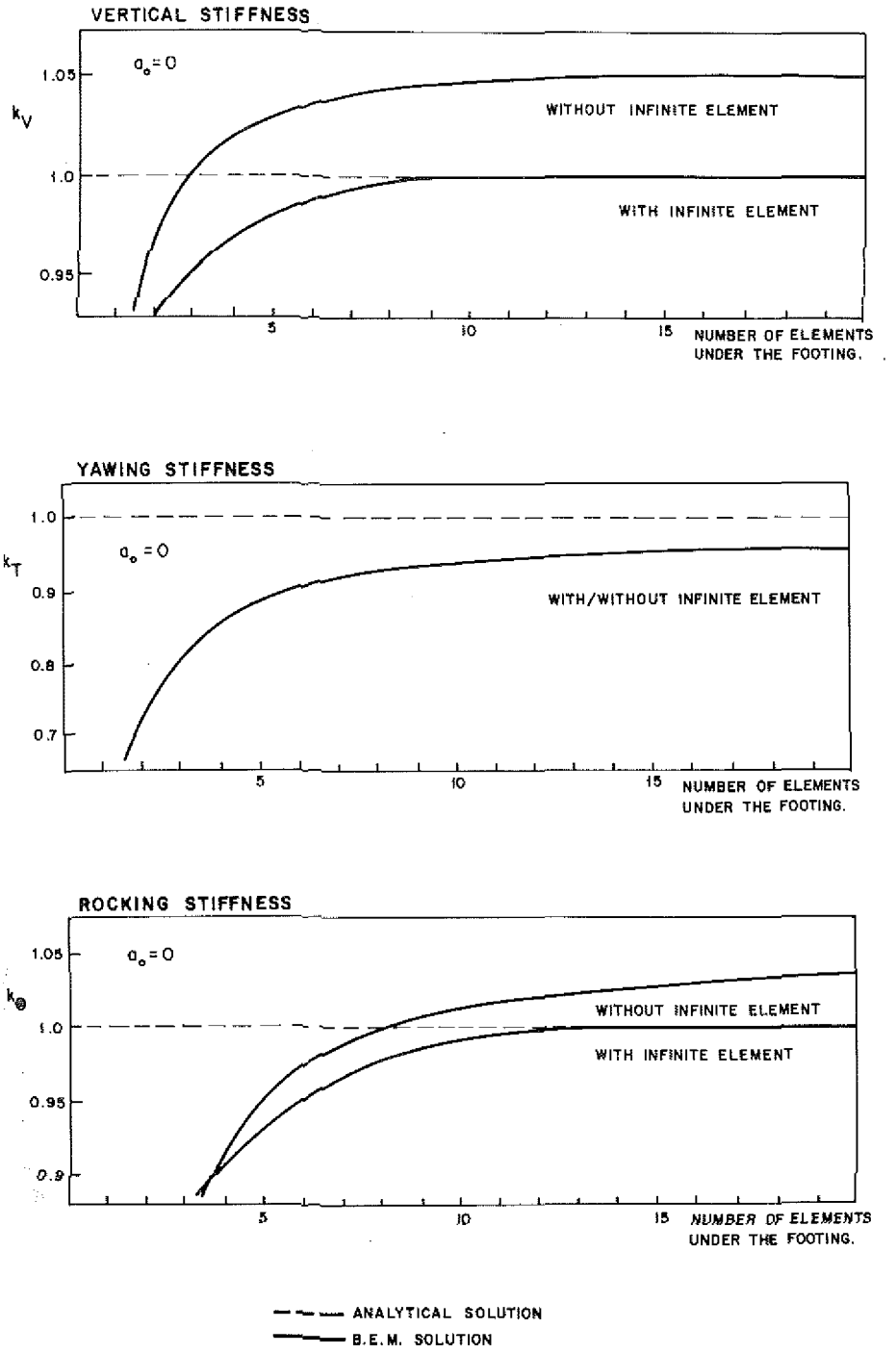

Fig. 39. Convergence of static solution discretizing only under the footing or adding an exterior infinite element.

Table 5
Stresses and displacements under a circular footing subjected to various modes of deformation.

Imposed displacement	Stresses	Displacements
(a) torsion	$\tau_\rho = 0 \quad \sigma_z = 0$ $\tau_\theta = \tau'_\theta(\rho)$	$u_\rho = 0 \quad u_z = 0$ $u_\theta = u'_\theta(\rho)$
(b) vertical	$\tau_\theta = 0 \quad \tau_\rho = \tau'_\rho(\rho)$ $\sigma_z = \sigma'_z(\rho)$	$u_\theta = 0 \quad u_\rho = u'_\rho(\rho)$ $u_z = u'_z$
(c) horizontal	$\tau_\rho = \tau'_\rho \cos\theta$ $\tau_\theta = -\tau'_\theta \sin\theta$ $\sigma_z = -\sigma'_z \cos\theta$	$u_\rho = u'_\rho \cos\theta$ $u_\theta = -u'_\theta \sin\theta$ $u_z = u'_z \cos\theta$
(d) rocking	ditto	ditto

obvious modifications. The integrals are done numerically, using the transformation indicated in Fig. 38(a, b), while sometimes it is also useful to develop infinite elements, as shown in Fig. 38(c), according to the law

$$\theta = \tfrac{1}{2}\pi\eta\,, \qquad \rho = \rho_2 + 2\,\frac{\rho_2 - \rho_1}{1-\xi}\,\xi\,. \tag{5.24}$$

Figure 39 shows some comparisons between stiffnesses computed using elements only under the rigid footing or adding infinite elements to represent the free-field region.

Closing this section, we would like to mention that treatment of axisymmetric elastic bodies with non-axisymmetric boundary conditions is also possible by expanding the variables of the problem in a series of orthogonal functions, e.g. Fourier series, of the polar angle and reducing the problem to a sequence of two-dimensional, angularly independent problems like the ones treated in this section [99, 80, 100].

6. Anisotropy

The treatment of anisotropic elastic bodies is a field relatively scarce in publications, in comparison with the isotropic elastic ones. The difficulty lies in the fundamental solution. Only for plane problems or for certain three-dimensional cases is it possible to obtain closed-form expressions.

Rizzo and Shippy [96] presented the first application of the BEM to plane anisotropic problems, while Vogel and Rizzo [111] presented an integral representation for three-dimensional problems. Wilson and Cruse [115] used the point-load solution

$$U_{ij}(x, y) = \frac{1}{8\pi^2 |x-y|} \oint_{|\xi|=1} K_{ij}^{-1}(\xi)\,, \tag{6.1}$$

which gives the displacement at point y due to a point force applied at x in the form of a line integral taken on the unit circle in the plane passing through x and normal to $x - y$ with an integrand

$$K_{ij}^{-1}(\xi) = [C_{ijkm}\xi_k\xi_m]^{-1}, \tag{6.2}$$

where C_{ijkm} represents the elastic constants of the material. This representation reduces only to closed form for the Kelvin case (isotropic material) or for transversely anisotropic materials (Pan and Chou [87] and Kobayashi and Nishimura [71]).

Wilson and Cruse [115] decided to treat what they called the modulation function

$$G_{ij}(n_1, n_2) = \int_{|\xi|=1} K_{ij}^{-1}(\xi), \tag{6.3}$$

where (n_1, n_2) is the orientation of $x - y$, by means of an interpolation technique, generating data bases for a variety of materials and managing them from an external computer core.

Because of the difficulties related to that presentation, Nishimura and Kobayashi [83] have recently offered an alternative, using an indirect approach where the Fourier transform is used to generate a simple layer potential approximated by piecewise-constant elements in place of the point-load solution.

Crouch [42] and Crouch and Starfield [44] have also shown how to apply the displacement discontinuity method to anisotropic elasticity. Figure 40, taken from [44], represents, for instance, their results for the tangential stress at the boundary of a circular hole in an orthotropic plate.

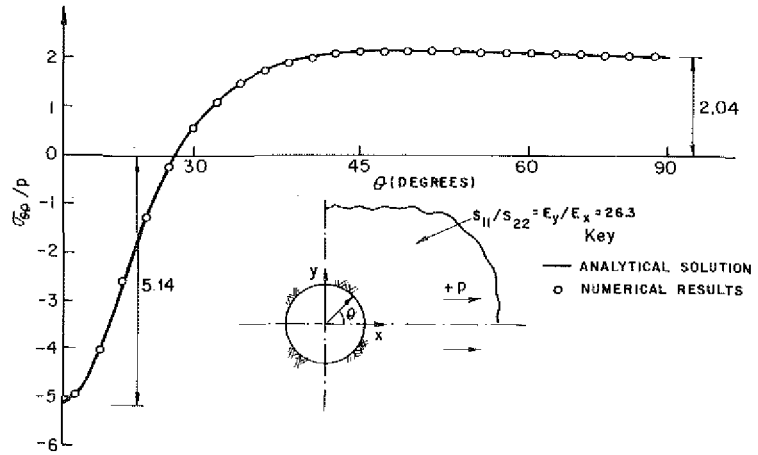

Fig. 40. Tangential stress around the boundary of a circular hole in an orthotropic plate.

7. Additional topics

Three complementary topics are included in this section. First, a discussion on the bending of thin plates and shallow shells; second, the coupling of boundary and finite elements; and finally, some hints on the possibility of developing adaptive boundary elements are briefly discussed. We think that, although some important research has already been done on the last two subjects, they deserve more attention in the future.

7.1. Bending of thin plates and shallow shells

The BEM has also been successfully applied to the analysis of thin elastic flexural plates. Both the indirect [66, 9, 84, 109] and the direct [55, 21, 104, 109] approaches have been used. The first work in this area is that of Jawson and Maiti [66] who presented an indirect approach based on the use of potentials. Comprehensive reviews of the topic can be seen in Tottenham [109] and Stern [105]. In general, the fundamental solution is based on the response to a concentrated load acting on an infinite plate, although other possibilities do exist, as shown by Altiero and Sikarskie [9]. Paris and Leon [88] have also shown the possibility of using the Marcus approach. Finally, a series of authors have presented extensions to finite deformations, buckling and shallow shell response [68].

It is well known [112] that the governing equation for thin plate flexure is

$$\nabla^2\nabla^2 w = p/D \,, \tag{7.1}$$

where w is the vertical deflection, p is the distributed loading acting on the plate, h is the plate thickness and the bending rigidity $D = Eh^3/12(1-\nu^2)$, with E and ν being the modulus of elasticity and Poisson's ratio, respectively.

Defining

$$M = D\nabla^2 w \,, \tag{7.2}$$

the governing equation can be written as

$$\nabla^2 M = p$$

and both can be treated along the same lines of potential problems to produce a pair of coupled equations

$$\begin{aligned} cM + \int_{\partial\Omega} Mq^* &= \int_{\partial\Omega} \frac{\partial M}{\partial n}\,\phi^* + \int_{\Omega} p\phi^* \,, \\ cw + \int_{\partial\Omega} wq^* &= \int_{\partial\Omega} \frac{\partial w}{\partial n}\,\phi^* + \int_{\Omega} \frac{M}{D}\,\phi^* \,, \end{aligned} \tag{7.3}$$

where ϕ^* is the fundamental solution of the Laplacian equation and M represents the value of the invariant

$$M = \frac{M_n + M_s}{1 + \nu} , \tag{7.4}$$

with M_n and M_s being the bending moments along two orthogonal directions [112].

The usual technique of discretization allows one to write

$$\begin{aligned} \boldsymbol{AM} &= \boldsymbol{BM}_{,n} + \mathbf{P}^0 , \\ \boldsymbol{Aw} &= \boldsymbol{Bw}_{,n} + \boldsymbol{M}^0 , \end{aligned} \tag{7.5}$$

where $\boldsymbol{A}$ and $\boldsymbol{B}$ are the influence matrices described in the chapter on potential problems and the comma indicates differentiation.

A very important possibility for application occurs when the boundary is simply supported and then both problems are decoupled so that it is possible to solve them in turn. In this case, it must be observed that $\boldsymbol{A}$ and $\boldsymbol{B}$ need to be computed only once.

The direct method can be obtained by considering the weak formulation of the equilibrium equation of the plate of the form

$$\frac{\partial^2 M_x}{\partial x^2} + 2\frac{\partial^2 M_{xy}}{\partial x \partial y} + \frac{\partial^2 M_y}{\partial y^2} = -p , \tag{7.6}$$

where M_x and M_y are the bending moments and M_{xy} is the twisting moment. After multiplication of both terms of (7.6) by a virtual displacement and integration by parts, it is obtained that

$$\begin{aligned} &\int_\Omega M_x \frac{\partial^2 w^*}{\partial x^2} + 2M_{xy}\frac{\partial^2 w^*}{\partial x \partial y} + M_y \frac{\partial^2 w^*}{\partial y^2} \\ &\quad = \int_\Omega p w^* - \int_{\partial\Omega} M_n \frac{\partial w^*}{\partial n} - \int_{\partial\Omega} M_{ns}\frac{\partial w^*}{\partial s} + \int_{\partial\Omega} Q w^* , \end{aligned} \tag{7.7}$$

where, as usual

$$\begin{aligned} &M_n = M_x n_1^2 + M_y n_2^2 + 2M_{xy} n_1 n_2 , \\ &M_{ns} = -M_x n_1 n_2 + M_y n_1 n_2 + M_{xy} n_1^2 - M_{xy} n_2^2 , \\ &n^{\mathrm{T}} = (n_1, n_2) , \qquad Q = Q_x n_1 + Q_y n_2 , \\ &Q_x = \frac{\partial M_x}{\partial x} + \frac{\partial M_{xy}}{\partial y} , \qquad Q_y = \frac{\partial M_y}{\partial y} + \frac{\partial M_{xy}}{\partial x} . \end{aligned} \tag{7.8}$$

It can be seen that the right-hand side of (7.7) is a bilinear symmetric form in w, w^* after the introduction of the definitions

$$M_x = -D\left(\frac{\partial^2 w}{\partial x^2} + \nu \frac{\partial^2 w}{\partial y^2}\right),$$

$$M_y = -D\left(\frac{\partial^2 w}{\partial y^2} + \nu \frac{\partial^2 w}{\partial x^2}\right),$$

$$M_{xy} = -(1-\nu)D \frac{\partial^2 w}{\partial x \partial y}.$$

Thus, a reciprocity relationship can immediately be written by interchanging w and w^* in (7.7) and subtracting the resulting equation from (7.7). This has the form

$$\int_\Omega p^* w - \int_{\partial\Omega} M_n^* \frac{\partial w}{\partial n} - \int_{\partial\Omega} M_{ns}^* \frac{\partial w}{\partial s} + \int_{\partial\Omega} Q^* w$$
$$= \int_\Omega \frac{p}{D} w^* - \int_{\partial\Omega} M_n \frac{\partial w^*}{\partial n} - \int_{\partial\Omega} M_{ns} \frac{\partial w^*}{\partial s} + \int_{\partial\Omega} Q w^*, \tag{7.9}$$

or, upon introducing

$$Q_{ef} = Q + \frac{\partial M_{ns}}{\partial s}, \qquad q = -\frac{\partial w}{\partial n}, \qquad q^* = -\frac{\partial w^*}{\partial n}$$

and applying integration by parts on the third integral on both sides, the form

$$\int_\Omega p^* w + \int_{\partial\Omega} M_n^* q + \int_{\partial\Omega} Q_{ef}^* w + \sum |M_{ns}^* w|$$
$$= \int_\Omega p w^* + \int_{\partial\Omega} M_n q^* + \int_{\partial\Omega} Q_{ef} w^* + \sum |M_{ns} w^*|, \tag{7.10}$$

where M_{ns} and M_{ns}^* are the possible concentrated forces in corners.

Using a fundamental solution, for instance,

$$w^* = (1/8\pi) r^2 \ln r, \tag{7.11}$$

we obtain the basic relations

$$cw = \int_\Omega p w^* - \int_{\partial\Omega} Q_{ef}^* w + \int_{\partial\Omega} M_n^* \frac{\partial w}{\partial n} - \int_{\partial\Omega} M_n \frac{\partial w^*}{\partial n}$$
$$+ \int_{\partial\Omega} Q_{ef} w^* + \sum_1^N |M_{ns} w^*| - \sum_1^N |M_{ns}^* w|, \tag{7.12}$$

$$c\frac{\partial w}{\partial n} = \int_{\Omega} p\frac{\partial w^*}{\partial n} - \int_{\partial\Omega} \frac{\partial Q^*_{ef}}{\partial n} w + \int_{\partial\Omega} \frac{\partial M^*_n}{\partial n}\frac{\partial w}{\partial n} - \int_{\partial\Omega} M_n \frac{\partial^2 w^*}{\partial n^2}$$
$$+ \int_{\partial\Omega} Q_{ef}\frac{\partial w^*}{\partial n} + \sum_1^N \left| M_{ns}\frac{\partial w^*}{\partial n}\right| - \sum_1^N \left|\frac{\partial M^*_{ns}}{\partial n} w\right| , \qquad (7.13)$$

where (7.13) was derived from (7.12) by differentiation. The pair of boundary integral equations (7.12) and (7.13) relate the variables w, $\partial w/\partial n$, M_n, Q_{ef} and is discretized along the same lines described in the previous sections, producing the set of equations

$$\begin{aligned} \boldsymbol{A}_1\boldsymbol{w} + \boldsymbol{B}_1\boldsymbol{w}_n + \boldsymbol{C}_1\boldsymbol{M}_n + \boldsymbol{D}_1\boldsymbol{Q}_{ef} &= \mathbf{P}_1 , \\ \boldsymbol{A}_2\boldsymbol{w} + \boldsymbol{B}_2\boldsymbol{w}_n + \boldsymbol{C}_2\boldsymbol{M}_n + \boldsymbol{D}_2\boldsymbol{Q}_{ef} &= \mathbf{P}_2 , \end{aligned} \qquad (7.14)$$

where $\boldsymbol{A}_i$, $\boldsymbol{B}_i$, $\boldsymbol{C}_i$ and $\boldsymbol{D}_i$ are the corresponding influence matrices. The imposition of boundary conditions allows the solution of the problem.

It is important to notice that, once again, the appearance of corners produces problems of the same type as in plane elasticity, due to the discontinuity of normals and the related variables. The solution is similar, i.e. if the w field is regular it is possible to add continuity conditions to solve the dilemma, while if there is a singularity, for instance of the re-entrant corner type, an asymptotic expansion can be used. More details can be found in Stern [104].

The treatment of shallow shells has been discussed by Forbes and Robinson [55], Newton and Tottenham [82] and Tottenham [109].

More recently Kamiya et al. [68] have presented interesting results for elastic plates experiencing finite deformations according to Berger's equation

$$\nabla^2\nabla^2 w - \kappa^2(\nabla^2 w + k_x + k_y) = p/D , \qquad (7.15)$$

where k_x, k_y are the curvatures and

$$\frac{\kappa^2 h^2}{12} = \frac{\partial u}{\partial x} + \frac{\partial v}{\partial y} + \tfrac{1}{2}\left[\left(\frac{\partial w}{\partial x}\right)^2 + \left(\frac{\partial w}{\partial y}\right)^2\right] - (k_x + k_y)w , \qquad (7.16)$$

with u and v being the in-plane displacements. It can be seen that this equation differs from Eq. (7.1) only in the second term, so that the previous scheme can be repeated, except that P_1 and P_2 in (7.14) now contain the contribution from the nonlinear terms.

If the in-plane displacement is restricted on the boundary such that

$$u = v = 0 \qquad \text{on } \partial\Omega , \qquad (7.17)$$

the magnitude of the parameter κ^2 can be estimated by integrating Eq. (7.16),

producing

$$\kappa^2 = \frac{12}{h^2 A_\Omega} \int_\Omega \tfrac{1}{2}\left[\left(\frac{\partial w}{\partial x}\right)^2 + \left(\frac{\partial w}{\partial y}\right)^2\right] - (k_x + k_y)w \,, \tag{7.18}$$

where A_Ω is the area of the domain. Kamiya et al. [68] suggest the use of an iterative approach to solve the nonlinearities and extend the solution to take into account the influence of temperature, as well as the finite deflection and post buckling deformation problems.

Figure 41 shows the application of the Marcus approach to the deflection of a square plate with simply supported, fixed and free edges [89]. The domain integral has been computed using a regular mesh of 5, 9 and 25 cells, where the values are assumed as constants, while the boundary has been discretized into 16, 32 and 64 linear elements.

Figure 42 shows results for the application of the indirect BEM along with an interesting modification suggested by Fukui [56], to treat corner solutions.

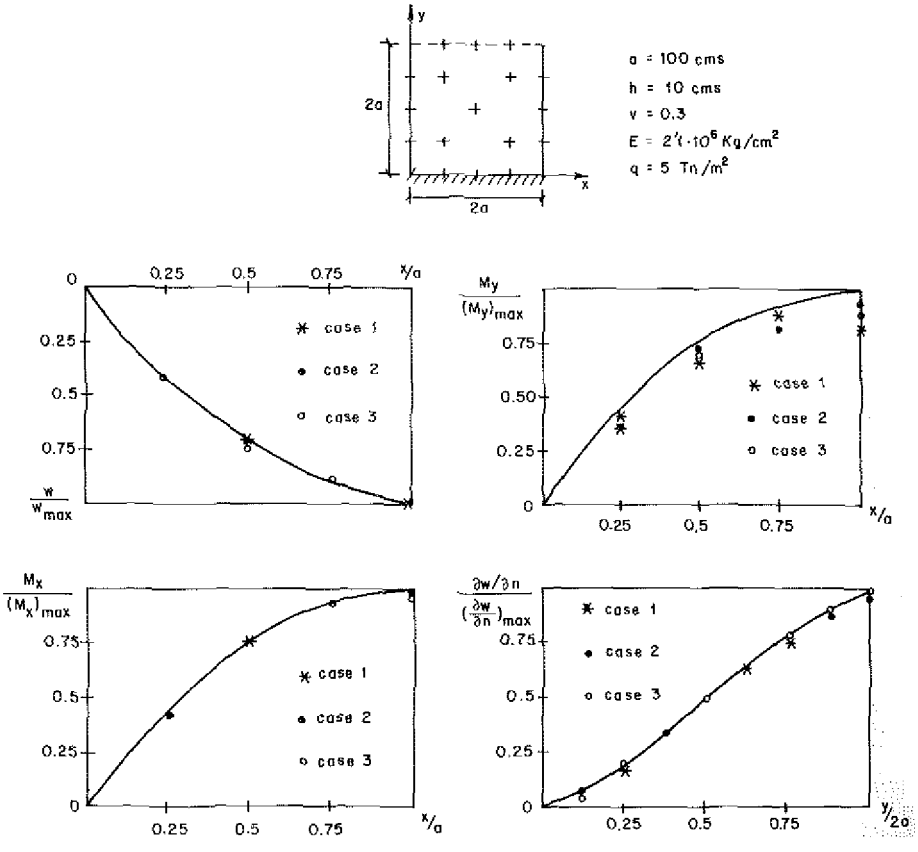

Fig. 41. Analysis results for a square plate using the BEM–Marcus approach.

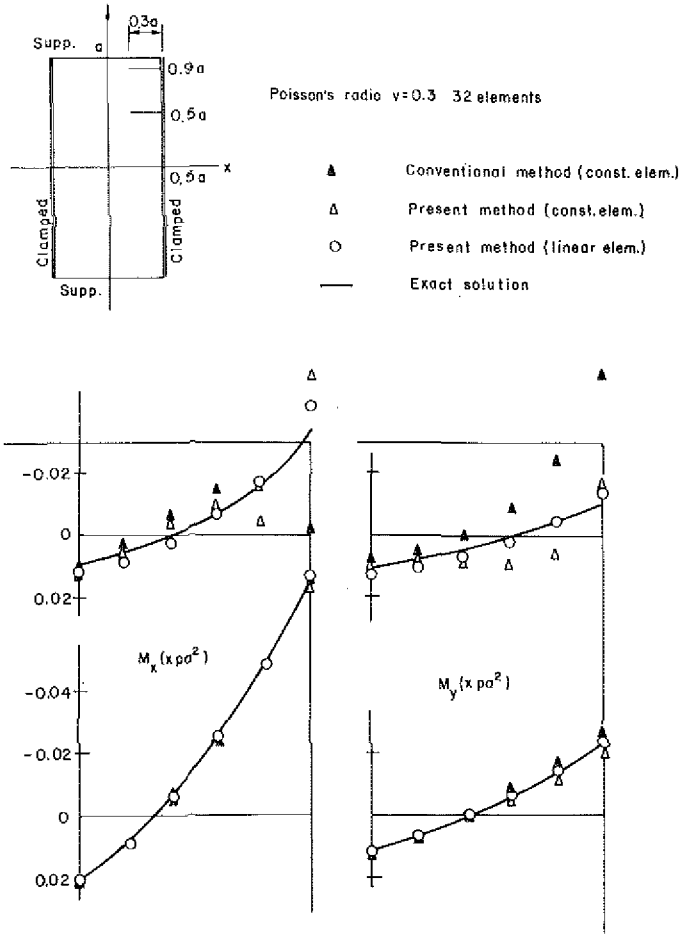

Fig. 42. Stress analysis of a rectangular plate.

7.2. BEM-FEM coupling

There are situations, such as nonlinearities, volume details, etc., where FEM versatility makes it unbeatable in treating a limited zone of the domain, while, in the remaining zones, the uniformity and extension counsel treatment with the BEM. The example in Figure 43 is typical of modelling soil–structure or fluid–structure or soil–fluid–structure interaction. The structure must be analyzed in detail and it is good to have extensive information throughout its domain, thereby requiring modelling by the FEM. On the other hand, the soil or the fluid are of interest only along the interfaces. Their size and homogeneity thus warrant the use of the BEM. Kelly et al. [69] and Margulies [77] have presented review-type articles on the subject.

The solution is a zoning, and it is important to note that the BEM works with

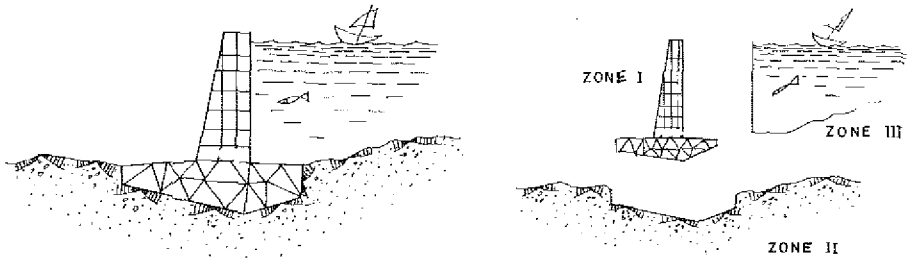

Fig. 43. The general problem of soil–structure–fluid interaction.

tractions while the FEM works with equivalent forces concentrated at the nodes. A previous integration is therefore necessary. In addition, there are problems motivated by the unsymmetric features of the BEM matrices. Thus, for each zone treated with the BEM

$$\boldsymbol{A}\boldsymbol{u} = \boldsymbol{B}\boldsymbol{t} \tag{7.19}$$

so that

$$\boldsymbol{t} = \boldsymbol{B}^{-1}\boldsymbol{A}\boldsymbol{u} \tag{7.20}$$

which will be used to obtain concentrated nodal forces. But $\boldsymbol{B}^{-1} \cdot \boldsymbol{A}$ is non-symmetric as discussed by Hartmann [58]. In particular, the non-symmetry implies that, due to the fact that the sum of the elements along columns is different from zero, the equilibrium condition is violated.

There have been several proposals to symmetrize $\boldsymbol{B}^{-1} \cdot \boldsymbol{A}$ from the simplest one

$$\tfrac{1}{2}[\boldsymbol{B}^{-1}\boldsymbol{A} + (\boldsymbol{B}^{-1} \cdot \boldsymbol{A})^{\mathrm{T}}] , \tag{7.21}$$

justified on variational reasons by Zienkiewickz [118, 81] or Brebbia and Walker [28] to the materialization of Hartmann [58] recommended by Tullberg and Bolteus [110]. In this sense, it seems that a good method might be the one that consists of the following steps:

(a) The elements of every column are added;

(b) the result is divided by the number of rows and the residuals are incorporated into every column element;

(c) the matrix is then symmetrized using (7.21).

Figure 44 presents a typical example of the above-mentioned procedure taken from Alarcón [4]. A lined tunnel was built after excavation of a trench which was filled a-posteriori to restore the original landscape. Due to the symmetries, it is only necessary to analyze half of the structure. The BEM was used to study the

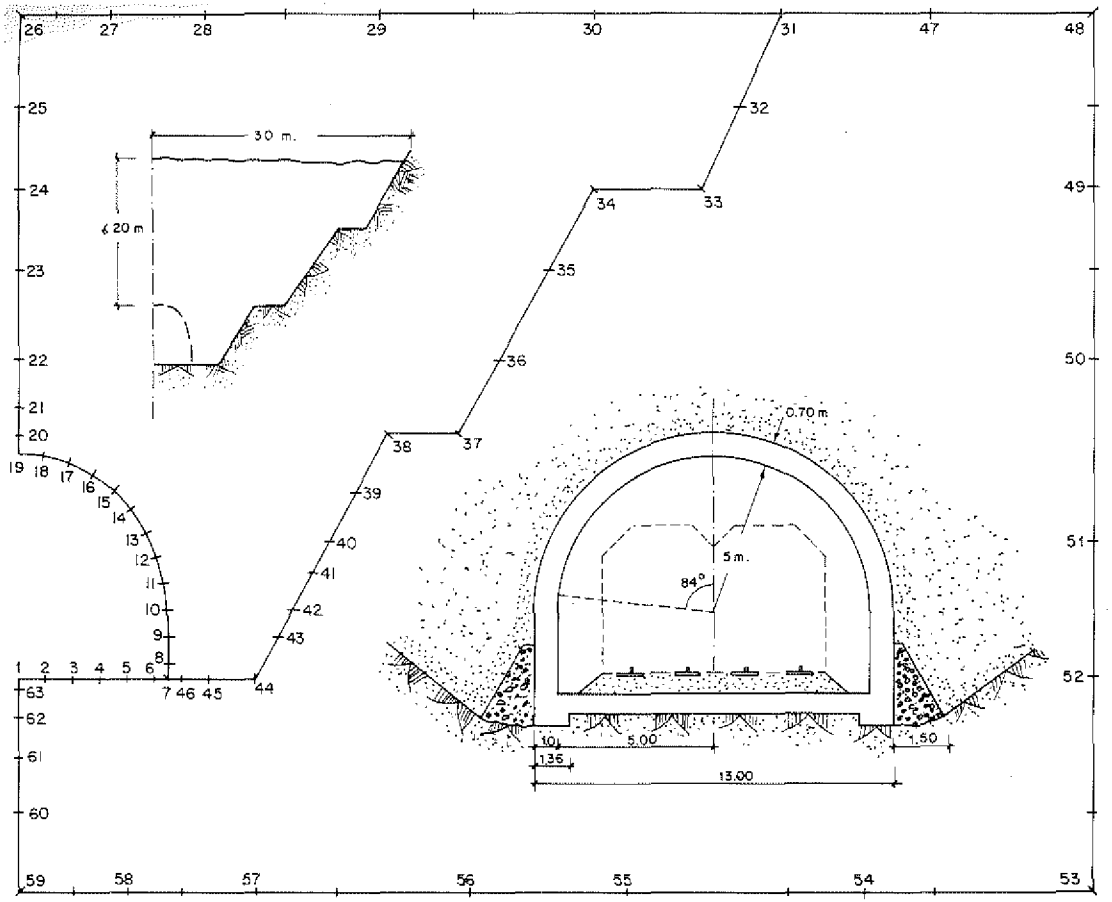

Fig. 44. Geometry and boundary discretization for the stress analysis of a lined tunnel.

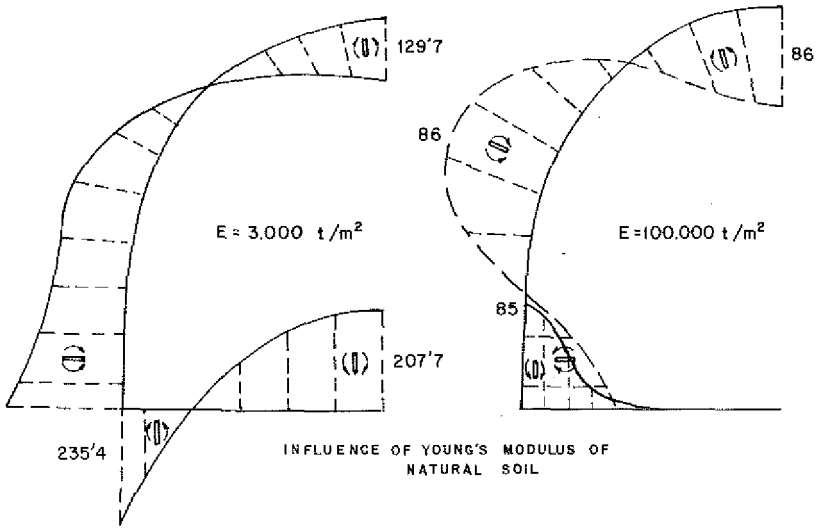

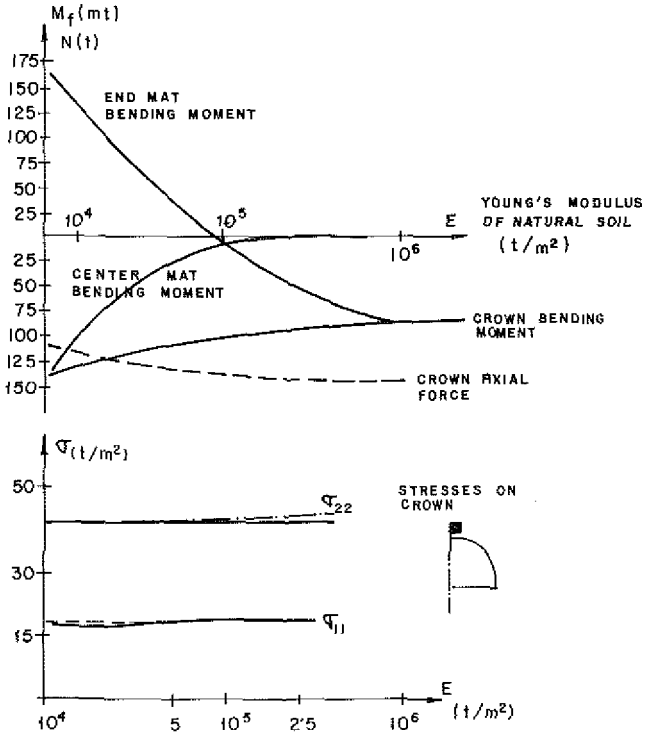

Fig. 45. Stress analysis results for the soil–structure system of Fig. 44.

earth region, while the liner was modelled through beam elements after condensation of the rotational degrees of freedom. Figure 45 shows some results of the parametric studies done with the model.

Another useful procedure akin to the BEM is sometimes used to build the stiffness matrix $\boldsymbol{K}^s$ of the soil through its definition stating that K_{ij} is the force appearing at the degree of freedom i when a unit displacement is imposed at the degree of freedom j. In this way, it is possible to treat soil–structure interaction problems as those of Figure 46 corresponding to a plate on a half-space. The interface is discretized using plane rectangular constant elements which can be thought of as boundary elements for the soil. These elements are given, in turn, unit displacements along the vertical and horizontal degrees of freedom. If only the vertical response is of concern, it suffices to give unit vertical displacements to obtain the resulting forces with the aid of the Boussinesq solution [112], in this way building a matrix $\boldsymbol{K}^s$, column by column. For its part, the plate can be discretized, using the FEM, with three degrees of freedom per node. The rotational degrees of freedom are condensed following a standard Gauss procedure and then translated along the depth of the plate to obtain its stiffness $\boldsymbol{K}^p$. The global matrix K for the soil-structure system is thus obtained as $\boldsymbol{K} = \boldsymbol{K}^s + \boldsymbol{K}^p$. After the common displacements $\boldsymbol{u}$ have been obtained, it is possible to get the contact pressures, by carrying out the product $\boldsymbol{K}^s\boldsymbol{u}$. Figures 47(a) and (b) show results obtained in this way, as compared with those presented by Cheung [40].

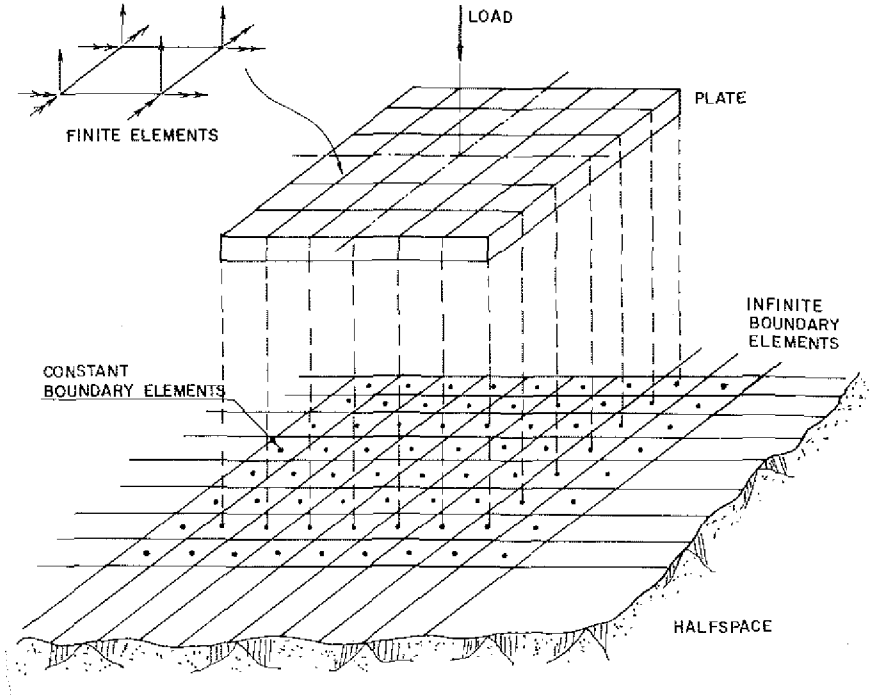

Fig. 46. Discretization scheme for a rectangular plate on an elastic half-space soil medium.

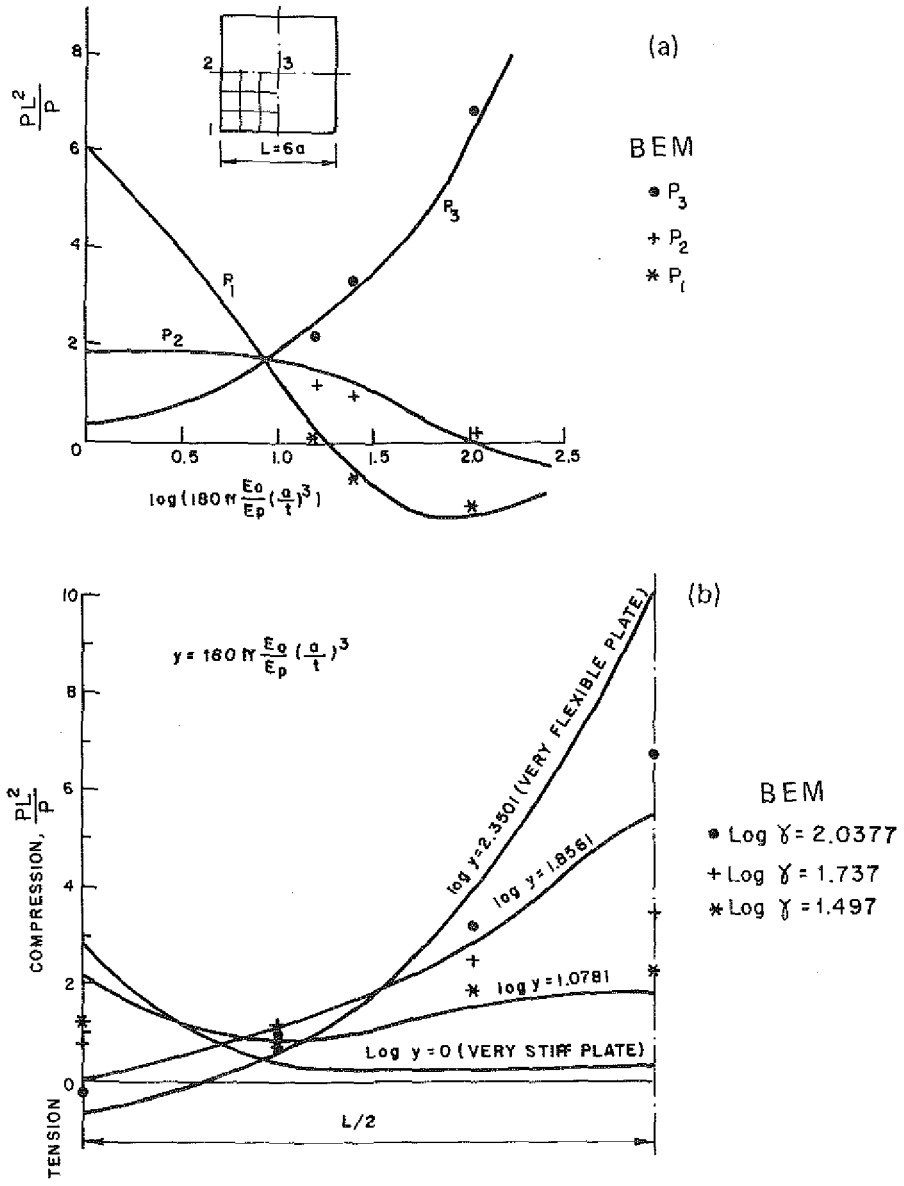

Fig. 47. Contact pressure results for the soil–foundation system of Fig. 46.

With the same procedure, using, for instance, the elements developed in section 5.5, it is possible to study soil–pile interaction problems. Another alternative has been proposed by Butterfield and Banerjee [37–39] and Banerjee et al. [13–15], which utilizes Mindlin's solution [35] for homogeneous and Kelvin's solution [76] with interface and surface discretization for layered half-spaces. Figure 48, taken from Banerjee and Butterfield [14], presents, for instance, the

case of a pile group. The geometry and discretization can be seen in Fig. 48(a), while the average vertical stress over the pile cross-section is shown in Fig. 48(b).

Additional applications of the BEM–FEM coupling technique can be found in [27, 23, 19]. The coupling of the BEM with the finite difference method has also been utilized [94].

7.3. Adaptive boundary elements

It is well known from the FEM that it is common to distinguish between two types of convergence, i.e. the h-convergence and the p-convergence. The first refers to the improvement of results obtained by refining the mesh. Due to the correspondence element – nodal variables – interpolation function, that implies a progressive adjustment of the results there where the refinement has been carried

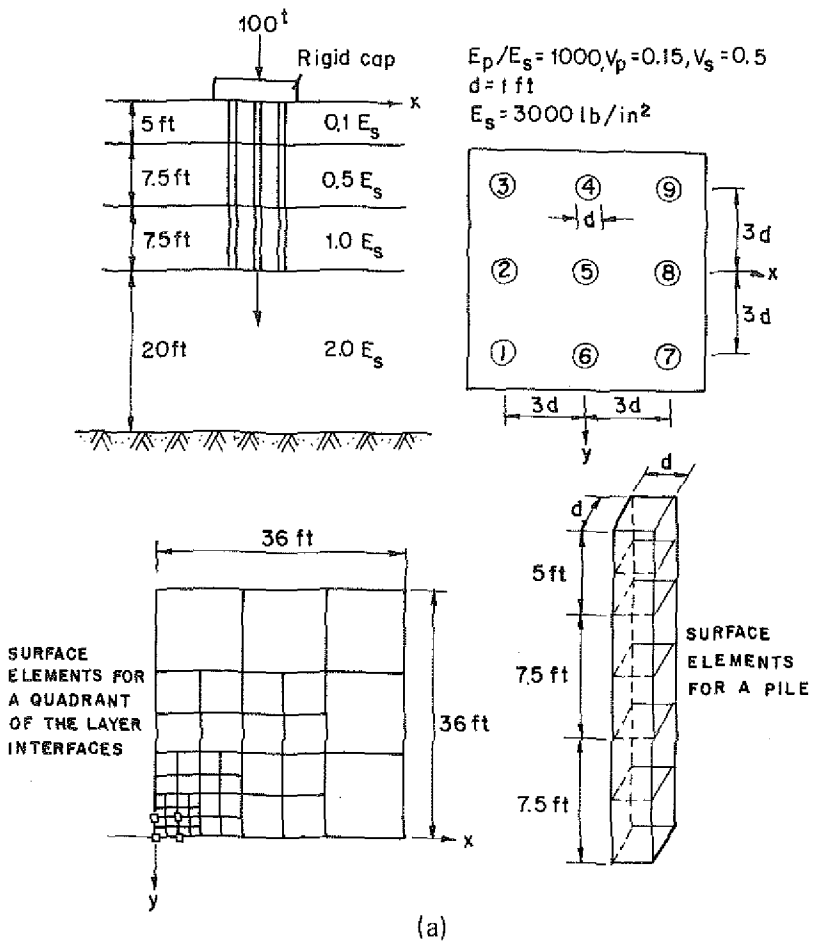

Fig. 48. Stress analysis of a vertically loaded group of piles embedded in a layered soil.

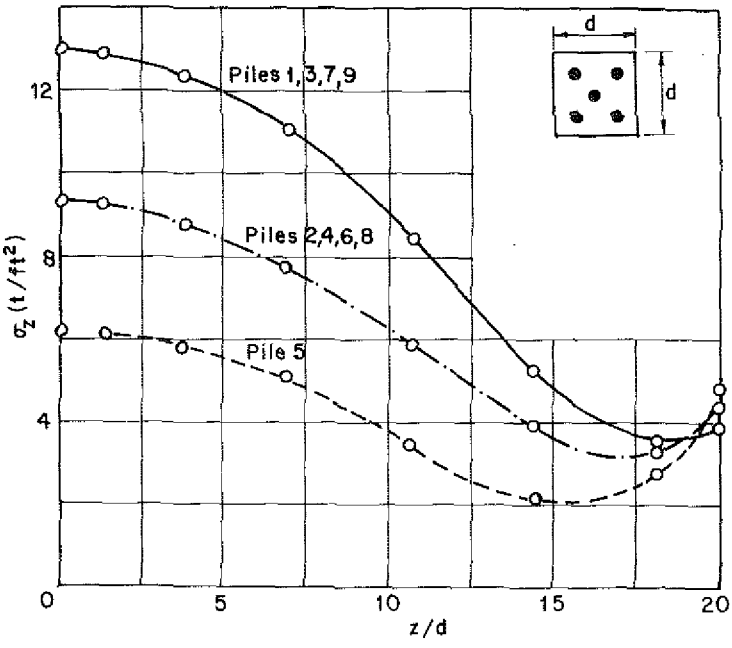

(b)

Fig. 48. (continued).

out. It is the most widely used method when, pragmatically, one wants to have an idea of the quality of the results. Its main disadvantage lies in the fact that every refinement requires the computation of different "stiffness" matrices, so that the information must be recomputed for every case, making the cost of this method quite high.

The second method analyzes p-convergence, or refinement of the approach by increasing the degree of the polynomial defined over every element. The idea is to compromise between the original Ritz idea of globally defined shape functions and the FEM of small support ones. The first step is, therefore, to define a rough mesh of elements and a hierarchy of functions inside them. With this intermediate decision between globality and locality, it is possible, on the one hand, to maintain a certain versatility for adjusting by pieces and, on the other, to refine intelligently because, as it happens with the Fourier series, the effect of adding a new term is decreasing, thus allowing truncation when a pre-established level of precision has been reached. In addition, and because every hierarchy of functions has a support fixed from each beginning, each refinement step uses all the previous computations. These ideas constitute the so-called adaptive procedures.

It seems that the first proposal was made by Zienkiewicz et al. [116] and since then, Szabo et al. [107], Peano et al. [92, 93] have contributed to the development of the method. The operating process follows these steps:

(a) establishment of a mesh on the model;

(b) definition of a hierarchy of function inside every element;

(c) establishment of an "indicator" to point to regions needing new shape functions;

(d) establishment of an "a-posteriori estimator", evaluating the error and predicting precisely when the process can be stopped.

A method following the previous steps is known as self-adaptive and is especially attractive for use with the BEM. It is well known that the BEM works with full matrices due to the globally based property of the fundamental solution, so that, except for the physical significance of the coefficients, it is not important to use locally based functions to interpolate the data or the unknowns. In order to reduce the computational effort, the idea of using hierarchical shape functions presents itself as an exciting posibility. The general isoparametric idea of the direct method, discussed in the previous sections, has been useful in the com-

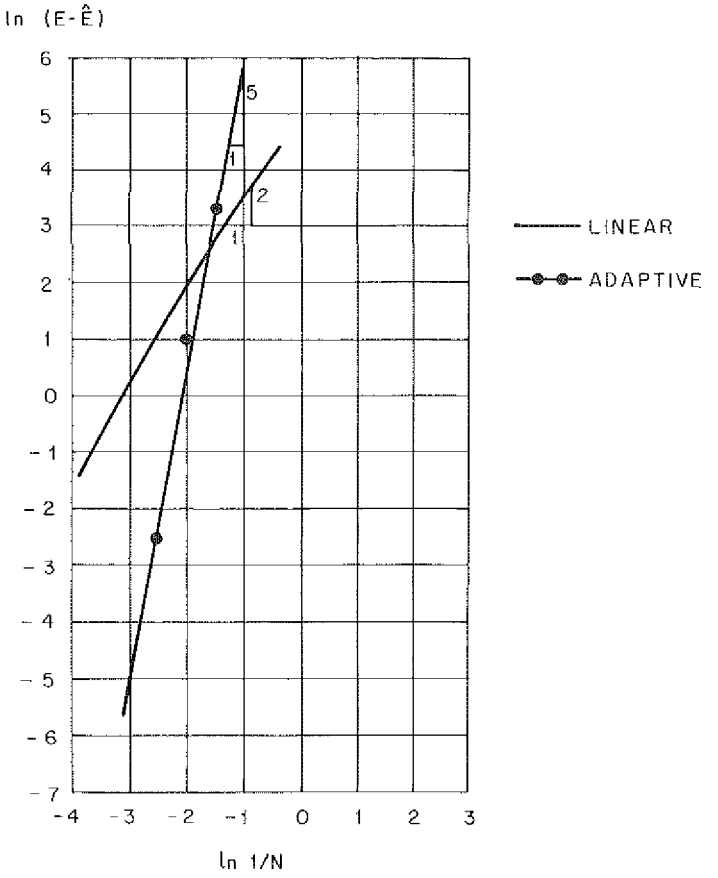

Fig. 49. Rate of convergence for adaptive boundary elements used to solve Neumann's problem in the square.

puterization of the method, but it is artificial to create elements by local shape functions when a banded structure is impossible to obtain. In addition, the rigidity introduced is enormous and as soon as the nodal points and the interpolation degree has been fixed, everything is fixed (i.e. geometry, collocation points, interpolation of data, etc.), when, usually, it is better to treat the geometry, the data and the unknowns independently.

The first attempt to adapt these ideas to the BEM as applied to potential problems was made by Alarcón [5] and subsequent advances on the subject have been presented by Alarcón et al. [6–8]. Application of adaptive procedures to elastostatics is quite straightforward.

Figure 49 shows the results (error in energy versus the inverse of the number of degrees of freedom) obtained for the classical Neumann problem in the square. As shown there and in [6–8], the increase in accuracy in comparison with the classical direct method is encouraging. In our opinion, adaptive boundary elements represent one of the more promising paths for the development of boundary elements.

Acknowledgement

The authors gratefully acknowledge Professor D. Beskos for useful comments and discussion. Financial support under Research Project 05.14 for the Comision Asesora de Investigación Cientifical y Tecnica (C.A.I.C.Y.T.) is gratefully acknowledged.

References

[1] E. Alarcón, C. Brebbia and J. Domínguez, The Boundary Element Method in Elasticity, *International Journal of Mechanical Sciences* **20**, 625–639 (1978).

[2] E. Alarcón, A. Martín and F. París, Boundary Elements in Potential and Elasticity Theory, Computers and Structures **10**, 341–362 (1979).

[3] E. Alarcón, A. Martín and F. París, Some Minor Problems with BEM, in: *Applied Numerical Modelling*, E. Alarcón and C.A. Brebbia, Eds. (Pentech Press, London, 1979) pp. 591–600.

[4] E. Alarcón, Identification of Pressures and Maintenance in Railway Tunnels, in: *Computational Methods and Experimental Measurements*, G.A. Keramidas and C.A. Brebbia, Eds. (Springer-Verlag, Berlin, 1982) pp. 516–526.

[5] E. Alarcón, Elementos de Contorno Adaptables, *Hormigón y Acero* **149**, 47–58 (1983).

[6] E. Alarcón, A. Reverter and J. Molina, Hierarchical Boundary Elements, in: *NASA Symposium on Advances and Trends in Structures and Dynamics*, A.K. Noor, Ed. (Washington D.C., 1984) pp. 441–443; also in *Computers and Structures* **20**, 151–156 (1985).

[7] E. Alarcón and A. Reverter, On the Possibility of Adaptive Boundary Elements, in: *Proceedings of the International Conference on Accuracy Estimates and Adaptive Refinements in Finite Element Computations*, I. Babuska, E.R.A. Oliveira and O.C. Zienkiewicz, Eds (Technical University of Lisbon, Lisbon, 1984) pp. 25–34.

[8] E. Alarcón and A. Reverter, P-Adaptive Boundary Elements, *International Journal for Numerical Methods in Engineering* **23**, 801–829 (1986).

[9] N. Altiero and D. Sikarskie, A. Boundary Integral Method Applied to Plates of Arbitrary Plan Form, *Computers and Structures* **9**, 163–168 (1978).
[10] N.J. Altiero and S.D. Gavazza, An Effective Boundary-Integral Approach for the Mixed Boundary-Value Problems of Linear Elastostatics, *Applied Mathematical Modelling* **3**, 99–104 (1979).
[11] J.J. Anza, El Método de los Elementos de Contorno en Problemas Termoelásticos, Ph.D. Thesis, School of Industrial Engng, Polytechnical University of Madrid, Spain (1981).
[12] I. Babuska and W.C. Rheinboldt, A Posteriori Error Estimate for the F.E.M., *International Journal for Numerical Methods in Engineering* **12**, 1597–1615 (1978).
[13] P.K. Banerjee, Integral Equation Methods for Analysis of Piece-wise Non-homogeneous Three-Dimensional Elastic Solids of Arbitrary Shape, *International Journal of Mechanical Sciences* **18**, 293–303 (1976).
[14] P.K. Banerjee and R. Butterfield, An Integral Equation Method for the Analysis of Boundary Value Problems in Irregularly Stratified Media, in: *Numerical Methods in Soil Mechanics and Rock Mechanics*, G. Borm and H. Meissner, Eds. (Karlsruhe, 1976) pp. 141–163.
[15] P.K. Banerjee and T.G. Davies, The Behaviour of Axially and Laterally Loaded Single Piles Embedded in Nonhomogeneous Soils, *Géotechnique* **28**, 309–326 (1978).
[16] P.K. Banerjee and R. Butterfield, Eds., *Developments in Boundary Element Methods*–1 (Applied Science, London, 1979).
[17] P.K. Banerjee and R. Butterfield, *Boundary Element Methods in Engineering Science* (McGraw Hill, London, 1981).
[18] P.K. Banerjee and R.P. Shaw, Eds., *Developments in Boundary Element Methods*–2 (*Applied Science, London*, 1982).
[19] G. Beer, J.L. Meek and R.G. Friday, Efficient Analysis of Problems in Geomechanics, in: *Numerical Methods in Geomechanics Edmonton*, Z. Eisenstein, Ed. (A.A. Balkema, Rotterdam, 1982) pp. 5–13.
[20] R. Benjumea and D.L. Sikarskie, On the Solutions of Plane Orthotropic Elasticity Problems by an Integral Equation Method, *Journal of Applied Mechanics* **39**, 801–808 (1972).
[21] G.P. Bézine, Boundary Integral Formulation for Plate Flexure with Arbitrary Boundary Conditions, *Mechanics Research Communications* **5**, 197–206 (1978).
[22] B.H.G. Brady, A Direct Formulation of the Boundary Element Method of Stress Analysis for Complete Plane Strain, *International Journal of Rock Mechanics and Mining Sciences & Geomechanics Abstracts* **16**, 235–244 (1979).
[23] B.H.G. Brady and A. Wassyng, A Coupled Finite Element-Boundary Element Method of Stress Analysis, *International Journal of Rock Mechanics and Mining Science & Geomechanics Abstracts* **18**, 475–485 (1981).
[24] C.A. Brebbia, *The Boundary Element Method for Engineers* (Pentech Press, London, 1978).
[25] C.A. Brebbia, Ed., *Recent Advances in Boundary Element Methods* (Pentech Press, London, 1978).
[26] C.A. Brebbia and R. Nakaguma, Boundary Elements in Stress Analysis, *Journal of the Engineering Mechanics Division of the ASCE* **105** (EM1), 55–69 (1979).
[27] C.A. Brebbia and P. Georgiou, Combination of Boundary and Finite Elements in Elastostatics, *Applied Mathematical Modelling* **3**, 212–220 (1979).
[28] C.A. Brebbia and S. Walker, *Boundary Element Techniques in Engineering* (Newnes–Butterworths, London, 1980).
[29] C.A. Brebbia, Ed., *New Developments in Boundary Element Methods* (CML Publications, Southampton, 1980).
[30] C.A. Brebbia, Ed., *Boundary Element Methods* (Springer-Verlag, Berlin, 1981).
[31] C.A. Brebbia, Ed., *Progress in Boundary Element Methods*, Vol. 1 (Pentech Press, London, 1981).
[32] C.A. Brebbia, Ed., *Boundary Element Methods in Engineering* (Springer-Verlag, Berlin, 1982).
[33] C.A. Brebbia, T. Futagami and M. Tanaka, Eds., *Boundary Elements* (Springer-Verlag, Berlin, 1983).
[34] C.A. Brebbia, Ed., *Progress in Boundary Element Methods*, Vol. 2 (Pentech Press, London, 1983).

[35] C.A. Brebbia, J.C.F. Telles and L.C. Wrobel, *Boundary Element Techniques* (Springer-Verlag, Berlin, 1984).
[36] C. Burgos, M. Doblaré, E. Alarcón, Automatic Mesh Generation Processor for 3-D Parabolic Boundary Discretization, *Advances in Engineering Software* **5**, 142–147 (1983).
[37] R. Butterfield and P.K. Banerjee, The Elastic Analysis of Compressible Piles and Pile Groups, *Géotechnique* **21**, 43–60 (1971).
[38] R. Butterfield and P. K. Banerjee, The Problem of Pile Group-Pile Cap Interaction, *Géotechnique* **21**, 135–142 (1971).
[39] R. Butterfield, The Application of Integral Equation Methods to Continuum Problems in Soil Mechanics, in: *Stress–Strain Behavior of Soils*, R.H.G. Parry, Ed., (G.T. Foulis & Co., Henley-on-Thames, Oxfordshire, 1972) pp. 573–587.
[40] Y.K. Cheung, Beams, Slabs and Pavements, in: *Numerical Methods in Geotechnical Engineering*, C.S. Desai and J.T. Christian, Eds., (McGraw-Hill, New York, 1977) pp. 176–210.
[41] M. Cristescu and G. Loubignac, Gaussian Quadrature Formulas for Functions with Singularities in $1/r$ Over Triangles, in: *Recent Advances in Boundary Element Methods*, C.A. Brebbia, Ed. (Pentech Press, London, 1978) pp. 375–390.
[42] S.L. Crouch, Solution of Plane Elasticity Problems by the Displacement Discontinuity Method: I & II, *International Journal for Numerical Methods in Engineering* **10**, 301–343 (1976).
[43] S.L. Crouch, Analysis of Stresses and Displacements Around Underground Excavations: An Application of the Displacement Discontinuity Method, Geomechanics/NSF Report, Dept. of Civil & Mineral Engng, University of Minnesota, Minneapolis (1976).
[44] S.L. Crouch and A.M. Starfield, *Boundary Element Methods in Solid Mechanics* (George Allen & Unwin, London, 1983).
[45] T.A. Cruse, Numerical Solutions in Three Dimensional Elastostatics, *International Journal of Solids and Structures* **5**, 1259–1274 (1969).
[46] T.A. Cruse, Application of the Boundary-Integral Equation Method to Three Dimensional Stress Analysis, *Computers and Structures* **3**, 509–527 (1973).
[47] T.A. Cruse, An Improved Boundary-Integral Equation Method for Three Dimensional Elastic Stress Analysis, *Computers and Structures* **4**, 741–754 (1974).
[48] T.A. Cruse, D.W. Snow and R.B. Wilson, Numerical Solutions in Axisymmetric Elasticity, *Computers and Structures* **7**, 445–451 (1971).
[49] T.A. Cruse and R.B. Wilson, Advanced Applications of Boundary-Integral Equation Methods, *Nuclear Engineering and Design* **46**, 223–234 (1978).
[50] D. Danson, Linear Isotropic Elasticity with Body Forces, in: *Progress in Boundary Element Methods*, Vol. 2, C.A. Brebbia, Ed. (Pentech Press, London, 1983) pp. 101–135.
[51] M. Doblaré and E. Alarcón, A Three-Dimensional B.I.E.M. Program, in: *Finite Element Systems: A Handbook*, C.A. Brebbia, Ed. (Springer-Verlag, Berlin, 1982) pp. 325–345.
[52] J. Domínguez, Cálculo de Tensiones en las Inmediaciones de Anclajes: Applicación del Método de los Elementos de Contorno, Ph.D. Thesis, School of Industrial Engng., University of Seville, Spain (1978).
[53] J. Domínguez, F. del Caño and E. Alarcón, B.I.E.M. in Solid Mechanics, in: *3rd Engineering Mechanics Division Speciality Conference ASCE*, Univ. of Texas at Austin, (ASCE, New York, 1979) pp. 793–796.
[54] W.S. Dunbar and D.L. Anderson, The Displacement Discontinuity Method in Three Dimensions, in: *Boundary Element Methods*, C.A. Brebbia, Ed. (Springer-Verlag, Berlin, 1981) pp. 153–165.
[55] D.J. Forbes and A.R. Robinson, Numerical Analysis of Elastic Plates and Shallow Shells by an Integral Equation Method, *Structural Research Series Report No.* 345, University of Illinois, Urbana, Illinois (1969).
[56] T. Fukui, On Corner Solutions by Indirect B.I.E.M., in: *Boundary Elements*, C.A. Brebbia, T. Futagami and M. Tanaka, Eds. (Springer-Verlag, Berlin, 1983) pp. 929–938.
[57] S. Gómez-Lera, F. París and E. Alarcón, Treatment of Singularities in 2-D Domains Using BIEM, *Applied Mathematical Modelling* **6**, 111–118 (1982).
[58] F. Hartmann, The Derivation of Stiffness Matrices from Integral Equations, *Applied Mathematical Modelling* **5**, 355–365 (1981).

[59] F. Hartmann, Elastostatics, in: *Progress in Boundary Element Methods*, Vol. 1, C.A. Brebbia, Ed. (Halsted Press, New York, 1981) pp. 84–167.
[60] U. Heisse, Comparison of Round-Off-Errors in Integral Equation Formulations of Elastostatical Boundary Value Problems, *Computer Methods in Applied Mechanics and Engineering* **28**, 145–177 (1981).
[61] U. Heisse, Removal of the Zero Eigenvalues of Integral Operator in Elastostatic Boundary Value Problems, *Acta Mechanica* **41**, 41–61 (1981).
[62] U. Heisse, Solution of Integral Equations for Plane Elastostatical Problems with Discontinuously Prescribed Boundary Values, *Journal of Elasticity* **12**, 293–312 (1982).
[63] G.C. Howell and W.S. Doyle, An Assessment of the Boundary Integral Equation Method for In-Plane Elastostatics Problems, *Applied Mathematical Modelling* **6**, 245–256 (1982).
[64] G.C. Howell and W.S. Doyle, The Plane Stress/Strain Analysis of Non-Homogeneous Continua by the Boundary Integral Equation Method, *Computers and Structures* **17**, 603–610 (1983).
[65] M.A. Jaswon, M. Maiti and G.T. Symm, Numerical Biharmonic Analysis and Some Applications, *International Journal of Solids and Structures* **3**, 309–332 (1967).
[66] M.A. Jaswon and M. Maiti, An Integral Equation Formulation of Plate Bending Problems, *Journal Engineering Mathematics* **2**, 83–93 (1968).
[67] M.A. Jaswon and G.T. Symm, *Integral Equation Methods in Potential Theory and Elastostatics* (Academic Press, New York, 1977).
[68] N. Kamiya, Y. Sawaki and Y. Nakamura, Finite and Postbuckling Deformations of Heated Plates and Shallow Shells, in: *Boundary Elements*, C.A. Brebbia, T. Futagami and M. Tanaka, Eds. (Springer-Verlag, Berlin, 1983) pp. 507–516.
[69] D.W. Kelly, G.G.W. Mustoe and O.C. Zienkiewicz, Coupling Boundary Element Methods with other Numerical Methods, in: *Developments in Boundary Element Methods – 1*, P.K. Banerjee and R. Butterfield, Eds. (Applied Science, London, 1979) pp. 251–285.
[70] T. Kermanidis, A. Numerical Solution for Axially Symmetrical Elasticity Problems, *International Journal of Solids and Structures* **11**, 493–500 (1975).
[71] S. Kobayashi and N. Nishimura, Green's Tensors for Elastic Half-Spaces: An Application of Boundary Integral Equation Method, *Memoirs Faculty Engineering, Kyoto Univ.* **42**, 228–241 (1980).
[72] G. Kuhn and W. Möhrmann, Boundary Element Method in Elastostatics: Theory and Applications, *Applied Mathematical Modelling* **7**, 97–105 (1983).
[73] J.C. Lachat and J.O. Watson, A Second Generation Integral Equation Program for Three-Dimensional Elastic Analysis, in: *Boundary-Integral Equation Method: Computational Applications in Applied Mechanics*, T.A. Cruse and F.J. Rizzo, Eds. (ASME, New York, 1975) pp. 85–100.
[74] J.C. Lachat and J.O. Watson, Effective Numerical Treatment of Boundary Integral Equations: A Formulation for Three-Dimensional Elastostatics, *International Journal for Numerical Methods in Engineering* **10**, 991–1005 (1976).
[75] J.C. Lachat and J.O. Watson, Progress in the Use of Boundary Integral Equations Illustrated by Examples, *Computer Methods in Applied Mechanics and Engineering* **10**, 273–289 (1977).
[76] A.E.H. Love, *A Treatise on the Mathematical Theory of Elasticity* (Dover Publ., New York, 1944).
[77] M. Margulies, Combination of the Boundary Element and Finite Element Methods, in: *Progress in Boundary Element Methods*, Vol. 1, C.A. Brebbia, Ed. (Halsted Press, New York, 1981) pp. 258–288.
[78] A. Martín, I. Rodríguez and E. Alarcón, Mixed Elements in the Boundary Theory, in: *New Developments in Boundary Element Methods*, C.A. Brebbia, Ed. (Comp. Mech. Centre Publ., Southampton, 1980) pp. 34–42.
[79] C.E. Massonnet, Numerical Use of Integral Procedures, in: *Stress Analysis*, O.C. Zienkiewicz and G.S. Holister, Eds. (Wiley, London, 1965) pp. 198–235.
[80] M. Mayr, W. Drexler and G. Kuhn, A Semianalytical Boundary Integral Approach for Axisymmetric Elastic Bodies with Arbitrary Boundary Conditions, *International Journal of Solids and Structures* **16**, 863–871 (1980).

[81] G.G.W. Mustoe, F. Volait and O.C. Zienkiewicz, A Symmetric Direct Boundary Integral Equation Method for Two Dimensional Elastostatics, *Res Mechanica* **4**, 57–82 (1982).
[82] D.A. Newton and H. Tottenham, Boundary Value Problems in Thin Shallow Shells of Arbitrary Plan Form, *Journal of Engineering Mathematics* **2**, 211–224 (1968).
[83] N. Nishimura and S. Kobayashi, A Boundary Integral Equation Formulation for Three Dimensional Anisotropic Elastostatics, in: *Boundary Elements*, C.A. Brebbia, T. Futagami and M. Tanaka, Eds. (Springer-Verlag, Berlin, 1983) pp. 345–354.
[84] Y. Niwa, S. Kobayashi and T. Fukui, An Application of the Integral Equation Method to Plate-Bending Problems, *Memoirs of the Faculty of Engineering, Kyoto University* **36**, 140–158.
[85] Y. Niwa, S. Kobayashi and T. Fukui, Stresses and Displacements Around an Advancing Face of a Tunnel, in: *Procedings of the 4th International Congress on Rock Mechanics*, Montreux, Switzerland (A.A. Balkema, Rotterdam, 1979) pp. 703–710.
[86] E.R.A. Oliveira, Plane Stress Analysis by a General Integral Method, *Journal of the Engineering Mechanics Division of the ASCE* **94**, (EM1), 79–101 (1968).
[87] Y.C. Pan and T.W. Chou, Green's Functional Solutions for Semi-Infinite Transverselly Isotropic Materials, *International Journal of Engineering Sciences* **17**, 545–551 (1979).
[88] F. París and S. León, Aplicación del Método de los Elementos de Contorno a Placas con Ecuaciones de Contorno Arbitrarias, *Anales de Ingenieria Mecanica, Gijon, Spain* **2**, 30–37 (1984).
[89] C. Patterson and M.A. Sheikh, Regular Boundary Integral Equations for Stress Analysis, in: *Boundary Element Methods*, C.A. Brebbia, Ed. (Springer-Verlag, Berlin, 1981) pp. 85–104.
[90] C. Patterson and M.A. Sheikh, Non-Conforming Boundary Elements for Stress Analysis, in: *Boundary Element Methods*, C.A. Brebbia, Ed. (Springer-Verlag, Berlin, 1981) pp. 137–152.
[91] C. Patterson and M.A. Sheikh, A Regular Boundary Element Method for Coupled Subdomains, in: *Proceedings of the International Conference on Numerical Methods for Coupled Problems*, R.W. Lewis, P. Bettes and E. Hinton, Eds. (Pineridge Press, Swansea, 1981) pp. 115–126.
[92] A.G. Peano, Hierarchies of Conforming Finite Elements, *Ph.D. Thesis*, Department of Civil Engng., Washington University, Saint Louis (1975).
[93] A. Peano, A. Pasini, R. Riccioni and L. Sardella, Adaptive Approximation in Finite Element Structure Analysis, *Computers and Structures* **10**, 333–342 (1979).
[94] R. Rangogni and M. Reali, The Coupling of the Finite Difference Method and the Boundary Element Method, *Applied Mathematical Modelling* **6**, 233–236 (1982).
[95] F.J. Rizzo, An Integral Equation Approach to Boundary Value Problems of Classical Elastostatics, *Quarterly of Applied Mathematics* **25**, 83–95 (1967).
[96] F.J. Rizzo and D.J. Shippy, A Method for Stress Determination in Plane Anisotropic Elastic Bodies, *Journal of Composite Materials* **4**, 36–61 (1970).
[97] F.J. Rizzo and D.J. Shippy, An Advanced Boundary Integral Equation Method for Three-Dimensional Thermoelasticity, *International Journal for Numerical Methods in Engineering* **11**, 1753–1768 (1977).
[98] F.J. Rizzo and D.J. Shippy, The Boundary Element Method in Thermoelasticity, in: *Developments in Boundary Element Methods*-1, P.K. Banerjee and R. Butterfield, Eds. (Applied Science, London, 1979) pp. 155–172.
[99] F.J. Rizzo and D.J. Shippy, A Boundary Integral Approach to Potential and Elasticity Problems for Axisymmetric Bodies with Arbitrary Boundary Conditions, *Mechanics Research Communications* **6**, 99–103 (1979).
[100] D.J. Shippy and F.J. Rizzo, On the Effectiveness of Three Boundary Integral Equation Formulations for Certain Axisymmetric Elastostatic Problems, *Res Mechanica* **4**, 43–56 (1982).
[101] C. Somigliana, Sopra gli Integrali delle Equazioni della Isotropia Elastica, *Il Nuovo Cimento*, Serie III, **36**, 28–39, 113–126 (1894).
[102] C. Somigliana, Sopra l'Equilibrio di un Corpo Elastico Isotropo, *Il Nuovo Cimento*, Serie III, **17**, 140–148, 272–276; **18**, 91–96, 161–166 (1885); **19**, 84–90, 278–282; **20**, 181–185 (1886).
[103] C. Somigliana, Sul Potenziale Elastico, *Annali di Mathematica Pura ed Applicata*), Serie III, **7**, 129–140 (1902).
[104] M. Stern, A General Boundary Integral Formulation for the Numerical Solution of Plate Bending Problems, *International Journal of Solids and Structures* **15**, 769–782 (1979).

[105] M. Stern, Boundary Integral Equations for Bending of Thin Plates, in: *Progress in Boundary Element Methods*, Vol. 2, C.A. Brebbia, Ed. (Pentech Press, London, 1983) pp. 158–181.
[106] A.H. Stroud and D. Secrest, *Gaussian Quadrature Formulas* (Prentice-Hall, Englewood Cliffs, N.J., 1966).
[107] B.A. Szabo and A.U. Metha, *P*-Convergent Finite Element Approximations in Fracture Mechanics, *International Journal for Numerical Methods in Engineering* **12**, 551–560 (1978).
[108] G.R. Tomlin and R. Butterfield, Elastic Analysis of Zoned Orthotropic Continua, *Journal of the Engineering Mechanics Division of the ASCE* **100** (EM3), 511–529 (1974).
[109] H. Tottenham, The Boundary Element Method for Plates and Shells, in: *Developments in Boundary Element Methods*–1, P.K. Banerjee and R. Butterfield, Eds. (Applied Science, London, 1979) pp. 173–205.
[110] O. Tullberg and L. Bolteus, A Critical Study of Different Boundary Element Stiffness Matrices, in: *Boundary Element Methods in Engineering*, C.A. Brebbia, Ed. (Springer-Verlag, Berlin, 1982) pp. 621–635.
[111] S.M. Vogel and J.F. Rizzo, An Integral Equation Formulation of Three Dimensional Anisotropic Elastostatic Boundary Value Problems, *Journal of Elasticity* **3**, 203–216 (1973).
[112] E. Volterra and J.H. Gaines, *Advanced Strength of Materials* (Prentice-Hall, Englewood Cliffs, NJ, 1971).
[113] L.J. Wardle and J.M. Crotty, Two-Dimensional Boundary Integral Equation Analysis for Non-homogeneous Mining Applications, in: *Recent Advances in Boundary Element Methods*, C.A. Brebbia, Ed. (Pentech Press, London, 1978) pp. 233–251.
[114] J.O. Watson, Advanced Implementation of the Boundary Element Method for Two- and Three-Dimensional Elastostatics, in: *Developments in Boundary Element Methods*–1, P.K. Banerjee and R. Butterfield, Eds. (Applied Science, London, 1979) pp. 31–63.
[115] R.B. Wilson and T.A. Cruse, Efficient Implementation of Anisotropic Three-Dimensional Boundary Integral Equation Stress Analysis, *International Journal for Numerical Methods in Engineering* **12**, 1383–1397 (1978).
[116] O.C. Zienkiewicz, B.M. Irons, F.E. Scott and J.S. Campbell, Three-Dimensional Stress Analysis, in: *Proceedings of the IUTAM Symposium on High Speed Computing of Elastic Structures* (University of Liege Press, Liege, 1971) pp. 413–443.
[117] O.C. Zienkiewic, Marriage a la Mode–The Best of Both Worlds (Finite Elements and Boundary Integrals), in: *Innovative Numerical Analysis in Applied Engineering Science*, T.A. Cruse et al, Eds. (CETIM, Senlis, France, 1977) pp. 19–26.
[118] O.C. Zienkiewicz, *The Finite Element Method* (McGraw-Hill, London, 1977).